



**UNIVERSITÀ DEGLI STUDI DI MILANO**  
**FACOLTÀ DI SCIENZE E TECNOLOGIE**

Corso di Laurea Magistrale in Fisica

**On the nature of soft and collinear scales in  
Higgs boson production at NNLO**

Relatore: **Prof. Stefano Forte**

Candidato: **Mattia Capuano**

Matricola: 09294A

---

ANNO ACCADEMICO 2022/2023

# Introduction

In experimental particle physics the main observables measured at particle accelerators, such as the Large Hadron Collider, are total and differential cross sections of scattering processes. Cross sections can be computed in the Quantum Field Theory framework through perturbative expansions: the calculation of each order of the expansion increases the precision of the prediction. In order to test the validity of the Standard Model of particle physics and to rule out possible extensions, the precision of the predictions must reach the precision of the experiments, which in the last years has greatly increased because of ever-growing datasets and refined data analysis techniques.

One of the main tools we have for this purpose is resummation. Each term of the perturbative expansion features logarithmic contributions which are enhanced when the final products are in certain configurations at the boundary of the phase space. Resummation formulae make possible to sum over all such large logarithms at all orders in perturbation theory, increasing the precision of the prediction.

In this thesis we verify a resummation formula for the Higgs boson production process derived in [1]. In particular, the resummation formula resums logarithms appearing in the cross section differential with respect to the longitudinal rapidity of the Higgs boson, called rapidity distribution. Such logarithms become large in the threshold limit, that is when the energy of the process is just enough to produce an Higgs boson with given mass and rapidity. The explicit form and origin of the logarithms is predicted by the resummation formalism by studying the phase space integrals that give rise to dimensional quantities that are singular in the threshold limit, the soft and collinear scales. Since this is the core of the derivation, in order to verify the resummation formula we compare the expected logarithms with the NNLO result [2].

In chapter 1 we review the main tools and concepts of perturbative QCD necessary for cross section computations relevant for the subsequent sections. After presenting basic definitions and properties of QCD, we present two archetypal processes, deep inelastic scattering (DIS) and Drell-Yan production (DY), which will give us the opportunity to discuss some features of perturbative calculations. We then focus on the soft and collinear divergences

appearing in loop and phase space integrals and on their cancellation, introducing the problem of large logarithms. Finally, we define the dimensional regularization scheme, which is fundamental to understand how enhanced logarithms arise in actual computations.

In chapter 2 we present resummation. After a general introduction we focus on threshold resummation of DY and DIS total cross sections, reviewing the renormalization group equations approach presented in [3]. This is organized in two steps, the first is the derivation of the singular scales from the phase space integrals, and the second is the application of renormalization group equations to cross sections in order to get the resummation formulae. To carry this calculation we also give a short account of the Mellin transform, a mathematical tool necessary to derive the formulae.

In chapter 3 we extend the threshold resummation of total cross sections to that of the rapidity distribution of the Higgs boson production process, following [1]. After introducing the basic variables for the kinematics of rapidity distributions, we study the singular scales emerging from the phase space, identifying a soft and a collinear scale emerging respectively from soft and collinear emissions in the threshold limit. This leads us finally to the resummation formulae.

Lastly, chapter 4 is the core of the thesis, where we deal with the verification of the resummation formulae by comparison with the NNLO result of the Higgs boson production rapidity distribution. The rapidity distribution is studied first at LO and NLO in order to see in action some techniques introduced in the first chapter and to introduce some general features of the calculation. Then, we get to the NNLO order computation. We study the phase space for the case of two extra-emissions, rewriting the soft and collinear scales in terms of different variables. The result of the fully differential distribution in [2] is presented and rewritten in order to make manifest the singular logarithms depending on the soft and collinear scales we found. We notice that these are of the form predicted by the phase space analysis. We also check that they have the same origin by retracing their provenance in the original computation.

# Contents

<b>Introduction</b>	<b>2</b>
<b>1 Perturbative QCD</b>	<b>5</b>
1.1 Cross sections	5
1.2 QCD and particle physics	6
1.3 QCD and renormalization	7
1.4 Factorization	8
1.5 Energy scales	9
1.6 Inclusive processes: DIS and DY	10
1.6.1 Deep inelastic scattering	11
1.6.2 Drell-Yan production	13
1.7 Infrared singularities	14
1.8 Dimensional regularization	18
<b>2 Resummation</b>	<b>20</b>
2.1 Large logarithms and resummation	20
2.2 Threshold resummation of total cross sections	22
2.2.1 Phase space analysis	23
2.2.2 Mellin space	27
2.2.3 Derivation of resummation formulae	29
2.3 From total to differential cross sections resummation	32
<b>3 Resummation of rapidity distributions</b>	<b>34</b>
3.1 Higgs boson production at hadron colliders	35
3.2 Fully differential distribution	36
3.3 Threshold variables of the rapidity distribution	38
3.3.1 Kinematical configurations in the threshold limit	41
3.4 Factorization in Mellin space	42
3.4.1 Hadronic kinematics	42
3.4.2 Factorization in Mellin-Fourier space	43
3.4.3 Factorization in Mellin-Mellin space	44
3.4.4 Threshold limit in $(N, M)$ and $(N_1, N_2)$	45
3.5 Phase space	45

3.6	Resummation of the rapidity distribution . . . . .	50
3.6.1	Singular scales in Mellin-Mellin space . . . . .	50
3.6.2	Resummation formulae: doubly soft limit . . . . .	51
3.6.3	Resummation formulae: singly soft limit . . . . .	52
3.7	The question of verification . . . . .	53
<b>4</b>	<b>Gluon fusion at NNLO</b>	<b>55</b>
4.1	Gluon fusion at LO . . . . .	56
4.2	Gluon fusion at NLO . . . . .	56
4.2.1	Virtual contribution at NLO . . . . .	57
4.2.2	Real contribution at NLO . . . . .	57
4.2.3	NLO in $(x, u, m_H^2)$ . . . . .	60
4.2.4	NLO in $(x_1, x_2, m_H^2)$ . . . . .	62
4.3	Gluon fusion at NNLO . . . . .	63
4.3.1	Relevant variables . . . . .	63
4.3.2	Phase space at NNLO . . . . .	64
4.3.3	The fully differential distribution at NNLO . . . . .	69
4.3.4	Retracing logarithms . . . . .	75
	<b>Conclusions</b>	<b>78</b>
<b>A</b>	<b>Mathematical tools</b>	<b>80</b>
A.1	Plus distribution . . . . .	80
A.2	Mellin transform . . . . .	81
	<b>Bibliography</b>	<b>84</b>

# Chapter 1

## Perturbative QCD

1.1	Cross sections . . . . .	5
1.2	QCD and particle physics . . . . .	6
1.3	QCD and renormalization . . . . .	7
1.4	Factorization . . . . .	8
1.5	Energy scales . . . . .	9
1.6	Inclusive processes: DIS and DY . . . . .	10
1.6.1	Deep inelastic scattering . . . . .	11
1.6.2	Drell-Yan production . . . . .	13
1.7	Infrared singularities . . . . .	14
1.8	Dimensional regularization . . . . .	18

In this chapter we briefly summarize key concepts of Quantum Chromodynamics (QCD) necessary to understand and fix notations for the following chapters. Focus is on phase space rather than amplitude calculations. After a short discussion on differential cross sections and QCD, its fundamental properties are presented together with a basic discussion of the relevant energy scales. We then introduce two archetypical processes in QCD, deep inelastic scattering and Drell-Yan production, crucial for the next chapter, and, finally, tackle the problem of soft and collinear divergences in cutoff and dimensional regularization schemes.

### 1.1 Cross sections

In this section we define the relevant observables in particles physics, cross sections, and how special relativity, through phase spaces, bridges cross sections and amplitudes, the core of quantum field theory models.

Given a scattering event, the main observables measured at particle accelerators are *total* and *differential cross sections*. Total cross sections ( $\sigma$ ) represent the rate at which a process occur, having fixed the energy of the colliding particles. Differential cross sections ( $d\sigma/d\{x\}$ ) are the rate of the occur-

rences of a process having fixed also a particular set of final state kinematical variables  $\{x\}$ . Quantum field theory gives the theoretical framework to predict cross sections. Squared amplitudes, functions containing all the information on the possible final kinematical configurations, are calculated through Feynman diagrams. Differential cross sections are obtained by integrating out from squared amplitudes all the variables that are not measured, that is to say all the final four-momenta in the case of total cross sections. However when the mass-shell condition  $p_i^2 = m_i^2$  holds, four-momenta components are not independent and the actual integration is done on three-dimensional momenta using  $d^4p_i \delta^{(+)}(p_i^2 - m_i^2) = d^3p_i / 2p_i^0$ .

In practice, taking for example a  $2 \rightarrow n$  process, the most general differential cross section is

$$d\sigma = \Phi \prod_{i=1}^n \left( \frac{d^3p_i}{(2\pi)^3(2p_i^0)} \right) |\mathcal{M}(\{p_i\})|^2 \delta^{(4)}(p_1 + p_2 - \sum p_i) =: \Phi d\Pi_n |\mathcal{M}|^2, \quad (1.1.1)$$

where the four-dimensional delta imposes conservation of the total four-momentum.  $\Phi$  is a dimensional factor depending on incoming particles. Integrating on every  $p_i$  gives the total cross section. In the following, we will collectively denote total and differential cross sections as  $d\sigma$ .

In this formula the actual input from the QFT model that is being tested is in the squared amplitude. Clearly, total cross sections, involving the maximum number of integrations, are the less sensitive observables to details of  $|\mathcal{M}|^2$ , and so to those of the underlying theory. Differential cross sections however, even if more sensitive, require a greater dataset for a precise measurement. Recently, with ever-growing dataset, precision of measurements of differential cross sections has greatly increased but state-of-the-art theoretical predictions are not yet as precise.

When working with many integrals it is important to deal with variables with great care, identifying a set of independent variables. General considerations can be made that will aid us in next chapters. In principle the amplitude depends on all the possible components of the final and initial momenta, that is  $4(n+2)$ , considering mass-shell conditions ( $-(n+2)$  variables) and Poincaré invariance ( $-10$  variables),  $3n-4$  independent variables remain. For example, processes with two particles in the final state depend on 2 variables, which can be chosen among the Mandelstam variables  $s$ ,  $t$  and  $u$ .

## 1.2 QCD and particle physics

In this section we define Quantum Chromodynamics and its interacting particles, discussing how computations can only be made in a perturbative context and its role in precision physics.

Quantum Chromodynamics (QCD) is the field theory describing the in-

interactions between the constituents of hadrons (*partons*), such as protons and neutrons. It is a  $SU(3)$  gauge theory interacting with 6 fermions called *quarks* with different masses. The massless excitations of the gauge field are called *gluons*. Given the masses and the charges of the six *flavours* of quarks and the coupling constant  $\alpha_s$ , measured at a known energy, the Lagrangian of the theory is completely specified by symmetry constraints.  $SU(3)$  symmetry in particular implies that quarks have a charge, called *colour*, and that this charge is conserved. Other properties of gluons and quarks are polarization and spin (the first are vector fields, the second fermionic fields). We will only consider colour, polarization and spin averaged observables.

Quantum field theory gives the recipe to derive from the Lagrangian of the theory the Feynman rules necessary to calculate perturbatively squared amplitudes (see for example [4]). In particular any observable  $\mathcal{O}$  is written as a power series in the coupling constant

$$\mathcal{O} = \sum_{n=0}^{\infty} \mathcal{O}_n \alpha^n, \quad (1.2.1)$$

where the first non-trivial term is called *leading order* (LO), the following *next-to-leading order* (NLO) and so on. The general term is labelled as  $N^k\text{LO}$ . Name conventions may change depending on the process considered, we will see an example in the next sections.

The precision of the prediction increases by calculating more terms in the perturbative expansions. In QCD particularly, because of the size of the coupling constant ( $\alpha_s \sim 1/10$ ), for predictions with precision comparable with experiments, computations should go at least beyond NLO.

### 1.3 QCD and renormalization

In this section we discuss the consequences of renormalization on QCD observables.

The procedure of renormalization, necessary to cancel ultraviolet divergences occurring in loop integrals, introduces an energy dependence in the coupling constant  $\alpha_s$ . The dependence of the coupling constant on the energy is captured by the process independent *beta function* defined as

$$\beta(\alpha_s(\mu^2)) := \frac{d \ln \alpha_s(\mu^2)}{d \ln \mu^2}. \quad (1.3.1)$$

The function is calculated perturbatively defining the coefficients of the expansion in the following way

$$\beta(\alpha_s) = -\alpha_s^2(\beta_0 + \beta_1 \alpha_s + \beta_2 \alpha_s^2 \dots). \quad (1.3.2)$$



The leading coefficient is

$$\beta_0 = \frac{33 - 2n_f}{12\pi}, \quad (1.3.3)$$

where  $n_f$  is the number of flavours that enter in the computation. It is customary, as it will be done subsequently, to choose as perturbative parameter  $\alpha_s/2\pi$  so that  $\beta_0 = 33 - 2n_f/6$ . For the observed number of quarks,  $\beta_0$  is negative, this has important phenomenological consequences. Observing the definition of beta function one sees that, if the beta function is negative, as the energy grows the coupling constant decreases: QCD is said to be an *asymptotical free* theory. At low energies the coupling constant eventually is greater than 1 and the perturbative expansion breaks down. At this level QCD is very strongly coupled, which is, at least intuitively, the reason for the property of *confinement*, that is the quarks and gluons are never observed as free particles but rather as bound states. Because we are not able to make any analytical prediction at the non-perturbative level, experimental input is needed when calculating cross sections for processes involving hadrons. This will be discussed in the next section.

Viewing the definition of beta function as a differential equation and solving it at leading order one obtains an approximate trend for  $\alpha_s$ ,

$$\alpha_s(Q^2) = \frac{\alpha(\mu^2)}{1 + \beta_0 \alpha_s(\mu^2) \ln \frac{Q^2}{\mu^2}}. \quad (1.3.4)$$

The denominator is singular for  $Q =: \Lambda_{QCD} \approx 100\text{MeV}$ , the *Landau pole*. Even if at these energies the actual behaviour of the coupling constant is unknown because the perturbative approximation fails, conventionally the Landau pole defines the energy scale of non-perturbative QCD.

Fixing the renormalization energy at  $\Lambda_{QCD}$ , at high energies the coupling constant is approximately

$$\alpha_s(Q^2) = \frac{1}{\beta_0 \ln \frac{Q^2}{\Lambda_{QCD}^2}}. \quad (1.3.5)$$

## 1.4 Factorization

In this section we introduce the fundamental concept of QCD factorization, which makes possible to calculate hadronic cross sections from partonic cross sections and the experimentally measured Parton Distribution Functions. This is just a general explanation, many important features and examples will be discussed in subsequent sections.

Only cross section relative to scattering between the fundamental fields of the theory, partons, can be calculated through perturbative QCD. However, as a consequence of confinement, quarks and gluons are never found as free

particles, but rather as bound states in hadrons such as protons, which we are not able to describe analytically. Therefore, we can only measure *hadronic* cross sections but we can only compute *partonic* cross sections.

*Factorization* is the property of perturbative QCD that makes possible to link experiments with theory. Factorization states that scattering involving hadrons can be regarded as a scattering involving a single parton carrying a fraction  $z$  of the total momentum of the hadron it belongs to.

Consider for example a scattering process between a single parton with momentum  $p$  and any another particle with momentum  $k$ . The particle may scatter with a gluon, a quark or an antiquark. The hadronic cross section is a combination of the partonic ones, integrating on all possible value of the momentum fraction  $\xi$  and weighing each partonic cross section with the probability of finding that given parton  $h$  carrying a fixed momentum fraction  $\xi$ ,  $f_h(\xi)$

$$d\sigma(k, p) = \sum_{h=g,q,\bar{q}} \int_{\tau}^1 d\xi f_h(\xi) d\sigma_h(k, \xi p). \quad (1.4.1)$$

This result is trivially extended to processes with more than one incoming parton, such as proton collisions

$$d\sigma(p_1, p_2) = \sum_{h_1, h_2=g,q,\bar{q}} \int_{\tau_1}^1 d\xi_1 \int_{\tau_2}^1 d\xi_2 f_{h_1}(\xi_1) f_{h_2}(\xi_2) d\sigma_{h_1 h_2}(\xi_1 p_1, \xi_2 p_2). \quad (1.4.2)$$

The lower limits of integration are scaling variables depending on the process considered (see next sections) The probability distributions  $f_h(\xi)$  are called parton density functions (PDFs). They are the experimental input of factorization, making up for the lack of knowledge of the non-perturbative hadron structure. PDFs are process independent, so they can be extracted by data through fitting procedures potentially from any process.

Factorization as stated holds only at tree level: virtual corrections induce on PDFs an energy dependence on the *factorization scale*  $\mu_F^2$ . This will be discussed in coming sections. Even though we have given here an intuitive account, factorization can be justified through rigorous field-theoretic arguments depending on the process considered.

## 1.5 Energy scales

To have a grasp with the actual experimental energy scales and in order to partially justify some approximations, in this section we present the relevant energy scales of QCD and LHC physics.

In table 1.1 approximate masses of the known quark flavours are shown.

The masses extend on a very wide range of energies. The center-of-mass energy at the LHC is almost 14 TeV, but since PDFs peak at some momen-

flavour	up (u)	down (d)	charm (c)	strange (s)	top (t)	bottom (b)
mass	2.5 MeV	5 MeV	1.3 MeV	0.1 GeV	173 GeV	4.2 GeV

Table 1.1: Masses of the six quarks flavours in the  $\overline{MS}$  scheme.

tum fraction  $\xi < 1$ , on average partons carry away a small energy of the total available (approximately  $1/3$  for *valence* quarks and  $1/10$  for gluons), leaving an effective energy for the parton scattering of approximately 1 TeV. For the Higgs boson production process the relevant hard scale is close to its mass, 125 GeV. At this energy the first five quarks can be taken to be massless while the mass of the top quark is infinite, so that we will actually consider only 5 massless flavours. A detailed discussion of this approximation can be found in [5].

## 1.6 Inclusive processes: DIS and DY

Having now acquired the most basic knowledge to build partonic cross sections in QCD, in this section we consider two basic semi-inclusive processes, Deep Inelastic Scattering and Drell-Yan production. We see that they can be taken to depend only on two variables, an hard scale and a dimensionless quantity. This gives us the opportunity to define the fundamental threshold limit.

In QCD *semi-inclusive* processes, the subset of strongly interacting products, referred collectively as  $X$ , is not experimentally measured. This is because in particle detectors it is not possible to distinguish which hadron comes from the process under examination: some may be produced from different processes or some may be colliding hadrons that have not interacted at all. We will see that inclusiveness has also important consequences in regularizing calculations.

Analytically, inclusive processes have two important features. Firstly, calculating cross sections, four-momenta of extra emissions are always integrated on, so that the cross section will be eventually differential on kinematical properties of the measured radiation. Secondly, it is necessary to sum over all the possible cross sections relative to processes with different final products that are not measured. This must be done consistently with the order of perturbation, because different processes, even at tree level, may contribute differently in the perturbative expansion. We will now see an application studying two of the most important processes in QCD, deep inelastic scattering (DIS) and Drell-Yan production (DY).

### 1.6.1 Deep inelastic scattering

Deep inelastic scattering is the scattering between an electron, or any other lepton, and a proton

$$p + e \rightarrow e + X. \quad (1.6.1)$$

Schematically DIS is represented in figure 1.1.

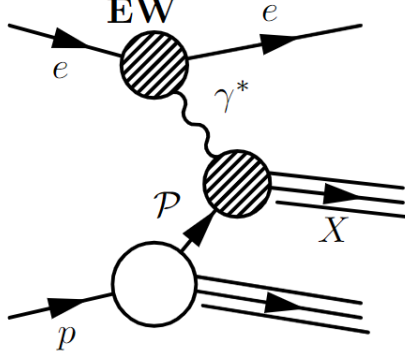


Figure 1.1: Schematic representation of DIS. From the white bubble, representing the proton, the scattering parton  $\mathcal{P}$  is extracted. This subprocess is dealt with factorization. The **EW** bubble represents the sum of electroweak corrections to the electron-photon scattering. The bubble in the center is the sum of QCD and EW corrections to the parton-photon scattering.  $X$  is the set of emitted QCD radiation.

The process has both Electroweak (EW) and QCD corrections, for this reason the perturbative expansion is defined with respect to both coupling constants. However, QCD corrections are dominant on EW corrections both because the strong coupling constant is greater and as a consequence of large logarithms (see next chapter). Only starting from higher-orders EW correction starts to be comparable with QCD corrections. We will focus only on QCD corrections, and for this reason only the sub-process  $\gamma^* + p \rightarrow X$  will be considered.<sup>1</sup>

For DIS the factorization can be formulated through the Operator Product Expansion (see for example chapter 8 of [4]).

The computation proceeds considering the three different partonic inclusive processes, gluon-initiated  $\gamma^* + g \rightarrow X$ , quark-initiated  $\gamma^* + q \rightarrow X$  and antiquark-initiated  $\gamma^* + \bar{q} \rightarrow X$ . The inclusive processes combines all possible processes with different final products than can be built consistently with the Feynman rules. Take for example the quark scattering, the first possible out-

<sup>1</sup>We could also consider the subprocesses  $Z^* + p \rightarrow X$ , and  $W^* + p \rightarrow X$ , but for brevity we will only refer to photon-mediated DIS.

comes are  $\gamma q \rightarrow q$ ,  $\gamma q \rightarrow qg$ ,  $\gamma q \rightarrow qgg$  and  $\gamma q \rightarrow qq\bar{q}$ . At tree level, processes with more emissions carry higher powers of the coupling constant. Therefore the cross section at leading order is trivially

$$d\sigma_{LO} = d\sigma_{2 \rightarrow 1}^{(0)} = \Phi d\Pi_2 |\mathcal{M}_{2 \rightarrow 2}^{(0)}|^2. \quad (1.6.2)$$

At NLO the  $2 \rightarrow 2$  processes starts contributing. The tree diagram  $\mathcal{M}_{2 \rightarrow 2}^{(0)}$  carries a power of  $\sqrt{\alpha_s}$  so that the squared amplitude carries  $\alpha_s$ . From the  $2 \rightarrow 1$  process the sum of QCD 1-loop diagrams  $\mathcal{M}_{2 \rightarrow 1}^{(1)}$  carries a power of  $\alpha_s$ , so that at this order only its interference with the tree diagram must be considered for consistency with the perturbative expansion. The total correction is

$$d\sigma_{NLO} = d\sigma_{2 \rightarrow 1}^{(1)} + d\sigma_{2 \rightarrow 2}^{(0)}, \quad (1.6.3)$$

where

$$d\sigma_{2 \rightarrow 1}^{(1)} = \Phi d\Pi_2 (|\mathcal{M}_{2 \rightarrow 1}^{(0)}|^2 + 2\text{Re}[\mathcal{M}_{2 \rightarrow 1}^{(0)*} \mathcal{M}_{2 \rightarrow 1}^{(1)}]) \quad (1.6.4)$$

$$d\sigma_{2 \rightarrow 2}^{(0)} = \Phi d\Pi_3 |\mathcal{M}_{2 \rightarrow 2}^{(0)}|^2 \quad (1.6.5)$$

and so forth for higher orders. Integrations on four-momenta of emitted parton has been omitted, it must be kept in mind that they are necessary when considering inclusive cross sections.

Starting from NLO, the process with the extra emissions is usually called *real contribution*, while the others *virtual contributions*.

After computing at a given order the partonic processes, they must be summed in the factorization formula. In the case of DIS the first contributions to the hadronic cross section from the gluon initiated process is  $\gamma g \rightarrow q\bar{q}$ .

For later application it is useful to discuss here the relevant variables of the total cross section. Consider first the process  $\gamma^*(q^\mu) + q(p^\mu) \rightarrow q(k^\mu)$ . By integrating on the final four-momentum, the process must depend only on Lorentz scalars built on initial state four-momenta. The possibilities are  $Q^2 = -q^2$  (keep in mind that the photon is an intermediate state, so is off-shell) and  $s = (p + q)^2$ . Applying conservation of energy  $s = k^2 = 0$ , so that the only relevant *hard scale* is  $Q^2$ . For the general process  $\gamma + q \rightarrow X$  the final state is off-shell, so that now  $s$  is not 0 anymore. Expanding  $s = (p + q)^2 = -Q^2 + 2(pq)$  we can see that  $s$  can be exchanged with the dimensionless variable  $x := \frac{Q^2}{2(pq)}$  so that

$$s = \frac{Q^2(1 - x)}{x}, \quad (1.6.6)$$

and the total cross section written with the correct dependencies is  $\sigma(Q^2, x)$ . When  $x \rightarrow 1$  the kinematics reduces to that of the LO, that is to say it is the limit where all the extra emissions have small four-momenta except for a

single final quark that must always be produced in order for color to be conserved. This limit is called *threshold*, *soft* or *high- $x$*  limit, and will be relevant for the next chapters. In the  $x \rightarrow 0$  limit the center of mass energy  $\sqrt{s}$  is big compared to  $\sqrt{Q^2}$ , for this reason it is called *high-energy limit* or simply *small- $x$*  limit.

The variables we have defined have been calculated in the partonic center-of-mass frame of reference. In the following we will always prefer partonic quantities over the hadronic ones, but it must be noted that experimentally one deals with the latter. Differentiating the hadronic momenta with capital letters, define the hadronic counterpart of  $x$   $\tau$ , defined as  $\tau = Q^2/2(PQ)$ . From the parton momentum fraction  $P = \xi p$ , the relation between  $x$  and  $\tau$  is  $x = \tau/\xi$ . For energy conservation  $x \leq 1$ , that implies  $\xi \geq \tau$ . Physically, for fixed  $\tau$ , the minimum parton momentum fraction must be such that the scattering parton is at rest. Clearly, a smaller value is not possible. From these considerations we are able to give a proper expression to the factorization formula

$$\sigma(\tau, Q^2) = \int_{\tau}^1 d\xi f(\xi) \hat{\sigma}\left(x = \frac{\tau}{\xi}, Q^2\right). \quad (1.6.7)$$

### 1.6.2 Drell-Yan production

*Drell-Yan production* (DY) or *Weak-boson production*, is the proton-proton collision producing a vector boson eventually decaying into a lepton pair (for this reason the process is also called *Lepton Pair Production*)

$$\begin{aligned} p_1 + p_2 &\rightarrow \gamma^*(q) + X, \\ p_1 + p_2 &\rightarrow Z^*(q) + X, \\ p_1 + p_2 &\rightarrow W^*(q) + X. \end{aligned} \quad (1.6.8)$$

Schematically DY is represented in figure 1.2.

At LO order the first partonic process contributing to the hadronic cross section is  $q(p_1) + \bar{q}(p_2) \rightarrow \gamma^*(q) + X$ . As done with DIS we study the possible independent variables necessary to describe the total cross section. Generally a process with four particles is described by two independent variable, as was shown before. Now, because both of the final particles are not on shell the variables become 4. A typical choice is the set  $(s, Q^2, p_T^2, y)$ , where  $Q^2 = q^2$  and  $p_T^2$  and  $y$  are respectively the transverse momentum and the longitudinal rapidity of the weak boson in the partonic center-of-mass frame of reference. To get the total cross section both of these two variables are integrated on, leaving only  $s$  and  $Q^2$ .

Analogously to DIS we define the dimensionless variable  $x := \frac{Q^2}{s}$ , which, for energy conservation, ranges between 0 and 1, and we exchange  $s$  with  $x$ ,

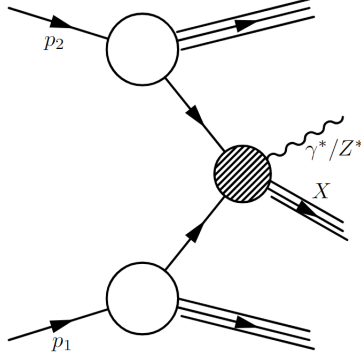


Figure 1.2: Schematic representation of DY. White bubbles represent protons. Perturbative QCD is enclosed in the shaded bubble.

so that the independent set of variables is  $(x, Q^2)$  and we can write  $\sigma(x, Q^2)$ <sup>2</sup>. In the threshold limit  $x \rightarrow 1$ ,  $s = Q^2$ , which again occurs when all the extra QCD emissions vanish. Physically it is the limit where the energy of the colliding particles is strictly sufficient to produce a weak boson with mass  $Q^2$ . Again, when  $x \rightarrow 0$ , the high-energy limit, the energy of the center of mass is far greater than the hard scale of the process.

Defining the hadronic scaling variable  $\tau$ , in terms of the parton momentum fractions  $\xi_1$  and  $\xi_2$ , we have  $x = \frac{\tau}{\xi_1 \xi_2}$ , and the full factorization formula is

$$\sigma(\tau, Q^2) = \int_{\tau}^1 d\xi_1 f_1(\xi_1) \int_{\tau/\xi_1}^1 d\xi_2 f_2(\xi_2) \hat{\sigma}\left(x = \frac{\tau}{\xi_1 \xi_2}, Q^2\right). \quad (1.6.9)$$

## 1.7 Infrared singularities

In this section we introduce infrared singularities, divergences recurring in QCD computations. We differentiate in particular soft and collinear singularities and see, through an example in DIS, how the first cancel in inclusive processes to give finite results and how the second must be included in PDFs' evolution in order to be eliminated. This gives naturally the opportunity to introduce soft scales, large logarithms and their resummation.

Because gluons are massless and because we work in massless quarks approximations, integrals appearing in amplitudes calculations and in the phase space manifest *infrared* (IR) *singularities*. Two different types of IR singularities occur, *soft* and *collinear*<sup>3</sup>. The first arises when a gluon has no energy (*soft emission*) and the second when the gluon (or quark) momentum is parallel to the parton it was emitted from (*collinear emission*). In turn, collinear

<sup>2</sup>Notice that what it is here called  $\sigma$  in literature it is sometimes referred to as  $\frac{d\sigma}{dQ^2}$

<sup>3</sup>In literature IR singularity may be referred only to soft singularities

emissions fall into two categories: initial-state and final-state collinear emissions. They arise when the gluon is emitted from an initial-state or final-state parton respectively.

For *infrared-safe observables*, by definition, soft singularities always cancel summing divergent loop diagrams with corresponding divergent phase space integrals for real emissions diagrams. To understand precisely how the cancellation works we will now see an example taken from DIS. Consider the partonic subprocess  $\gamma^* + q \rightarrow q$ . The LO order diagram is (fig. 1.3)

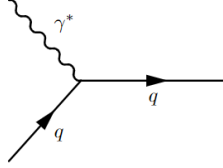


Figure 1.3: LO diagram for  $\gamma^* + q \rightarrow q$

The QCD 1-loop corrections to this process are shown in fig. 1.4

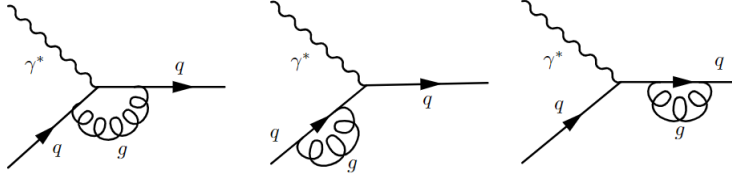


Figure 1.4: QCD loops contributing to  $\gamma^* + q \rightarrow q$  at NLO.

Using Feynman rules one can show explicitly that the loop integrals in the virtual momentum  $l^\mu$  of the last two diagrams, not only display the typical UV singularity for  $l^\mu \rightarrow \infty$ , but are also divergent for  $l^\mu \rightarrow 0$ . This divergence, properly isolated, cancels with the singularity arising in the phase space integral for a soft gluon emission on the same external legs, corresponding to the following two diagrams (fig. 1.5).

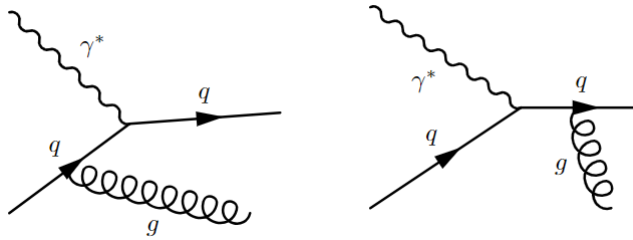


Figure 1.5: *Real emission* diagrams cancelling loop IR divergences.

Therefore when calculating loop corrections to the process  $\gamma^* + q \rightarrow q$  one



should consistently add diagrams with soft gluons emission to cancel soft singularities. The first contributions are called *virtual*, because they come from integrating on the momentum of a virtual gluon, while the second are called *real* contributions, because they come from the phase space integration of a real emitted gluon. Considering inclusive processes these singularities cancel naturally and no diagrams must be added by hand.

In this example we have mentioned diagrams for simplicity, but when considering process with different final states what is actually summed are cross sections. In practice divergent integrals are regularized, for example introducing an IR cutoff  $\Lambda^2$  and equation 1.6.3 becomes

$$d\sigma_{NLO} = \lim_{\Lambda^2 \rightarrow 0} \left[ d\sigma_{2 \rightarrow 2}^{(1)}(\Lambda^2) + d\sigma_{2 \rightarrow 3}^{(0)}(\Lambda^2) \right]. \quad (1.7.1)$$

The single cross sections, containing loops and real emissions respectively, are singular, the sum is finite.

The cancellation of collinear singularities is more delicate. Consider first an initial-state and a final-state emission (fig. 1.6)

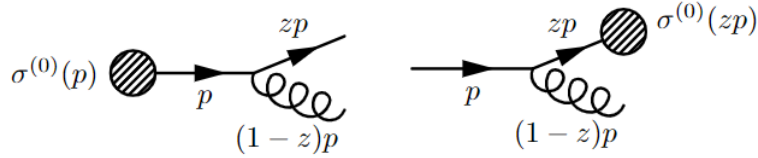


Figure 1.6: Final-state and initial-state IR emissions

In the collinear limit the cross section factorizes into a singular term containing the singularity multiplying the cross section for the process without the emission,  $\sigma^{(0)}$ . While in first case the singular term is multiplied by  $\sigma^{(0)}(p)$ , in the second it is multiplied by  $\sigma^{(0)}(zp)$ . Because the virtual corrections is obviously proportional to  $\sigma^{(0)}(p)$ , the cancellation occurs only in the first case while in the second a residue proportional to  $\sigma^{(0)}(zp) - \sigma^{(0)}(p)$  is left. The leftover terms have universal forms. Considering the case of single emission this is

$$\Gamma^{(res)} = \int_0^{k_{T,max}^2} \frac{dk_T^2}{k_T^2} \int_x^1 dz [\sigma^0(zp) - \sigma^0(p)] \frac{p(z)}{1-z}. \quad (1.7.2)$$

$k_T^2$  is the transverse momentum of the emitted parton,  $x$  is the scaling variable defined in the previous section (clearly  $z$  cannot be 0 or the final state could not be produced). In the soft limit ( $z \rightarrow 1$ ) the divergence  $1/(1-z)$  is cancelled by the numerator, while in the collinear limit ( $k_T^2 \rightarrow 0$ ) the first integral is manifestly logarithmically divergent.

In order to introduce some notation we shortly rewrite the result. Firstly

by introducing a *plus distribution* (see appendix), it becomes

$$\Gamma^{(res)} = \int_0^{k_{T,max}^2} \frac{dk_T^2}{k_T^2} \int_x^1 dz \sigma^0(zp) \left( \frac{p(z)}{1-z} \right)_+. \quad (1.7.3)$$

Then, defining the *splitting function*  $P(z)$ , we are finally left with

$$\Gamma^{(res)} = \int_0^{k_{T,max}^2} \frac{dk_T^2}{k_T^2} \int_x^1 dz \sigma^0(zp) P_{i \rightarrow j}(z). \quad (1.7.4)$$

Splitting functions  $P_{ij}$  are universal factors that appear in soft-collinear singularities. They depend on the partons  $i$  and  $j$  involved in the emission.

Finally we deal with the collinear singularity. Its treatment is similar to the cancellation of UV divergences in renormalization. While in the latter case divergences are absorbed into the coupling constant, defining the running coupling constant, in the case of initial-state collinear singularities the divergence is absorbed into PDFs, which acquire a scale dependence coming from regularization. This is physically motivated because PDFs are measured quantities, and, as such, in QFT they must depend on the energy at which they are measured. This is the effect of the aforementioned virtual corrections to PDFs. In principle also finite terms could be included into PDFs, but by choice we will always adopt the  $\overline{MS}$  scheme, which prescribes the inclusion into bare quantities of only divergent pieces.

To understand in simple terms how this works in practice we calculate the collinear integral introducing an IR cutoff,

$$\Gamma^{(res)} = \ln \frac{k_{T,max}^2}{\Lambda^2} \int_x^1 dz \sigma(zp) P(z). \quad (1.7.5)$$

The improved parton distribution function is defined as the bare parton distribution function,  $f_0(\xi)$ , plus a term cancelling from the partonic cross section the dependence from the regularizing scale  $\Lambda^2$ , such that the remaining function is

$$\Gamma^{(res)} = \ln \frac{k_{T,max}^2}{\mu_F^2} \int_x^1 dz \sigma(zp) P(z), \quad (1.7.6)$$

where PDFs have been defined at the energy  $\mu_F^2$ , called factorization scale. It is similar to the renormalization scale  $\mu_R$  and often they are taken to be the same, defining for short  $\mu = \mu_F = \mu_R$ . Also similarly as what is done in UV renormalization, initial-state collinear poles can be cancelled manually by absorbing them in the PDFs as just described or by adding counterterms to the cross section that cancel the poles as will be done in subsequent chapters.

In the threshold limit, by definition, any extra emitted radiation is soft, so  $k_T^2$  must go to 0, and so must its maximum value  $k_{T,max}^2$ . That means that  $k_{T,max}^2$  is a dimensional quantity which must go to 0 in threshold limit. This

is what defines a *soft scale*. Therefore  $k_{T,max}^2$  can be written as a product of an *hard scale* and a function going to 0 for  $x \rightarrow 1$ , such as  $(1-x)$ . The exact dependence is a function of the structure of the phase space and it will be greatly discussed in the next chapter. For simplicity let us write  $k_{T,max}^2 = Q^2(1-x)$ ,

$$\Gamma^{(res)} = \ln \frac{Q^2(1-x)}{\mu^2} \int_x^1 dz \sigma(zp) P(z). \quad (1.7.7)$$

The result displays two logarithms,  $\ln(1-x)$  and  $\ln Q^2/\mu^2$ . Compare the second with 1.3.5. This tells us that

$$\alpha_s(Q^2) \ln \frac{Q^2}{\mu_F^2} = 1. \quad (1.7.8)$$

This combination occurs also at higher orders as  $\alpha^k \ln^k$ , spoiling the convergence of the perturbative series. This problem can be simply solved by setting  $\mu_F^2 = Q^2$ , that is to say by evaluating the PDF at the energy level of the hard scale.

What looks to be a computational trick can be justified formulating rigorously factorization in DIS. In this context one can see that by imposing invariance of the physical hadronic cross section on the scale  $\mu$ , PDFs satisfy a *renormalization group equation*. The equation links PDFs at different scales. The solution at the desired perturbative order that links  $f(\xi, Q^2)$  and  $f(\xi, \mu^2)$  displays exactly the same analytical structure of the collinear universal factor. Thus all the logarithms  $\ln^k \frac{Q^2}{\mu^2}$  multiplied by splitting functions make up exactly for the factors necessary to evolve the PDFs from  $\mu^2$  to  $Q^2$ . Evolving PDFs absorb the logarithms into the solution of the renormalization group equation. This is the first example of *resummation* we encounter: logarithmic contributions are resummed at all order through renormalization group equations.

The remaining logarithm,  $\ln(1-x)$  is singular for  $x \rightarrow 1$ . Close to the threshold limit it is very large, thus causing again instability in the perturbative series. Resummation of these logarithms, which is the motivation for this thesis, is discussed in the next chapter.

## 1.8 Dimensional regularization

For higher order computations it is convenient to regularize divergent integrals adopting *dimensional regularization*. Not only this regularization scheme preserves Lorentz invariance and gauge symmetry, it also proves to be more efficient in computations, highlighting the structure of singularities appearing in calculations. In this section we give its definition and state how, through a fundamental distributional identity, it gives rise to plus distributions and logarithms

In dimensional regularization every integral computed in 4 dimensions, be it a loop integral or a phase space integral, is computed in  $d = 4 - 2\epsilon$  dimensions, where  $\epsilon$  must be taken negative to have infrared divergences regularized. The limit  $\epsilon \rightarrow 0$  is always implicit and it is crucial that it be taken only at the end of the calculation. We will now see some explicit recurrent computation in order to understand readily the structure of calculations in next chapters.

The phase space measure in  $d$ -dimension [1.1.1](#) is replaced with

$$d\phi_n(\epsilon) = \prod_{i=1}^n \frac{d^{d-1}p_i}{(2\pi)^{d-1}(2p_i^0)} \delta^{(d)}(p_1 + p_2 - \sum p_i). \quad (1.8.1)$$

Divergent integrals become finite but they acquire a term proportional  $1/\epsilon$ .  $\epsilon$ -finite terms comes from the interference of poles with exponentials in  $\epsilon$ . Take for example the regularized collinear-divergent integral

$$\mathcal{I}_{coll} = \int_0^{k_{T,max}^2} \frac{dk_T^2}{(k_T^2)^{1+\epsilon}}, \quad (1.8.2)$$

Using again  $k_{T,max}^2 = Q^2(1-x)$  and solving

$$\Lambda_{soft} = \frac{1}{\epsilon} [Q^2(1-x)]^\epsilon. \quad (1.8.3)$$

We have obtained the predicted exponential. Now by simple Taylor expansion the pole is isolated

$$\frac{1}{\epsilon} [Q^2(1-x)]^\epsilon = \frac{1}{\epsilon} \left[ 1 + \epsilon \ln Q^2(1-x) + \mathcal{O}(\epsilon^2) \right] = \frac{1}{\epsilon} + \ln Q^2(1-x) + \mathcal{O}(\epsilon). \quad (1.8.4)$$

The pole cancels with PDFs renormalization, leaving only finite terms.

In this context plus distributions in any variable, say  $1-z$ , arise from the following distributional identity (proof in the appendix)

$$(1-z)^{-1-\epsilon} = \frac{\delta(1-z)}{\epsilon} + \left( \frac{1}{1-z} \right)_+ + \epsilon \left( \frac{\ln(1-z)}{1-z} \right)_+ + \frac{\epsilon^2}{2!} \left( \frac{\ln^2(1-z)}{(1-z)} \right)_+ + \dots \quad (1.8.5)$$

Depending on the order of the pole multiplying the identity a different finite logarithm survives and the remaining terms are cancelled or disappear with  $\epsilon \rightarrow 0$ .

A final note on dimensional analysis. In dimensional regularization the coupling constant acquires a mass dimension  $d_\alpha = 2\epsilon$ . In order to keep the constant adimensional the renormalization energy scale is introduced so that  $\alpha$  is replaced with the combination  $\alpha\mu^{2\epsilon}$ .

## Chapter 2

# Resummation

2.1	Large logarithms and resummation . . . . .	20
2.2	Threshold resummation of total cross sections . . . . .	22
2.2.1	Phase space analysis . . . . .	23
2.2.2	Mellin space . . . . .	27
2.2.3	Derivation of resummation formulae . . . . .	29
2.3	From total to differential cross sections resummation . . . . .	32

We have seen how IR divergences give rise to logarithmic contributions as residue of their cancellation and how such logarithms spoil the convergence of the perturbative series. In this chapter we discuss the technique of resummation, which solves this problem by resumming the large logarithms at all orders in perturbation theory. First we formally introduce the problem of large logarithms and discuss resummation in full generality. Then, focusing on threshold resummation, we present a derivation of resummation formulae of total cross sections of Drell-Yan production and deep inelastic scattering, following [3]. To accomplish this, we first present a factorization of phase space that will finally establish the form and the origin of threshold logarithms in terms of soft scales. After a small detour on the Mellin transform and its utility, we apply renormalization group equations to get to the final formulae in Mellin space. Finally the formalism is briefly generalized to differential cross sections [6]. A practical application will be given in the next section to resum the rapidity distribution of Higgs boson production.

### 2.1 Large logarithms and resummation

In this section we return to the question of large logarithms introduced in section 1.7, stating formally the problem and how resummation provides a solution. Resummation is a broad topic: we define and differentiate with generality different types of resummation and their features.

Discussing cancellation of IR divergences in section 1.7 we have pointed out the rise of logarithms potentially spoiling the perturbative expansion. We have already identified two types of such logarithms

$$L(Q^2) = \ln \frac{Q^2}{\mu^2}, \quad L(x) = \ln(1 - x). \quad (2.1.1)$$

Both appear at higher powers in the case of a greater number of parton emissions.

The first type of logarithm spoils the perturbative series because, by equation 1.3.5, the combination  $\alpha^k(Q^2) \ln^k \frac{Q^2}{\mu^2}$  is of order 1. It can be dealt by evolving PDFs at the hard scale of the process as briefly exemplified in the previous chapter. The second logarithm belongs to the family of *large* or *enhanced* logarithms, logarithms that are divergent on the boundary of phase space. Close to these regions every term of the power expansion becomes very large thus making the truncation of the perturbative series ineffective.

Resummation makes possible to sum over all such logarithmic contributions appearing at every order. Summing terms at all orders, increases the precision of the prediction. For this reason resummation has an important role in precision phenomenology at particle accelerators, as discussed in the introduction.

Several resummation techniques exist depending on the kinematics of the process considered (i), the observables (ii), whether differential or not, and most importantly in which regions of the phase space are resummed logarithms singular in (iii).

Consider for example a process with a relevant final set of products and take its cross section differential respectively to their combined transverse momentum,  $\frac{d\sigma}{dp_T^2}$ . A set of independent variables is made up by the hard scale  $Q^2$ , the threshold variable  $x$  and the transverse momentum  $p_T^2$ . We differentiate three main types of resummation. *Threshold, soft* or *high- $x$*  resummation, referring to logarithms singular in the threshold limit  $x \rightarrow 1$ , *high-energy* or *small- $x$*  resummation, that resums logarithms enhanced in the high-energy limit  $x \rightarrow 0$ , and finally *transverse momentum* or *small- $p_T$*  resummation with logarithms singular when the transverse momentum is small. These three regions are depicted in figure 2.1.

Resummation of different kinematical region is usually performed separately, but several successful attempts have been made for joint resummation. In this thesis we will only focus on threshold resummation.

When considering any resummation formula another point must be considered. As we have mentioned, at higher-orders logarithms with higher powers appear, but the result generally also displays logarithms with smaller powers, i.e. subleading logarithms. The first resummation formulae that had been derived were able to resum only leading logarithms (LL), that is to say loga-

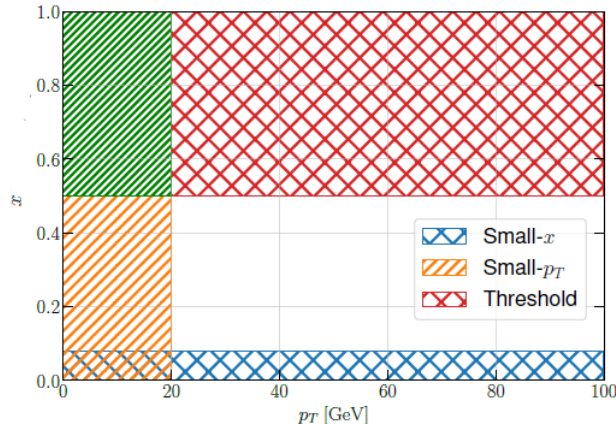


Figure 2.1: Phase space diagram for the transverse momentum distribution of a production process.  $x$  is the threshold variable. The three kinematic limits relevant for resummation are highlighted: threshold (in red), transverse momentum (in orange) and high-energy (in blue). Figure adapted from [7].

rithms that carry the highest power at any order. The resummation formulae we derive include all logarithmic contributions, both leading and subleading.

## 2.2 Threshold resummation of total cross sections

In this section threshold resummation is formulated for total cross sections for partonic processes. The result will be generalized to differential cross sections.

Consider the total cross section of a process involving two particles in the initial state. Let the total cross section be specified by a single hard scale  $Q^2$  and by the threshold variable  $x$ . Kinematically such processes belong to two archetypes:

- Deep inelastic scattering (DIS):  $\gamma^*(q) + \mathcal{P}(p_1) \rightarrow \mathcal{P}(p_2) + X$
- Drell-Yan (DY):  $\mathcal{P}(p_1) + \mathcal{P}(p_2) \rightarrow \gamma^*(q) + X,$

where  $\mathcal{P}$  is a parton and  $X$  is the collection of inclusive strongly interacting radiation. The main difference between the two processes is that the hard scale  $Q^2$  is the virtuality of an initial-state particle in the case of DIS and of the final product in the case of Drell-Yan production. In the DY family falls also *Higgs production*, where  $\gamma^*$  is replaced by an Higgs boson and the hard scale is its mass  $m_H^2$ . We have seen in the previous chapter the exact definition of the hard scale and of the threshold variable for each process.

Threshold resummation refers to the resummation of large logarithms singular in the limit  $x \rightarrow 1$ . Different formalisms exist to perform resummation.

One of the main approaches is based on factorization of the amplitudes and of the phase space in a product of singular terms which explicitly exponentiates in the threshold limit. We follow a different approach based on the application of the renormalization group equation presented in [3]. Particularly, the derivation proceeds in two stages:

1. Determination of the origin and of the exact dependence of large logarithms on the threshold variable by identification of the soft scale arising from the phase space;
2. Use of renormalization group equations to determine the resummation formulae.

### 2.2.1 Phase space analysis

In this section we will show how soft logarithms arise from  $d$ -dimensional phase space calculation for DIS and DY total cross sections. We will consider in detail only the phase space for Drell-Yan production, the case of DIS is analogous. Further details for any passage may be found in [3].

Take a DY process with two incoming partons with momenta  $p$  and  $p'$ . Let  $Q$  be the four-momentum of the weak boson and  $k_1, \dots, k_n$  the four-momenta of the extra emissions. The regularized phase space measure is

$$d\phi_{n+1}(p + p'; Q, k_1, \dots, k_n) = \frac{d^{d-1}Q}{(2\pi)^{d-1}2Q^0} \frac{d^{d-1}k_1}{(2\pi)^{d-1}2k_1^0} \cdots \frac{d^{d-1}k_n}{(2\pi)^{d-1}2k_n^0} (2\pi)^d \delta^{(d)}(p_1 + p_2 - Q - k_1 - \cdots - k_n). \quad (2.2.1)$$

To get the total cross section all components of every momenta must be integrated. At the end, as discussed in the previous chapter, the remaining variables must be  $x$  and  $Q^2$ . They can be made explicit without performing any explicit integration rewriting all integration variables in terms of dimensionless quantities. To accomplish this the phase space is factorized into 2-body phase spaces applying the following identity recursively

$$d\phi_n(P; k_1, \dots, k_n) = \int_{M_{n-1,inf}^2}^{M_{n-1,sup}^2} \frac{dM_{n-1}^2}{(2\pi)} d\phi_2(P; P_{n-1}, k_n) d\phi_{n-1}(P_{n-1}; k_1, \dots, k_{n-1}). \quad (2.2.2)$$

In practice an intermediate momentum  $P_{n-1} = k_1 + \cdots + k_{n-1}$  with virtuality  $M_{n-1}^2$  has been introduced to separate the  $n$ -th emission from others. The extrema of the virtuality are

$$(m_1 + \cdots + m_{n-1})^2 \leq M_{n-1}^2 \leq (\sqrt{P^2} - m_n)^2.$$



Applying recursively on [2.2.1](#)

$$d\phi_{n+1}(p+p'; Q, k_1, \dots, k_n) = \int_{Q^2}^s \frac{M_n^2}{2\pi} d\phi_2(p+p'; k_n, P_n) \int_{Q^2}^{M_n^2} \frac{M_{n-1}^2}{2\pi} d\phi_2(p+p'; k_{n-1}, P_{n-1}) \\ \dots \int_{Q^2}^{M_3^2} \frac{M_2^2}{2\pi} d\phi_2(k_1; k_2, P_2) d\phi_2(P_2; k_1, Q).$$

Because each two-body phase space is Lorentz-invariant, they can be evaluated using difference frame of references. Choosing the center-of-mass frame the two-body phase spaces are

$$d\phi_2(P_{i+1}; P_i, k_i) = N(\epsilon) M_{i+1}^{-2\epsilon} \left(1 - \frac{M_i^2}{M_{i+1}^2}\right)^{1-2\epsilon} d\Omega_i. \quad (2.2.3)$$

Where  $N(\epsilon) = \frac{1}{2(4\pi)^{2-2\epsilon}}$ . Now we exchange the dimensional integration variables with the adimensional fractions

$$z_i = \frac{M_i^2 - Q^2}{M_{i+1}^2 - Q^2} \quad (2.2.4)$$

so that  $M_i^2 - Q^2 = (s - Q^2) z_n \dots z_i$ , where  $i = 2, \dots, n$ ,  $P_{n+1} := p + p'$  and  $P_1 := Q$ . Combining all together

$$d\phi_{n+1}(p+p'; Q, k_1, \dots, k_n) = 2\pi \left[ \frac{N(\epsilon)}{2\pi} \right]^n s^{-n(1-\epsilon)} (s - Q^2)^{2n-1-2n\epsilon} d\Omega_n \dots d\Omega_1 \\ \int_0^1 dz_n z_n^{n-2+(n-1)(1-2\epsilon)} (1 - z_n)^{1-2\epsilon} \dots \int_0^1 dz_2 z_2^{1-2\epsilon} (1 - z_2)^{1-2\epsilon}.$$

The only kinematic variables that remain after integration are  $s$  and  $Q^2$ . Now focus on the  $\epsilon$  exponentials in these variables. We have seen in [section 1.8](#) that these give rise to logarithms. Exchanging  $s$  with  $x$  these exponentials become

$$s^{-n(1-\epsilon)} (s - Q^2)^{2n-1-2n\epsilon} = \frac{1}{s - Q^2} \left[ \frac{(s - Q^2)^2}{s} \right]^{n-n\epsilon} = x^{1-2n+2n\epsilon} \frac{[Q^2(1-x)^2]^{n-n\epsilon}}{Q^2(1-x)}. \quad (2.2.5)$$

We have finally isolated the soft scale we have mentioned studying collinear singularities in the IR cutoff and dimensional regularization (eqs. [1.7.6](#) and [1.8.2](#)). We see that, in the case of DY total cross section, the soft scale is  $Q^2(1-x)^2$ . Physically it is contained in the extrema of integration of collinear and soft emissions, and for this reason we managed to extract it by writing all integrals in terms of adimensional variables on a constant range.

To get the correct exponent, this factor must be combined with dimensional factors coming from the integration of the squared amplitude

$|\mathcal{M}_{n+1}(Q^2, s; z_2, \dots, z_n; \Omega_1, \dots, \Omega_n)|^2$ . Factors of  $[Q^2(1-x)^2]^{-n}$  must come out from tree diagrams contributing to soft singularities, while loop diagrams may also carry a  $[Q^2(1-x^2)]^{-\epsilon}$  factor for each loop integration computed in dimensional regularization<sup>1</sup>. This finally leaves a factor of

$$\Lambda_{soft} = (Q^2)^{-1-k\epsilon}[(1-x)]^{-1-2k\epsilon}, \quad (2.2.6)$$

where  $k$  ranges from 1 to  $n$ . We have thus found the form of the distributional identity 1.8.5. Plus distributions arise through interference of  $\epsilon$  factors in the identity with  $\epsilon$  poles coming from divergent integrals. Therefore to understand the final structure of logarithms the expected order of poles must be determined. Considering tree diagrams, poles arise only from phase space integrals. Clearly, each  $z_k$  and  $\Omega_k$  integration produces at most<sup>2</sup> one pole, so that counting the number of integrals we find that maximum pole order is  $\epsilon^{2n-1}$ . IR divergent loops must carry two more poles so that they can be cancelled by the two poles arising from an extra soft emission.

Consider now the bare partonic cross section and its perturbative coefficients

$$C^{(0)}(x, Q^2, \alpha_0, \epsilon) = \sum_{n=0}^{\infty} \alpha_0^n C_n^{(0)}(x, Q^2, \epsilon). \quad (2.2.7)$$

The coefficient  $C_n^{(0)}$  is found by summing squared tree amplitudes with  $n$  emission, times the corresponding phase space, with squared 1-loop amplitudes with  $n-1$  emissions times its phase space and so on, up to squared amplitudes with purely virtual diagrams. From the first contribution (purely real) we have just derived the factor  $[Q^2(1-x^2)]^{-1-n\epsilon}$  from the phase space. Because there are no loops no additional corrections must be made. Consider the next contribution, with  $n-1$  emissions and one loop. Applying the same arguments, phase space gives  $[Q^2(1-x)^2]^{-1-(n-1)\epsilon}$  with at most a  $\epsilon^{2(n-1)-1}$  pole from phase space and an  $\epsilon^2$  pole from the loop diagram. Adding the optional loop factor the possible results are  $[Q^2(1-x)^2]^{-1-(n-1)\epsilon}$  and  $[Q^2(1-x)^2]^{-1-n\epsilon}$ , and so on for other contributions. Finally the purely virtual contribution has simpler phase space proportional to  $\delta(1-x)$ , but the  $n$  loops still contribute with up an  $\epsilon^{2n}$  pole. Notice that the order of poles is consistent with IR divergences cancellation.

Combining all these considerations we obtain the final structure of soft logs

---

<sup>1</sup>Of course not all diagrams contribute the same, real emissions from internal line for example do not carry IR singularities and so do not some loop integrals, such as the first in figure 1.4

<sup>2</sup>See previous footnote.

for the  $C_n^{(0)}$  coefficient

$$C_n^{(0)}(x, Q^2, \epsilon) = (Q^2)^{-n\epsilon} \left[ C_0(\epsilon) \delta(1-x) + \sum_{k=1}^n C_k(\epsilon) (1-x)^{-1-2k\epsilon} \right] + \mathcal{O}[(1-x)^0] \quad (2.2.8)$$

where  $\mathcal{O}[(1-x)^0]$  includes terms that are not singular for  $x \rightarrow 1$  but may be singular for  $\epsilon \rightarrow 0$ , such as purely collinear singularities cancelled by PDFs renormalization or UV singularities. The coefficients  $C_k(\epsilon)$  as argued must contain at most a pole of order  $2n-1$  for  $k > 0$ , while  $C_0(\epsilon)$  must contain a pole of order  $2n$ . The dependency on  $Q^2$  is fixed by dimensional analysis following from the mass dimension of  $\alpha_s$  in dimensional regularization discussed in section 1.8.

Finally, using equation 1.8.5, we can apply this result to see in practice the rise of soft logs. Consider for example the case  $n = 2$ . The final result is the sum on two real emission contributions with no loops (2R), 1 real emissions with 1 loop (1R1V) and no real emissions with two loops (2V),

$$C_n^{(0)}(x, Q^2, \epsilon) = (Q^2)^{-2\epsilon} \left[ C_0(\epsilon) \delta(1-x) + C_1(\epsilon) (1-x)^{-1-2\epsilon} + C_2(\epsilon) (1-x)^{-1-4\epsilon} \right] + \mathcal{O}[(1-x)^0]. \quad (2.2.9)$$

The last factor comes from the sum of 2R contributions with the 1R1V contributions having the loop integral IR divergent. The second comes from the 1R1V contribution with no IR divergent loop integrals and the first from the 2V contributions. The second and the third coefficients, containing a  $\epsilon^3$  pole, combined with the distributional identity give the finite logarithm  $\left( \frac{\ln^3(1-x)}{1-x} \right)_+$ , all remaining terms must cancel. Because we expect coefficients  $C_k(\epsilon)$  to contain also poles of smaller order, logarithms of the same type but with smaller powers must also originate. We have thus learnt that at a given order  $\alpha_s^n$  we have the following sequence of logarithms

$$\mathcal{D}_n(x) := \alpha_s^n \left( \frac{\ln^k(1-x)}{1-x} \right)_+ \quad 0 \leq k \leq 2n-1. \quad (2.2.10)$$

We define Leading Logarithms (LL) those of the form  $\alpha_s^k \mathcal{D}_{2k-1}(z)$ , Next-to-Leading logarithms (NLL)  $\alpha_s^k \mathcal{D}_{2k-2}(z)$  and so on. We will soon see why also  $k = 0$  terms are being included as logarithms. Notice that our preliminary analysis of large logarithms in section 1.7 did not predicted neither the  $(1-x)$  denominator nor the plus distribution. The distribution in particular regularizes the integral on the parton momentum fraction  $\xi$  which is contained implicitly in  $x$ .

The analysis that has been done for Drell-Yan can be repeated for DIS,

Process	hard scale	threshold variable	soft scale
DY: $\mathcal{P}(p) + \mathcal{P}(p') \rightarrow \gamma^*(q) + X$	final state	$x = Q^2/s$	$(s - Q^2)^2/Q^2 \rightarrow Q^2(1 - x)^2$
DIS $\gamma^*(q) + \mathcal{P}(p) \rightarrow \mathcal{P}(p') + X$	initial state	$x = Q^2/2(pq)$	$s \rightarrow Q^2(1 - x)$

Table 2.1: DY and DIS phase spaces

leading to the following result

$$d\phi_{n+1}(p + q; k_1, \dots, k_n, p') = 2\pi \left[ \frac{N(\epsilon)}{2\pi} \right]^n s^{n-1-n\epsilon} d\Omega_n \dots d\Omega_1 \quad (2.2.11)$$

$$\int_0^1 dz_n z_n^{n-2+(n-1)\epsilon} (1 - z_n)^{1-2\epsilon} \dots \int_0^1 dz_2 z_2^{1-2\epsilon} (1 - z_2)^{1-2\epsilon}.$$

$q$  is the four-momentum of the incoming virtual photon and  $p'$  is the momentum of the emitted parton at LO. Exchanging  $s$  with  $x$  we get the prefactor  $[Q^2(1 - x)]^{n-1-n\epsilon}$ , so that the soft scale in this case is simply  $Q^2(1 - x)$ . Thus, repeating the same considerations made for DY, the  $\mathcal{O}(\alpha_s^n)$  coefficient is

$$C_n^{(0)}(x, Q^2, \epsilon) = (Q^2)^{-n\epsilon} \left[ C_0(\epsilon) \delta(1 - x) + \sum_{k=1}^n C_k(\epsilon) (1 - x)^{-1-k\epsilon} \right] + \mathcal{O}[(1 - x)^0]. \quad (2.2.12)$$

Let us sum up what we have understood by now (table 2.1). Drell-Yan and deep inelastic scattering phase spaces for  $n$  emissions can be written making explicit the dependence on the hard scale and on the threshold variable by rewriting all the integrals in terms of adimensional integration variables. Doing this we found the soft scales  $Q^2(1 - x)^a$ , where  $a = 1$  for DIS and  $a = 2$  for DY. Physically such factors come from the extrema of integration on four-momenta of extra emissions. Counting the number of poles coming from soft and collinear integrals we found using identity 1.8.5 that imperfect cancellation of real and virtual contribution give rise at any order new powers of logarithms in the threshold variables. This led us to define leading logarithm and next <sup>$k$</sup> -to-leading logarithms.

### 2.2.2 Mellin space

Before getting to the derivation of resummation formulae, in this section we introduce the necessary *Mellin transform*, detailed in the appendix. We first see its definition and how plus distributions in real space become simple logarithms in Mellin space. Next, we see how under a Mellin transformation factorization equations become products and, finally, how the results of the previous section can be rewritten in Mellin space.

The Mellin transform exchanges the threshold variable  $x$  with a complex

variable  $N$  such that, given a function  $f(x)$ , its Mellin transform is

$$\mathcal{M}[f](N) := \int_0^1 dx x^{N-1} f(x). \quad (2.2.13)$$

First notice that in the limit  $|N| \rightarrow \infty$  the only finite contribution to the integral is given by  $f(1)$  so that the two limits  $x \rightarrow 1$ , that is the threshold limit, and  $|N| \rightarrow \infty$  yield the same result.

We can see this immediately by Mellin transforming the plus distributions  $\mathcal{D}_p(x)$  (see [3])

$$\int_0^1 dx x^{N-1} \left( \frac{\ln^p(1-x)}{1-x} \right)_+ = \frac{1}{p+1} \sum_{k=0}^{p+1} \Gamma^{(k)}(1) \left( \ln \frac{1}{N} \right)^{p+1-k} + \mathcal{O}\left(\frac{1}{N}\right). \quad (2.2.14)$$

The  $\ln^p(1-x)$  plus distributions are transformed into  $\ln^{p+1} N$  plus subleading logs and  $N \rightarrow \infty$  suppressed terms. Employing this, 2.2.10 becomes

$$\mathcal{D}_n(N) = \ln^k N \quad 1 \leq k \leq 2n. \quad (2.2.15)$$

Secondly, under a Mellin transformation factorization formulae becomes simple products. Starting from DIS, the factorization formula 1.6.7 has exactly the form of a Mellin convolution, so that under Mellin transform we have

$$\sigma(\tau, Q^2) = (f \otimes \hat{\sigma})(\tau, Q^2) \quad \rightarrow \quad \sigma(N, Q^2) = f(N) \hat{\sigma}(N, Q^2). \quad (2.2.16)$$

This can be generalized to processes with two incoming partons such as DY. Starting from the factorization formula in  $x$ -space (also called *real space*), equation 1.6.9, defining  $\xi = \xi_1 \xi_2$  and the *parton density luminosity*

$$\mathcal{L}(\xi) = \int d\xi_1 f_1(\xi_1) f_2(\xi/\xi_1) = (f_1 \otimes f_2)(\xi), \quad (2.2.17)$$

The equation

$$\sigma(\tau, Q^2) = (\mathcal{L} \otimes \hat{\sigma})(\tau, Q^2) \quad \rightarrow \quad \sigma(N, Q^2) = \mathcal{L}(N) \hat{\sigma}(N, Q^2). \quad (2.2.18)$$

Finally, we notice that in Mellin space equations 2.2.8 and 2.2.12 become

$$C_n^0(N, Q^2, \epsilon) = \sum_{k=0}^n C_k(\epsilon) (Q^2)^{-(n-k)\epsilon} \left( \frac{Q^2}{N^a} \right)^{-k\epsilon} + \mathcal{O}\left(\frac{1}{N}\right), \quad (2.2.19)$$

where now the coefficients  $C_k(\epsilon)$  have been redefined so that each of them contains an  $\epsilon$  pole of order  $2n$ . Notice that the soft scale  $Q^2(1-x)^a$  has been mapped onto  $Q^2/N^a$ .

### 2.2.3 Derivation of resummation formulae

Finally, in this section we briefly derive the threshold resummation formulae for DY and DIS. Starting from the factorization formula in Mellin space we apply renormalization group equations to the partonic cross section to get the resummed result in terms of the unknown physical anomalous dimension of the hadronic cross section. By assuming a particular factorization of the partonic cross section, we are finally able to write the anomalous dimension in terms of the hard and soft scales of the process and in terms of a set of coefficients that can be determined by comparing the resummation formula with fixed order results. This section will not be detailed, for technicalities always refer to [3].

The derivation employs renormalization group techniques, that is to say the study of the dependence, called *anomalous dimensions*, of different quantities on the renormalization scales  $\mu^2 = \mu_R^2 = \mu_F^2$ . First start from the factorization formula in Mellin space with now dependence on  $\mu$  explicit

$$\sigma(N, Q^2, \alpha_s(\mu^2)) = \mathcal{L}(N, \mu^2) C(N, Q^2/\mu^2, \alpha_s(\mu^2)). \quad (2.2.20)$$

Inside  $\mathcal{L}$  has been included the LO result so that the perturbative expansion of the partonic cross section, renamed  $C$ , starts by a 1. In this context  $C$  is also called *coefficient function*. The hadronic cross section does not depend on  $\mu^2$  because it is the actual physical observable, so it cannot depend on an arbitrary scale, only on the hard scale. The dependence on the hard scale is called *physical anomalous dimension* and it is defined by

$$\gamma(N, Q^2/\mu^2, \alpha_s(\mu^2)) = \frac{d}{d \ln Q^2} \ln \sigma(N, Q^2). \quad (2.2.21)$$

This of course applies also to the partonic cross section because the parton luminosity does not depend on the hard scale

$$\gamma(N, Q^2/\mu^2, \alpha_s(\mu^2)) = \frac{d}{d \ln Q^2} \ln C(N, Q^2/\mu^2, \alpha_s(\mu^2)). \quad (2.2.22)$$

Interpreting the definition as a differential equation we obtain

$$C\left(N, \frac{Q^2}{\mu^2}, \alpha_s(\mu^2)\right) = C(N, 1, \alpha_s(Q^2)) \exp\left\{ \int_{\mu^2}^{Q^2} \frac{dk^2}{k^2} \gamma(N, \alpha_s(k^2)) \right\}. \quad (2.2.23)$$

This equation is analogous to PDFs evolution equations mentioned in section 1.7 that made resumming of  $\ln \frac{Q^2}{\mu^2}$  logarithms possible. Also in this case the exponential performs the task of resumming logarithms, that is to say by expanding it at the desired order in  $\alpha$  the resummed N<sup>k</sup>LL are retrieved. However in this form it is not very meaningful because it is not easy to say what exactly is  $\gamma$  in such full generality, while, in the case of PDFs, anoma-

lous dimensions can be shown to be the Mellin transform of splitting functions. Scope of the next steps will be finding an expression for  $\gamma$  which can be determined order-by-order comparing the resummation formula with fixed order results. Firstly we can write  $\gamma$  also in terms of the bare partonic cross section. Suppose WLOG  $C$  is multiplicatively renormalized in dimensional regularization

$$C(N, Q^2/\mu^2, \alpha_s(\mu^2)) = Z(N, \alpha_s(\mu^2), \epsilon) C^{(0)}(N, Q^2, \alpha_s^0, \epsilon), \quad (2.2.24)$$

where  $\alpha_s^0$  is the bare coupling constant and  $C^{(0)}$  the bare partonic cross section. Then,  $\gamma$  is

$$\gamma(N, Q^2/\mu^2, \alpha_s(\mu^2)) = -\epsilon \alpha_s^0 \frac{d}{d \ln \alpha_s^0} \ln C^{(0)}(N, Q^2, \alpha_s^0, \epsilon), \quad (2.2.25)$$

where we have used that  $Z$  does not depend on  $Q^2$ , since it is a process-independent function, and to change the variable of the derivative we have used the fact that for dimensional reasons we have already mentioned dependence on  $\alpha_s^0$  and  $Q^2$  must be through the combination  $Q^{-2\epsilon} \alpha_s^0$ .

Next we will assume that the bare partonic cross section can be factorized in Mellin space into the product of a bare coefficient function  $C^{(0,c)}$  including all the purely virtual contributions to the process, i.e having Born kinematics, and a bare coefficient function  $C^{(0,l)}$  including all contributions with real emissions. Using finally the result of the lengthy phase space analysis this translates to

$$C^{(0)}(N, Q^2, \alpha_s^0, \epsilon) = C^{(0,c)}(Q^2, \alpha_0, \epsilon) C^{(0,l)}(Q^2/N^a, \alpha_0, \epsilon); \quad (2.2.26)$$

$$C^{(0,c)}(Q^2, \alpha_0, \epsilon) = \sum_n C_n^{(0,c)}(\epsilon) Q^{-2n\epsilon} \alpha_0^n; \quad (2.2.27)$$

$$C^{(0,l)}(Q^2/N^a, \alpha_0, \epsilon) = \sum_n C_n^{(0,l)}(\epsilon) \left( \frac{Q^2}{N^a} \right)^{-n\epsilon}. \quad (2.2.28)$$

Applying the factorization to 2.2.25 we get straightforwardly

$$\gamma(N, Q^2/\mu^2, \alpha_s(\mu^2)) = \gamma^c(Q^2/\mu^2, \alpha_s(\mu^2), \epsilon) + \gamma^{(l)} \left( \frac{Q^2/N^a}{\mu^2}, \alpha_s(\mu^2), \epsilon \right) \quad (2.2.29)$$

where

$$\gamma^{(c)}(Q^2/\mu^2, \alpha_s(\mu^2)) = \epsilon \alpha_s^0 \frac{d}{d \ln \alpha_s^0} \ln C^{(0,c)}(Q^2, \alpha_0, \epsilon) \quad (2.2.30)$$

$$\gamma^{(l)} \left( \frac{Q^2/N^a}{\mu^2}, \alpha_s(\mu^2), \epsilon \right) = \epsilon \alpha_s^0 \frac{d}{d \ln \alpha_s^0} \ln C^{(0,l)}(Q^2/N^a, \alpha_0, \epsilon). \quad (2.2.31)$$

Recalling the definition of the physical anomalous dimension we infer that it

cannot depend on  $\mu$ , therefore by deriving with respect to  $\mu^2$  both sides of 2.2.29 we get two renormalization group equations for  $\gamma^{(l)}$  and  $\gamma^{(c)}$

$$-\frac{d}{d \ln \mu^2} \gamma^{(l)} \left( \frac{Q^2/N^a}{\mu^2}, \alpha_s(\mu^2), \epsilon \right) = \frac{d}{d \ln \mu^2} \gamma^{(c)}(Q^2/\mu^2, \alpha_s(\mu^2)) = \bar{g}(\alpha_s(\mu^2)) \quad (2.2.32)$$

where

$$\bar{g}(\alpha_s(\mu^2)) = \sum_n \bar{g}_n \alpha_s^n(\mu^2). \quad (2.2.33)$$

Summing both solutions we finally find an expression for  $\gamma$  that depends perturbatively only on a set of coefficients

$$\gamma(N, \alpha_s(Q^2)) = \bar{g}_0(\alpha_s(Q^2)) + \int_{Q^2}^{Q^2/N^a} \frac{d\lambda^2}{\lambda^2} \bar{g}(\alpha_s(\mu^2)), \quad (2.2.34)$$

where  $\bar{g}_0(\alpha)$  can also be expressed a series in  $\alpha$ . Substituting in 2.2.23 we find

$$C \left( N, \frac{Q^2}{\mu^2} \right) = C^{(c)} \left( \frac{Q^2}{\mu^2}, \alpha_s(Q^2) \right) \exp \left\{ \int_{\mu^2}^{Q^2} \frac{dk^2}{k^2} \int_{k^2}^{k^2/N^a} \frac{d\lambda^2}{\lambda^2} \hat{g}(\alpha_s(\lambda^2)) \right\}. \quad (2.2.35)$$

Two equivalent formulae are

$$C \left( N, \frac{Q^2}{\mu^2} \right) = C^{(c)} \left( \frac{Q^2}{\mu^2}, \alpha_s(Q^2) \right) \exp \left\{ \int_1^{N^a} \frac{dn}{n} \int_{n\mu^2}^{Q^2} \frac{dk^2}{k^2} \hat{g}(\alpha_s(k^2/n)) \right\} \quad (2.2.36)$$

$$C \left( N, \frac{Q^2}{\mu^2} \right) = C^{(c)} \left( \frac{Q^2}{\mu^2}, \alpha_s(Q^2) \right) \exp \left\{ a \int_0^1 dz \frac{z^{N-1} - 1}{1-z} \int_{\mu^2}^{Q^2(1-z)^a} \frac{dk^2}{k^2} \hat{g}(\alpha_s(k^2)) \right\} \quad (2.2.37)$$

Resummation for DY and DIS total cross sections is thus settled. Multiplying the *hard* coefficient function  $C^{(c)}$  by the resumming exponential the full coefficient function in the threshold limit is obtained. All threshold enhanced logarithms, leading and subleading, are resummed in the exponential and can be retrieved by expanding in  $\alpha$  both the hard coefficient function  $C^{(c)}$  and the function  $g$ . Expanding each of these consistently at any order one can find the structure of leading logarithms, according to table 2.2.

The coefficients  $g_i$  can be determined by comparison with fixed-order results. The higher the order the more coefficients can be found. Substituting back in the exponential, resummation is accomplished up to the logarithmic accuracy determined by the known coefficients.

To get resummation in real space it is necessary to compute the inverse Mellin transform of the resummation formulae. This integral however is divergent and extra theoretical effort is needed to deal with this problem, however



$N^k\text{LL}$	$g_i$ up to	$C^{(c)}$ up to	Accuracy ( $\alpha^n \ln^k N$ )
LL	$i = 1$	$\alpha_s^0$	$k = 2n$
NLL	$i = 2$	$\alpha_s^1$	$2n - 2 \leq k \leq 2n$
NNLL	$i = 3$	$\alpha_s^2$	$2n - 4 \leq k \leq 2n$

Table 2.2: Expansions necessary to get the desired logarithmic accuracy.

this is out of the scope of this thesis.

Remember that equations 2.2.36 give the resummed partonic cross section in the threshold limit. The complete  $N^k\text{LO}+N^j\text{LL}$  correction is found by adding to the resummed cross section the fixed order without large logarithms that are already included in the resumming exponential.

## 2.3 From total to differential cross sections resummation

In this section we deal in generality with the problem of resumming differential cross sections. We discuss the crucial differences with the total cross sections and explain how they can be resummed by generalizing the procedure of the previous section.

We have so far only considered total cross sections. Resumming differential cross sections is more delicate because they have a more complex phase space, which we have seen playing a fundamental role in resummation. The reason for this is manifest: differential cross sections depend on one more variable so in principle there are more hard and soft scales, that is to say possibly more logarithms to resum.

The two steps outlined in the previous sections must be generalized. Identification of soft scales from phase space analysis must be done case-by-case, we will see an example in the next chapter where the results for DY and DIS cross sections will be cleverly recycled. Derivation of resummation formulae can be repeated identically by generalizing the soft and hard decomposition (eq. 2.2.26). Take for example a process with two soft scales  $\Lambda_1^2(Q_1^2, N)$  and  $\Lambda_2^2(Q_2^2, N)$ , equation 2.2.26 becomes

$$C^0(N, Q_1^2, Q_2^2, \alpha_0, \epsilon) = C^{(0,c)}(Q_1^2, Q_2^2, \alpha_0, \epsilon) C^{(0,l_1)}(\Lambda_1^2(Q_1^2, N), \alpha_0, \epsilon) C^{(0,l_2)}(\Lambda_2^2(Q_2^2, N), \alpha_0, \epsilon), \quad (2.3.1)$$

so that the final resummation formulae are

$$C(N, Q_1^2/\mu^2, Q_2^2/\mu^2, \alpha_s(\mu^2)) = C^{(c)}(Q^2/\mu^2, \alpha_s(Q)^2) \exp \left\{ \int_1^{N^a} \frac{dn}{n} \int_{n\mu^2}^{Q_1^2} \frac{dk^2}{k^2} \bar{g}_1(\alpha_s k_1^2) + \int_1^{N^b} \frac{dn}{n} \int_{n\mu^2}^{Q_2^2} \frac{dk^2}{k^2} \bar{g}_2(\alpha_s(k^2)) \right\}, \quad (2.3.2)$$

and

$$C(N, Q_1^2/\mu^2, Q_2^2/\mu^2, \alpha_s(\mu^2)) = C^{(c)}(Q^2/\mu^2, \alpha_s(Q)^2) \exp \left\{ \int_0^1 dz \frac{z^{N-1} - 1}{1 - z} \left( \int_{\mu^2}^{\Lambda_1(Q^2, z)} \frac{dk^2}{k^2} \bar{g}_1(\alpha_s k_1^2) + \int_{\mu^2}^{\Lambda_2(Q_2^2, z)} \frac{dk_2^2}{k_2^2} \bar{g}_2(\alpha_s(k^2)) \right) \right\}. \quad (2.3.3)$$

Consider for example the resummation of transverse momentum distribution of a DY-like process, shown in [6]. The two soft scales are  $\Lambda_1(Q_1^2, x) = Q^2(1 - x)^2$  and  $\Lambda_2(Q_2^2, x) = Q p_T(1 - x)$ , that in Mellin space become respectively  $Q^2/N^2$  and  $Q p_T/N$ . The two equivalent resummation formulae therefore are

$$C(N, Q_1^2/\mu^2, Q_2^2/\mu^2, \alpha_s(\mu^2)) = C^{(c)}(Q^2/\mu^2, \alpha_s(Q)^2) \exp \left\{ \int_1^{N^2} \frac{dn}{n} \int_{n\mu^2}^{Q^2} \frac{dk^2}{k^2} \bar{g}_1(\alpha_s k_1^2) + \int_1^N \frac{dn}{n} \int_{n\mu^2}^{Q p_T} \frac{dk_2^2}{k_2^2} \bar{g}_2(\alpha_s(k^2)) \right\}, \quad (2.3.4)$$

and

$$C(N, Q_1^2/\mu^2, Q_2^2/\mu^2, \alpha_s(\mu^2)) = C^{(c)}(Q^2/\mu^2, \alpha_s(Q)^2) \exp \left\{ \int_0^1 dz \frac{z^{N-1} - 1}{1 - z} \left( \int_{\mu^2}^{Q^2(1-z)^2} \frac{dk^2}{k^2} \bar{g}_1(\alpha_s k_1^2) + \int_{\mu^2}^{Q p_T(1-z)} \frac{dk_2^2}{k_2^2} \bar{g}_2(\alpha_s(k^2)) \right) \right\}. \quad (2.3.5)$$

We have thus established how to perform resummation of differential cross sections generalizing the procedure presented for total cross sections. While the formulae are always the same, the key point of the derivation is understanding in detail the phase space in order to get the soft scales. In the next chapter we present a derivation of the soft scales for rapidity distributions and subsequent threshold resummation formulae following [1].

## Chapter 3

# Resummation of rapidity distributions

3.1	Higgs boson production at hadron colliders . . . . .	35
3.2	Fully differential distribution . . . . .	36
3.3	Threshold variables of the rapidity distribution . . . . .	38
3.3.1	Kinematical configurations in the threshold limit . . . . .	41
3.4	Factorization in Mellin space . . . . .	42
3.4.1	Hadronic kinematics . . . . .	42
3.4.2	Factorization in Mellin-Fourier space . . . . .	43
3.4.3	Factorization in Mellin-Mellin space . . . . .	44
3.4.4	Threshold limit in $(N, M)$ and $(N_1, N_2)$ . . . . .	45
3.5	Phase space . . . . .	45
3.6	Resummation of the rapidity distribution . . . . .	50
3.6.1	Singular scales in Mellin-Mellin space . . . . .	50
3.6.2	Resummation formulae: doubly soft limit . . . . .	51
3.6.3	Resummation formulae: singly soft limit . . . . .	52
3.7	The question of verification . . . . .	53

In this chapter we introduce the QCD-induced Higgs boson production and discuss the threshold resummation of its rapidity distribution following the derivation in [1].

Firstly, we present the Higgs boson production process and its most relevant partonic subprocess, gluon fusion, in the infinite top mass approximation. Next, we introduce the basics of Higgs boson production kinematics, discussing the differential cross section in both transverse momentum and longitudinal rapidity of the Higgs and the relevant independent variables involved. This is helpful for the subsequent discussion on the rapidity distribution, where we define the threshold limits, *singly* and *doubly soft*, both elucidating their physical meaning and highlighting the differences with respect to

the threshold limit of the total cross section. We find that the classic threshold variable  $x$  is no longer suitable and the new threshold variables  $x_1$  and  $x_2$  must be defined. Having understood which are the regions of the phase space that must be resummed, we get to the problem of factorization for the rapidity distribution and see how the Mellin-Fourier and Mellin-Mellin transformations solve it. Finally, we find the two hard and soft scales singular in the threshold limits by studying the general structure of the phase space. This is the core of the derivation that naturally takes us to the final resummation formulae by application of the formalism developed in the previous chapter.

This not the only way to derive threshold resummation of rapidity distribution. In the last section we briefly describe the effective field theory approach developed in an unpublished paper by F.J. Tackmann et alii [8] and the problem of verifying and comparing the two approaches, which is the motivation of this work that will be dealt in the next chapter.

### 3.1 Higgs boson production at hadron colliders

One of the most physically interesting processes at hadron colliders is the Higgs boson production

$$p + p \rightarrow H + X. \quad (3.1.1)$$

The process is important to study the properties of the Higgs boson and, subsequently, of the spontaneous symmetry breaking. In particle accelerators the Higgs boson decays in other particles, which are those that are actually measured, such as weak boson pairs or leptons, so the momentum of  $H$  in equation 3.1.1 is not on shell. However, we will always refer to its virtuality as  $m_H^2$ : keep in mind that this value is not fixed but it is a variable of the process. We can now understand the remark made in section 2.2, Higgs boson production is kinematically equivalent to DY production: in both cases the final state boson is not on-shell and the remaining particles are partons. As in DY production, the hard scale of the process is taken to be  $m_H^2$ .

The partonic subprocess we will consider in subsequent sections is the *gluon fusion* induced production

$$g + g \rightarrow H + X. \quad (3.1.2)$$

The gluons and the Higgs boson are mediated by a quark loop (see LO diagram 3.1) so in principle all the contributions with the six different quarks flavours in the loop should be considered, however the top quark, being the most massive, (table 1.1) is dominant. Because of the intermediate loop, the LO diagram carries a power of  $\alpha_s$ , one order more than the LO of the quark scattering induced production  $q\bar{q} \rightarrow H$ . However, numerically, at LHC gluon fusion, differently from DY production, turns out to be the dominant contribution, since the coupling between the Higgs boson and the top quark is proportional to its mass, that is very large. For a comparison between different

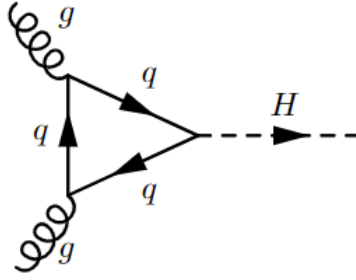


Figure 3.1: LO diagram for gluon fusion initiated Higgs boson production.

partonic process see for example figure 4.5 in [5].

As briefly discussed in section 1.5, the mass of the top quark can be considered infinite. This means in principle that final results can be simplified by taking the limit  $m_t^2 \rightarrow \infty$ , but in practice one can do this systematically by substituting the top mass Lagrangian with an *effective* low-energy Lagrangian coupling the gauge field (the gluon) and the Higgs boson. Diagrammatically the top mass loop collapses into three possible effective vertices that couples two, three or four gluons to the Higgs boson. For reference, the LO cross section is

$$\sigma = \frac{\alpha_s^2}{576\pi v^2} \delta(1-x) = \sigma_0 \delta(1-x) \quad (3.1.3)$$

where  $v$  is the vacuum expectation value of the Higgs field and  $x = \frac{m_H^2}{s}$ . Consistently with the discussion in section 1.6.2, because of the conservation of energy the dependence on  $x$  is trivial. Since the effective vertex is proportional to  $\sigma_0$ , at N<sup>k</sup>LO,  $\sigma_0$  can always be factorized.

## 3.2 Fully differential distribution

In this section we will determine the independent variables necessary to describe the completely inclusive differential cross section of the Higgs boson production. We will also collect a series of kinematical relations that will be useful in the next chapter.

Consider again gluon fusion

$$g(p_1) + g(p_2) \rightarrow H(p_H) + X(p_X). \quad (3.2.1)$$

Applying the same reasoning used in section 1.6.2 the process, after integrating on extra radiations, must depend on four variables. Two of these can be taken to be the same of the total cross section, that is to say  $s$  and  $m_H^2$ , the other two can be chosen in different ways. First of all, calculating the fully differential total cross section, observe that the Higgs boson momentum mea-

sure  $d^3p_H$  is not integrated. It is therefore natural to choose as variables the transverse component  $p_T^2$  and the longitudinal component  $p_z$  of the space momentum. The last one is always replaced by the longitudinal rapidity<sup>1</sup>  $y = \sqrt{m_H^2 + p_T^2} \sinh y$ <sup>2</sup>. Then, the fully differential distribution is written explicitly  $\frac{d^2\sigma}{dp_T^2 dy}(s, m_H^2, p_T^2, y)$ . We mention that in older works in place of the rapidity one can also find the *Feynman-x*  $x_F$ , the ratio between the longitudinal momentum and its maximum value (for details see [9]). This variable however will not be relevant for subsequent discussions.

Another choice [10] for the two variables is picking the Mandelstam invariants  $t = (p_2 - p_H)^2$  and  $u = (p_1 - p_H)^2$ . Because both of the final states are off-shell, the Mandelstam invariants are not necessarily dependent, since the usual Lorentz-invariant energy conservation relation is

$$s + t + u = m_H^2 + Q^2 \quad (3.2.2)$$

where  $Q^2 := p_X^2$ . The relation between rapidity and transverse momentum and the two Mandelstam variables can be found explicitly from the definitions. First in the partonic center-of-mass the four-momenta  $p_1$  and  $p_2$  are

$$p_1 = \frac{\sqrt{s}}{2} (1, 0, 0, 1) \quad (3.2.3)$$

$$p_2 = \frac{\sqrt{s}}{2} (1, 0, 0, -1), \quad (3.2.4)$$

while, by definition of rapidity and transverse momentum,  $p_H$  is

$$p_H = (\sqrt{m_H^2 + p_T^2} \cosh y, \vec{p}_T, \sqrt{m_H^2 + p_T^2} \sinh y). \quad (3.2.5)$$

The four-momentum  $p_X$  can be found trivially by applying conservation of total four-momentum  $p_1 + p_2 = p_X + p_H$ . Substituting such parametrization of four-momenta in the definition of Mandelstam invariants we find

$$\begin{aligned} t &= m^2 - \sqrt{s} \sqrt{m_H^2 + p_T^2} e^{-y} \\ u &= m^2 - \sqrt{s} \sqrt{m_H^2 + p_T^2} e^y. \end{aligned} \quad (3.2.6)$$

This set of equations gives explicitly the transformation  $(m_H^2, s, t, u) \rightarrow (m_H^2, s, p_T^2, y)$ .

---

<sup>1</sup>Starting from this point we will always refer to the longitudinal rapidity simply as rapidity.

<sup>2</sup>Recall that, by definition of rapidity,  $\sinh y_z = \beta_z \gamma_z$  where  $\beta_z = v_z = \frac{p_z}{E}$  and  $\gamma_z = 1/\sqrt{1 - \frac{p_z^2}{E^2}}$ . Using  $E^2 = m^2 + p_T^2 + p_z^2$  and isolating  $p_z$  from the definition we obtain the mentioned relation.

The Jacobian relates the two cross sections:

$$\frac{d^2\sigma}{dp_T^2 dy} = \left| \det \frac{\partial(t, u)}{\partial(p_T^2, y)} \right| \frac{d^2\sigma}{dt du} = s \frac{d^2\sigma}{dt du}. \quad (3.2.7)$$

Relations 3.2.6 can also be used to determine  $Q^2$  in terms of  $p_T^2$  and  $y$  using 3.2.2. This yields

$$Q^2 = s + m^2 - 2\sqrt{s}\sqrt{m_H^2 + p_T^2} \cosh y. \quad (3.2.8)$$

Through this relation  $Q^2$  can be exchanged with  $p_T^2$  or  $y$ . This equation also makes possible to calculate the limits of  $Q^2$  and  $p_T^2$ . By setting<sup>3</sup>  $Q^2 \geq 0$  and solving for  $p_T^2$  we find the maximum of the transverse momentum. Vice versa, isolating the transverse momentum and setting  $p_T^2 \geq 0$  we find the maximum of  $Q^2$ . We report the results for later purposes

$$\begin{aligned} 0 \leq p_T^2 &\leq \frac{(s + m^2)^2}{4s \cosh^2(y)} - m^2 \\ 0 \leq Q^2 &\leq s + m^2 - 2m\sqrt{s} \cosh y. \end{aligned} \quad (3.2.9)$$

### 3.3 Threshold variables of the rapidity distribution

In this section we focus on the rapidity distribution. In particular, we define the threshold limits, showing the differences with the total cross section case, and discuss, correspondingly, new variables appropriate for its parametrization. A final note will elucidate the actual kinematical configurations of the phase space that contribute to the threshold limits.

Integrating the fully differential cross section with respect to the rapidity  $y$  or the transverse momentum  $p_T^2$ , one calculates respectively the transverse momentum spectrum or the rapidity distribution. Now, because we are interested in resumming the rapidity distribution, we will study in detail the boundaries of the kinematic variables left out by the integration on  $p_T^2$ , that is to say the variables  $s$ ,  $m_H^2$ , and  $y$ . We expect a crucial difference regarding the total cross section case studied for the equivalent DY production. In that context we have seen that in the threshold limit  $x \rightarrow 1$ , all the extra emissions had to be soft. In the rapidity distribution, fixing rapidity, this is not possible in principle because at least one extra emission must recoil to the Higgs boson, so the limit  $x \rightarrow 1$  is not accessible, if not when  $y = 0$ . Equivalently, the threshold limit was defined as the limit where the center-of-mass energy is barely sufficient to produce an Higgs boson. The energy is clearly the least when the Higgs boson is produced at rest, but this limit is not pos-

---

<sup>3</sup> $Q^2$  must be positive because  $Q^2 = (k_1 + \dots + k_n)^2 = \sum 2(k_i k_j) = 2 \sum (k_i^0 k_j^0 - \vec{k}_i \vec{k}_j) = 2 \sum k_i^0 k_j^0 (1 - \cos \theta_{ij}) \geq 0$ .

sible when the rapidity is fixed to any value. Therefore the threshold limit must be generalized so that it is defined as the limit where the center-of-mass energy is barely sufficient to produce an Higgs boson *with fixed rapidity*. We will see in this section how to define analytically the newly settled threshold limit.

Having integrated on  $p_T^2$ , or, alternatively, on  $Q^2$ , equations 3.2.9 become

$$s + m^2 - 2m\sqrt{s} \cosh y \geq 0. \quad (3.3.1)$$

Now, solving for  $\sqrt{s}$  we find the limits of  $x = m^2/s$ , *having fixed rapidity*. First notice that the solutions of the associated equation are

$$x = \cosh y \pm |\sinh y| \quad (3.3.2)$$

so that when  $y \geq 0$ ,  $x \leq e^{-2y} \vee x \geq e^{2y}$ , viceversa for  $y \leq 0$ . Combining with  $0 \leq x \leq 1$  we finally find (see figure 3.2)

$$\begin{aligned} 0 \leq x \leq e^{-2y} & \quad \text{if } y \geq 0 \\ 0 \leq x \leq e^{2y} & \quad \text{if } y \leq 0 \end{aligned} \quad (3.3.3)$$

We have already interpreted physically this result: with fixed rapidity the

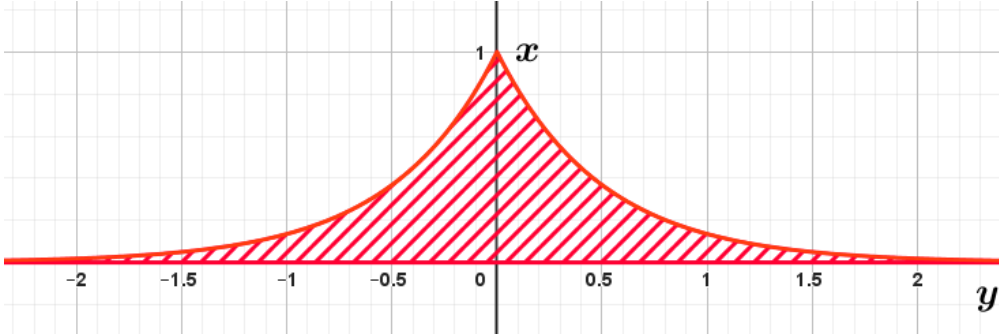


Figure 3.2: Phase space of rapidity distribution in the variables  $z = m_H^2/s$  and  $y$ .

center-of-mass energy must be greater than  $m_H^2$  in order to produce an Higgs moving longitudinally, thus  $x$  cannot be equal to 1, if not when  $y = 0$ .

For completeness we report the extrema of rapidity, fixing  $x$ , found by solving eq. 3.3.1

$$-\frac{1}{2} \ln \frac{1}{x} \leq y \leq \frac{1}{2} \ln \frac{1}{x}. \quad (3.3.4)$$

Now, we still would like to have a variable ranging from 0 to 1 that in the threshold limit approaches to 1. For this reason we define the new scaling variables  $x_1$  and  $x_2$  that interpolates on the extrema of  $x$  (we will actually work with the square root for reasons that will be clear later) in the two cases



found

$$\begin{cases} x_1 := \sqrt{x}e^y \\ x_2 := \sqrt{x}e^{-y} \end{cases} \quad (3.3.5)$$

In the case of positive rapidity the threshold limit is  $x \rightarrow e^{-2y}$  and therefore  $x_1 \rightarrow 1$ . Vice versa in the case of negative rapidity  $x_2 \rightarrow 1$ . This limit is also called *singly soft limit*. For  $y = 0$  both variables approach to 1 and so does  $x$ . This case is called *doubly soft limit* and it is physically equivalent to the threshold limit of the cross section.

We have thus found a new set of variables  $(x_1, x_2, m_H^2)$  that can be exchanged with the original set  $(s, m_H^2, y)$ . The inverse relation is

$$\begin{cases} x = x_1 x_2 \\ y = \frac{1}{2} \ln \frac{x_1}{x_2} \end{cases}, \quad (3.3.6)$$

where the Jacobian of the transformation is 1, so that the differential cross section does not acquire any additional multiplicative factor in the transformation. In this new set of variables the phase has simply the shape of a square (see figure 3.3) In literature it can also be found a variable,  $u$  (not

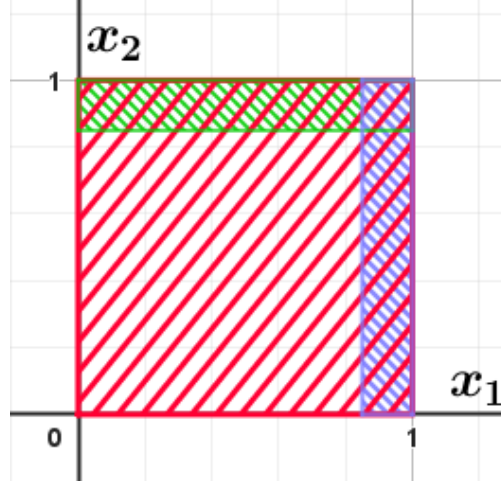


Figure 3.3: Phase space of rapidity distribution in the variables  $x_1$  and  $x_2$ . The threshold region have been highlighted with different colors: singly soft limit for positive rapidity (blue), negative rapidity (green), doubly soft limit (superposition).

to be confused with the Mandelstam invariant), ranging from 0 to 1 that includes both singly soft limits in its extrema:

$$u := \frac{e^{-y} - xe^y}{2(1-x)\cosh y}. \quad (3.3.7)$$

Notice that in terms of  $x_1$  and  $x_2$

$$\begin{aligned} u &= \frac{x_2(1-x_1^2)}{(1-x_1x_2)(x_1+x_2)}, \\ 1-u &= \frac{x_1(1-x_2^2)}{(1-x_1x_2)(x_1+x_2)}, \end{aligned} \quad (3.3.8)$$

so that  $x_1 \rightarrow 1$  implies  $u \rightarrow 1$  and  $x_2 \rightarrow 1$  implies  $u \rightarrow 0$ . Physically it can be shown  $u$  to be simply related to the angle of the emitted Higgs boson  $\theta$  in the center-of-mass frame

$$u = \frac{1 + \cos \theta}{2}. \quad (3.3.9)$$

The equation shows that  $x_1 \rightarrow 1$  implies  $\theta \rightarrow \pi$  and  $x_2 \rightarrow 1$  implies  $\theta \rightarrow -\pi$ , which implies that in the singly soft limit the Higgs boson is collinear. This has an obvious physical interpretation: in the threshold limit the transverse momentum of the Higgs boson must be 0 because the center-of-mass energy is barely enough to produce the Higgs with that given rapidity, so no energy is available for transverse momentum. In the doubly soft limit, since  $y = 0$ ,  $x_1 = x_2 = x$  and therefore  $u \rightarrow 1/2$ .

Now the rapidity distribution can be computed also in terms of the set of variables  $(x, u, m_H^2)$ , where the Jacobian of the transformation is

$$\frac{d\sigma}{du} = \frac{dy}{du} \frac{d\sigma}{dy} = \frac{(1-x)(1+x)}{2(1-u+ux)(-u-x+ux)} \frac{d\sigma}{dy}. \quad (3.3.10)$$

### 3.3.1 Kinematical configurations in the threshold limit

We have defined the appropriate threshold limits for the rapidity distribution and discussed their physical interpretation, now we would like to know what actual kinematical configurations of the final products contribute to the threshold limits. In the case of the total cross section we have already mentioned that threshold limit implies at rest production of the Higgs boson and that all extra-emissions are soft. For the rapidity distribution we have also observed that fixing the rapidity these two conditions cannot be satisfied, the first trivially, the second because, for momentum conservation, one parton must recoil against the Higgs and so it cannot be soft. In addition, discussing the  $u$  variable, we have shown that in the threshold limit  $p_T^2 \rightarrow 0$ . It is left to discuss the possible behaviour of the other partons  $k_1, \dots, k_{n-1}$ .

Using four-momentum conservation  $p_1 + p_2 = p_H + k_1 + \dots + k_n$  and the

explicit four-momenta parametrization, we have

$$\begin{aligned}
(k_1 + \dots + k_n)^2 &= (p_1 + p_2 - p_H)^2 = s - 2\sqrt{s}\sqrt{m_H^2 + p_T^2} \cosh y + m_H^2 + p_T^2 \\
&= \sum_{i,j} k_i^0 k_j^0 (1 - \cos \theta_{ij}).
\end{aligned}
\tag{3.3.11}$$

Since  $p_T^2 = 0$  in the threshold limit, the first line can simply be factorized as a polynomial in the variable  $\sqrt{s}$  to finally give

$$\sum_{i,j} k_i^0 k_j^0 (1 - \cos \theta_{ij}) = s(1 - x_1)(1 - x_2).
\tag{3.3.12}$$

We see that  $x_1 \rightarrow 1$  is satisfied not only if all the partons are soft, but also if they are all collinear. Of course integrating on the phase space both of these configurations are covered and they will give rise to different logarithmic contributions. This is studied in the following sections.

### 3.4 Factorization in Mellin space

In section 2.2.2 we have introduced the Mellin transform and its role in factorizing the factorization formulae. This factorization was the starting point in section 2.2.3 to derive resummation formulae. In this section we find will find how to get factorization for rapidity distribution using a double Mellin transform. In order to do this it is first necessary to define the variables of the hadronic rapidity distribution and their relation with the partonic ones.

#### 3.4.1 Hadronic kinematics

We first start from the four-momenta in the hadronic center-of-mass frame of reference

$$\begin{aligned}
P_1 &= \frac{\sqrt{S}}{2}(1, 0, 0, 1), & P_2 &= \frac{\sqrt{S}}{2}(1, 0, 0, -1) \\
P_H &= (\sqrt{m_H^2 + p_T^2} \cosh Y, \vec{p}_T, \sqrt{m_H^2 + p_T^2} \sinh Y),
\end{aligned}
\tag{3.4.1}$$

where  $P_1$  and  $P_2$  are the four-momenta of the incoming protons and  $Y$  and  $S$  are the rapidity and hadronic center-of-mass energy in this frame. Clearly the two frames of reference are related by a boost in the longitudinal direction, for this reason the transverse momentum is unchanged. Let as usual  $\xi_1$  and  $\xi_2$  be the two parton momentum fractions, so that  $p_i = \xi_i P_i$ . Applying this definition  $s = (p_1 + p_2)^2 = \xi_1 \xi_2 S$ , thus the partonic threshold variable  $x$  is trivially related to the hadronic threshold variable  $\tau = \frac{m_H^2}{S}$  with  $x = \frac{\tau}{\xi_1 \xi_2}$ .

The rapidities are related by the boost between the two frame of references. Now because the rapidity is additive, being  $w = \frac{1}{2} \ln \frac{\xi_1}{\xi_2}$  the rapidity of the boost between the two frame of references, the partonic rapidity is simply  $y = Y - w$ . Finally notice that fixing  $\tau$  and  $Y$  the momentum fractions  $\xi_1$  and  $\xi_2$  cannot range freely from 0 to 1. If they are too small there is not enough energy to produce the Higgs boson. The minimum value is found by setting  $x = \frac{\tau}{\xi_1 \xi_2} = 1$  and  $y = Y - w = 0$ . Solved (the equations are analogous to 3.3.6) we get the minimum values  $\tau_1 = \sqrt{\tau} e^Y$  and  $\tau_2 = \sqrt{\tau} e^{-Y}$ .

As for partonic cross sections, also hadronic cross sections can be described in terms of the two threshold variables  $\tau_1$  and  $\tau_2$ . Substituting in their definition  $\tau$  and  $Y$  in terms of  $x$  and  $y$ , we get the physically transparent result  $x_1 = \frac{\tau_1}{\xi_1}$  and  $x_2 = \frac{\tau_2}{\xi_2}$ .

### 3.4.2 Factorization in Mellin-Fourier space

Now we are ready to write the parton formula in the variables  $(\tau, Y, m_H^2)$ . We will adopt the same convention used in the previous chapter to name the partonic cross section  $C$ .

$$\frac{d\sigma}{dY}(\tau, Y, m_H^2) = \sum_{i,j=g,q,\bar{q}} \int_{\tau_1}^1 d\xi_1 f_i(\xi_1, \mu_F^2) \int_{\tau_2}^1 d\xi_2 f_j(\xi_2, \mu_F^2) \frac{dC_{ij}}{dy} \left( x = \frac{\tau}{\xi_1 \xi_2}, y = Y - w, m_H^2, \mu_F^2 \right). \quad (3.4.2)$$

By comparison with equation 1.6.9 we notice that it is not obvious how this should factorize under a Mellin transformation. First we rewrite the two kinematical constraints with  $\delta$  functions (the sum symbol and the dependences on the factorization scale will now be omitted)

$$\frac{d\sigma}{dY}(\tau, Y, m_H^2) = \int_0^1 \int_0^1 d\xi_1 d\xi_2 \int_0^1 \int_{y_{min}}^{y_{max}} dx dy [f_i(\xi_1) f_j(\xi_2) \delta(\tau - \xi_1 \xi_2 x) \delta(Y - y - w) \frac{dC_{ij}}{dy}(x, y, m_H^2)]. \quad (3.4.3)$$

Now, the first  $\delta$  has the correct structure for factorization in Mellin space, while the second is appropriate for factorization in Fourier space. This suggests to rewrite the differential cross section in Fourier-Mellin space, where  $\tau$  is mapped into  $N$  through a Mellin transformation and  $Y$  is mapped to  $M$  through a Fourier transformation

$$\frac{d\sigma}{dY}(N, M, m_H^2) = \int_0^1 d\tau \tau^{N-1} \int_{Y_{min}}^{Y_{max}} dY e^{iMY} \frac{d\sigma}{dY}(\tau, y, m_H^2). \quad (3.4.4)$$

Substituting inside this definition the factorization formula one gets the desired factorization by simply applying the  $\delta$  functions on  $\tau$  and  $Y$

$$\frac{d\sigma}{dY}(N, M, m_H^2) = f_i \left( N + i \frac{M}{2} \right) f_j \left( N - i \frac{M}{2} \right) \frac{dC_{ij}}{dy}(N, M, m_H^2), \quad (3.4.5)$$

where  $\frac{dC}{dy}(N, M, m_H^2)$  is the Fourier-Mellin transform of the partonic cross section with respect to  $x$  and  $y$  and the PDFs have been Mellin transformed mapping  $\xi_1$  and  $\xi_2$  into the variables  $N \pm i \frac{M}{2}$ .

### 3.4.3 Factorization in Mellin-Mellin space

We could also work out factorization in terms of the threshold hadronic variables  $(\tau_1, \tau_2, m_H^2)$ . Using this the factorization formula becomes

$$\frac{d\sigma}{dY}(\tau_1, \tau_2, m_H^2) = \int_{\tau_1}^1 d\xi_1 f_i(\xi_1) \int_{\tau_2}^1 d\xi_2 f_j(\xi_2) \frac{dC_{ij}}{dy} \left( x_1 = \frac{\tau_1}{\xi_1}, x_2 = \frac{\tau_2}{\xi_2}, m_H^2, \mu_F^2 \right). \quad (3.4.6)$$

This equation can now manifestly be factorized defining the doubly Mellin transformed hadronic cross section

$$\frac{d\sigma}{dY}(\tau_1, \tau_2, m_H^2) = \int_0^1 d\tau_1 \tau_1^{N_1-1} \int_0^1 d\tau_2 \tau_2^{N_2-1} \frac{d\sigma}{dY}(x_1, x_2, m_H^2). \quad (3.4.7)$$

Substituting inside the factorization formula we have

$$\frac{d\sigma}{dY}(N_1, N_2, m_H^2) = f_i(N_1) f_j(N_2) \frac{dC_{ij}}{dY}(N_1, N_2, m_H^2), \quad (3.4.8)$$

with obvious definitions. Comparing 3.4.4 and 3.4.7 we get the relation between the two sets of transformed variables

$$\begin{aligned} N_1 &= N + i \frac{M}{2}, \\ N_2 &= N - i \frac{M}{2}. \end{aligned} \quad (3.4.9)$$

$N_1$  and  $N_2$  are two complex variables so they have in principle four degree of freedoms, while  $N$  and  $M$ , since  $M$  is real, only three. However separating the real and imaginary part of  $N$  it is straightforward to see that they are constrained to have the same real part

$$\begin{aligned} N_1 &= \Re(N) + i[\Im(N) + M/2] \\ N_2 &= \Re(N) + i[\Im(N) - M/2]. \end{aligned} \quad (3.4.10)$$

Sets	Definitions	Singly soft limit	Doubly soft limit
$(x, y, m_H^2)$	$x = m_H^2/s$	$x \rightarrow e^{-2y} \vee x \rightarrow e^{2y}$	$x \rightarrow 1$
$(x_1, x_2, m_H^2)$	$\begin{cases} x_1 = \sqrt{x}e^{-y} \\ x_2 = \sqrt{x}e^y \end{cases}$	$\begin{cases} x_1 \rightarrow 1 \\ x_2 \rightarrow x \end{cases} \vee \begin{cases} x_1 \rightarrow x \\ x_2 \rightarrow 1 \end{cases}$	$x_1, x_2 \rightarrow 1$
$(x, u, m_H^2)$	$u = \frac{x_2(1-x_1^2)}{(1-x_1x_2)(x_1+x_2)}$	$u \rightarrow 1 \vee u \rightarrow 0$	$u \rightarrow \frac{1}{2}$
$(N, M, m_H^2)$	$\begin{cases} N \text{ Mellin of } x \\ M \text{ Fourier of } y \end{cases}$	$\begin{cases} \Im(N) \rightarrow \infty \\ M \rightarrow +\infty \end{cases} \vee \begin{cases} \Im(N) \rightarrow \infty \\ M \rightarrow -\infty \end{cases}$	$ N , M \rightarrow \infty$
$(N_1, N_2, m_H^2)$	$\begin{cases} N_1 = N + i\frac{M}{2} \\ N_2 = N - i\frac{M}{2} \end{cases}$	$ N_1  \rightarrow \infty \vee  N_2  \rightarrow \infty$	$N_1, N_2 \rightarrow \infty$

Table 3.1: Possible set of independent variables for the partonic rapidity distribution and their limits in the singly soft limit ( $y \neq 0$ ) and in the doubly softly limit ( $y = 0$ ).

### 3.4.4 Threshold limit in $(N, M)$ and $(N_1, N_2)$

Because we are ultimately interested in resumming in factorizing spaces, it is useful to ask what the singly and doubly soft limits correspond to in Mellin-Fourier and Mellin-Mellin spaces.

We have already discussed in 2.2.2 that the  $x \rightarrow 1$  limit in real space corresponds to the  $|N| \rightarrow \infty$  limit in Mellin space. Consider therefore the mapping  $(x_1, x_2) \rightarrow (N_1, N_2)$ . In the singly soft limit with  $x_2$  fixed and  $x_1 \rightarrow 1$ ,  $N_2$  must be fixed too and  $|N_1| \rightarrow \infty$ . However, consistently with equations 3.4.10, it is the imaginary part of  $N_1$  that must go to infinity. In particular we cannot take in principle neither  $\Im(N)$  or  $M$  fixed and the other to  $+\infty$  because it would in both cases imply  $N_2 \rightarrow \infty$ , so they must both go to  $\infty$  but such that  $\Im(N) \approx M/2$  so that  $N_2$  stays fixed and finite. The reasoning can of course be applied conversely when  $x_1$  is fixed and  $x_2 \rightarrow 1$ .

In the doubly soft limit  $x \rightarrow 1$  or, equivalently,  $x_1, x_2 \rightarrow 1$ , therefore  $N, N_1, N_2 \rightarrow \infty$ . From a well-known property of Fourier transformations we also have  $M \rightarrow \infty$ : Since  $y = 0$  in the doubly soft limit, in order to get a finite transformed function, the Fourier variable  $M$  must get to  $+\infty$  too to compensate for the increasingly oscillating factor  $e^{iMY}$ .

Table (3.1) sums up all the variables we have introduced and their relative limits.

## 3.5 Phase space

We are finally ready to set up the first of the two steps necessary to derive the resummation formulae: the determination of the soft scales from the phase space structure. This is the most subtle point of the derivation and for this

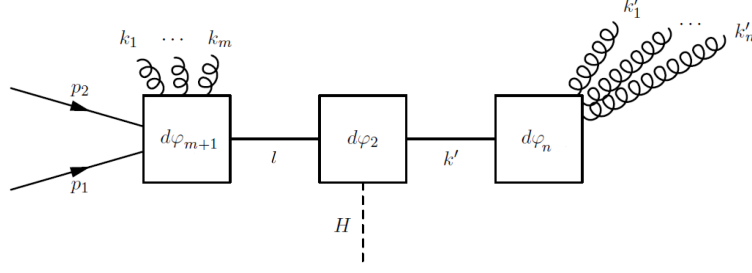


Figure 3.4: Decomposition of the phase for Higgs boson production and  $n + m$  emissions in  $n$  collinear extra emissions recoiling against the Higgs boson and  $m$  soft emissions.

reason its check will essentially be the objective of the next chapter. We follow the derivation in [1], which adopts the approach already applied in [6] and [11], which all stem from [3]. The general strategy is singling out from the phase space the independent variables of the rapidity distribution by writing all phase space integrals in terms of dimensionless variables on a fixed range. We discover two singular scales,  $m_H^2(1 - x_1)(1 - x_2)$  and  $m_H^2(1 - x_1)^2$ , respectively related to collinear and soft emissions.

We have shown in section 3.3.1 that configurations contributing to the threshold limit include both soft and collinear emissions. This motivates to differentiate among the total  $n + m$  emitted partons  $m$  that are soft in the threshold limit and  $n$  that in the threshold limit are collinear. This distinction is technically artificial since to calculate the rapidity distribution we integrate on all possible configurations, however it will soon prove to be extremely insightful. Firstly we write the four-momentum conservation as

$$p_1 + p_2 = p_H + k_1 + \dots + k_m + k'_1 + \dots + k'_n, \quad (3.5.1)$$

where the prime marks the collinear partons. By definition the phase space measure regularized in  $d = 4 - 2\epsilon$  dimensions is

$$\begin{aligned} d\phi_{n+m+1}(p_1, p_2; p_H, k_1, \dots, k_m, k'_1, \dots, k'_n) = \\ = \frac{d^{d-1}p_H}{(2\pi)^{d-1}2p_H^0} \frac{d^{d-1}k_1}{(2\pi)^{d-1}2k_1^0} \dots \frac{d^{d-1}k'_n}{(2\pi)^{d-1}2k'_n} (2\pi)^d \delta^{(d)}(p_1 + p_2 - p_H - k_1 - \dots - k'_n). \end{aligned} \quad (3.5.2)$$

Now we can employ equation 2.2.2 to decompose the total phase space as (see figure 3.4)

$$d\phi_{n+m+1} = \int \frac{dl^2}{2\pi} d\phi_{m+1}(p_1, p_2; l, k_1, \dots, k_m) \int \frac{d(k')^2}{2\pi} d\phi_2(l; p_H, k') d\phi_n(k'; k'_1, \dots, k'_n), \quad (3.5.3)$$

where  $d\phi_{m+1}(p_1 + p_2; l, \{k_i\})$  is the phase space with an incoming momentum

$p_1 + p_2$  producing a massive state  $l$  with  $m$  extra emissions,  $d\phi_2(l; p_H, k')$  is the phase space for the production of an Higgs boson with incoming and outgoing massive states  $l$  and  $k'$  and, finally,  $d\phi_n(k'; \{k'_j\})$  is the phase space for the production of  $n$  partons.

Up to now there is no particular physics involved in this decomposition, this is just a rewriting of the phase space measure 3.5.2. Notice that by integrating on all partonic four-momenta,  $d\phi_{m+1}$  and  $d\phi_n$  behave like total cross sections, so that the differential variables  $p_T^2$  and  $y$  arise only from the phase space  $d\phi_2$ , whence the Higgs is emitted. Now we will consider all the three phase spaces separately. In the following explicit integration symbols on partonic momenta are omitted and, employing Lorentz invariance, all the phase spaces will be computed in the respective center-of-mass frame of reference.

The phase space  $d\phi_2$  can be calculated explicitly. Starting from the definition

$$d\phi_2(l; p_H, k') = \frac{d^{d-1}p_H}{(2\pi)^{d-1}2p_H^0} \frac{d^{d-1}k'}{(2\pi)^{d-1}2(k')^0} (2\pi)^d \delta^{(d)}(l - p_H - k'), \quad (3.5.4)$$

the delta function can be used to eliminate integration on the space momenta of  $k'$  and the Higgs boson measure can be written as

$$d^{d-1}p_H = d^{d-2}\vec{p}_T d\vec{p}_z = \frac{1}{2} dp_T^2 |p_T|^{d-4} d\Omega_{d-2} dp_z = \frac{\pi^{1-\epsilon}}{\Gamma(1-\epsilon)} dp_T^2 |p_T|^{-2\epsilon} dp_z, \quad (3.5.5)$$

where  $d\Omega_d = \frac{2\pi^{d/2}}{\Gamma(d/2)}$ . Combining all together

$$d\phi_2(l; p_H, k') = \frac{(4\pi)^\epsilon |p_T|^{-2\epsilon}}{16\pi\Gamma(1-\epsilon)} \frac{\delta(\sqrt{l^2} - p_H^0 - k'^0)}{p_H^0 k'^0} dp_T^2 dp_z. \quad (3.5.6)$$

Now  $dp_z$  can be written straightforwardly in terms of  $dy$ , and the integration on the transverse momentum can be eliminated rewriting the Dirac  $\delta$  as  $\delta(p_T^2 - \tilde{p}_T^2)$ , The final result is

$$d\phi_2(l; p_H, k') = \frac{(4\pi)^\epsilon |\tilde{p}_T|^{-2\epsilon}}{32\pi^2\Gamma(1-\epsilon)\sqrt{l^2}} \sqrt{m_H^2 + \tilde{p}_T^2} \cosh(y) dy. \quad (3.5.7)$$

So far we have got

$$\begin{aligned} \frac{d\phi_{m+n+1}}{dy}(p_1, p_2; p_H, k_1, \dots, k'_n) &= \frac{(4\pi)^\epsilon}{32\pi^2\Gamma(1-\epsilon)} \cosh(y) \int \frac{dl^2}{\sqrt{l^2}} \\ d\phi_{m+1}(p_1, p_2; l, k_1, \dots, k_m) &\int \frac{d(k')^2}{2\pi} |\tilde{p}_T|^{-2\epsilon} \sqrt{m_H^2 + \tilde{p}_T^2} d\phi_n(k'; k_1, \dots, k'_n), \end{aligned} \quad (3.5.8)$$

where the integration on the transverse momentum of the Higgs boson has



been computed.

We have already noticed that  $\int d\phi_{m+1}$  and  $\int d\phi_n$  are equivalent to the phase space of a total cross section. Consider the first phase space. It is the production of a massive state  $l^2$  with the emission of  $m$  partons: we have already studied in depth this total cross section, it is exactly that of Drell-Yan production. In the threshold limit all the partons go soft, exactly as in DY. In section 2.2.1 we have shown that the associated soft scale is

$$\Lambda_{DY}^2 = \frac{(s - l^2)^2}{s}. \quad (3.5.9)$$

Similarly  $d\phi_n$  is equivalent to the total cross section of a process with a massive initial state and only massless final products: this is exactly the case of deep inelastic scattering. This phase space produces the soft scale

$$\Lambda_{DIS}^2 = (k')^2. \quad (3.5.10)$$

Notice that in the threshold limit also DIS total cross section is going to its threshold since all extra emissions are going collinear, which for DIS is sufficient to get to this limit.

These two soft scales however are not enough to establish the correct soft scales of the rapidity distribution since they depend on the integration variables  $l^2$  and  $(k')^2$ . It is therefore necessary to use the same strategy employed in section 2.2.1: the integration variables are written in terms of dimensionless variables on fixed ranges so to single out the explicit dependence of phase space on its independent variables.

Consider first  $l^2$ . Working with energy conservation of  $d\phi_{m+1}$  and  $d\phi_2$  we find

$$(\sqrt{m_H^2 + p_T^2} + |p_z|)^2 \leq l^2 \leq s, \quad (3.5.11)$$

that in the limit  $p_T^2 \rightarrow 0$  reduces to

$$m^2(\cosh y + |\sinh y|)^2 \leq l^2 \leq s. \quad (3.5.12)$$

In the threshold limit  $x_1 \rightarrow 1$  we have  $y \geq 0$  so that

$$m^2 e^{2y} \leq l^2 \leq s, \quad (3.5.13)$$

which in terms of threshold variables 3.3.5 it becomes

$$x_1^2 s \leq l^2 \leq s. \quad (3.5.14)$$

Now we define the dimensionless slider variable  $w \in [0, 1]$  interpolating between the extrema of  $l^2$

$$l^2 = x_1^2 s(1 - w) + sw = x_1^2 s + w(s - x_1^2 s), \quad (3.5.15)$$

and change subsequently the integration variable

$$\int \frac{dl^2}{\sqrt{l^2}} d\phi_{m+1} = \sqrt{s}(1-x_1^2) \int_0^1 \frac{dw}{\sqrt{x_1^2 + w(1-x_1^2)}} d\phi_{m+1}. \quad (3.5.16)$$

In terms of this variable the quantity  $(s-l^2)$  simply factorizes as  $m_H^2(1-x_1)^2(1-w)^2$  and so the soft scale factor arising from the integral is

$$\frac{1}{s-l^2} \left[ \frac{(s-l^2)^2}{s} \right]^{m-m\epsilon} \propto \frac{[m_H^2(1-x_1)^2]^{m+m\epsilon}}{m_H^2(1-x_1)} (1-w)^{-1+2m-2m\epsilon}, \quad (3.5.17)$$

as already argued when studying Drell-Yan production, we expect the integrals on the squared amplitude to carry contributions of the form  $[m_H^2(1-x_1)^2]^{-m}$  which leave factors of  $[1-x_1]^{-1+2m\epsilon}$  that, by interfering with poles, produce plus distributions with increasingly high powers as the order of poles, and so the number of soft emissions, increases.

Consider now the integral on  $(k')^2$ . Using again energy conservation we can show that

$$0 \leq (k')^2 \leq l^2 + m_H^2 - 2\sqrt{l^2} \sqrt{m_H^2 + p_z^2}. \quad (3.5.18)$$

Writing the RHS in terms of  $x_1$  and  $x_2$  and expanding in  $x_1$  we find

$$0 \leq (k')^2 \leq sw(1-z_1)(1-z_2). \quad (3.5.19)$$

Introducing again a dimensionless slider variable  $v$

$$(k')^2 = vsu(1-x_1)(1-x_2) \quad (3.5.20)$$

the integral on  $(k')^2$  becomes

$$\int_0^{k'_m ax} dk'^2 d\phi_n = (1-x_1)(1-x_2) su \int_0^1 dv d\phi_n. \quad (3.5.21)$$

In terms of the slider variable the soft scale is

$$(k'^2)^{-1+(n-1)-(n-1)\epsilon} \propto [m_H^2(1-x_1)(1-x_2)]^{-1+(n-1)-(n-1)\epsilon}, \quad (3.5.22)$$

that, again, combined the squared amplitudes, gives singular factors of  $[(1-x_1)(1-x_2)]^{-1-(n-1)\epsilon}$  that, by interference with  $\epsilon$  poles, produces plus distributions.

To sum up, using the techniques and the results of section 2.2.1 we have shown that the Higgs boson rapidity distribution depends on two singular scales

- $\Lambda_{DY}^2 = m_H^2(1-x_1)^2$ , rising from the DY-like phase subspace of soft emissions;

- $\Lambda_{DIS}^2 = m_H^2(1 - x_1)(1 - x_2)$ , rising from the DIS-like phase subspace of collinear emissions.

Of course in the case the singly soft limit  $x_2$  is fixed so for the DIS scale  $m_H^2(1 - x_2)$  is the hard scale, while in the doubly soft limit the only hard scale is  $m_H^2$ .

As already observed, the phase space decomposition we have employed is just a rewriting of the total phase space. Integrating on all partonic four-momenta all the possible kinematical configurations contributing to the threshold limit are covered, such as the case in which all the extra-emissions are collinear or the case in which they are all soft. The difference among these configurations is the maximum power of the singular logarithms they give rise to. For example, the integration region of the phase space where  $n + m$  partons are collinear, squared amplitudes coming from diagrams with  $n + m$  parton emissions on external legs will give the correct factors and poles to originate a logarithm of power  $n + m$  in the  $\Lambda_{DIS}^2$  scale. In the total phase space however it is also included the region where one of those parton is soft. Because softness implies collinearity, integration will give one more  $\epsilon$  pole that, by interference, may contribute to one more power of the collinear logarithm or to a single logarithm in the  $\Lambda_{DY}^2$  case. Tree diagrams where all partons are emitted on internal legs and region of phase spaces where no emission is soft or collinear do not originate to any logarithm and are therefore subleading in the threshold limit.

## 3.6 Resummation of the rapidity distribution

In this section finally write and discuss resummation formulae for the rapidity distribution applying equations 2.3.2 and 2.3.3. Firstly we discuss the explicit form of the singular scales in Mellin-Mellin space and their consequence on the resummation formulae. Secondly, we write the resummation formulae in the doubly soft limit, which is well known in literature and, finally, we write the resummation formulae for the singly soft limit, whose check is the final scope of this thesis.

### 3.6.1 Singular scales in Mellin-Mellin space

We have seen explicitly in the previous chapter that resummation must be performed in Mellin space, that is in the case of rapidity distributions the Mellin-Mellin space. Under this transformation we have observed that plus distributions become logarithms in Mellin space, which are the contributions that are materially resummed. Working with two Mellin variables the situation is slightly different and so it is worth to briefly discuss it.

Consider the DIS scale in the doubly soft limit  $(1 - x_1)(1 - x_2)$ . We have observed that combination of phase space and squared amplitude factors

give expressions of the form  $[(1-x_1)(1-x_2)]^{-1+\epsilon}$  that, interfering with poles, give rise to plus distributions. In Mellin-Mellin space these factors become

$$\begin{aligned} \int_0^1 dx_1 x_1^{N_1-1} \int_0^1 dx_2 x_2^{N_2-1} (1-x_1)^{-1+\epsilon} (1-x_2)^{-1+\epsilon} &= \\ = \int_0^1 dx_1 x_1^{-1+N_1} (1-x_1)^{-1+\epsilon} \int_0^1 dx_2 x_2^{-1+N_2} (1-x_2)^{-1+\epsilon} &= \beta(N_1, \epsilon) \beta(N_2, \epsilon), \end{aligned} \quad (3.6.1)$$

where we have used the definition of the  $\beta$  function. Using the equivalence of  $x \rightarrow 1$  and  $N \rightarrow \infty$  limit, shown in the previous chapter, we can apply the Stirling approximation on  $\beta$  functions

$$\beta(N, \epsilon) \approx \frac{1}{\epsilon} \frac{\Gamma(1+\epsilon)}{N^\epsilon} + \mathcal{O}\left(\frac{1}{N}\right). \quad (3.6.2)$$

Combining together, the Mellin-Mellin transform of the  $\Lambda_{DIS}^2$  scale gives contributions of the form

$$\int_0^1 dx_1 x_1^{N_1-1} \int_0^1 dx_2 x_2^{N_2-1} (1-x_1)^{-1+\epsilon} (1-x_2)^{-1+\epsilon} = \frac{1}{\epsilon^2} \frac{\Gamma(1+\epsilon)^2}{(N_1 N_2)^\epsilon}. \quad (3.6.3)$$

We see explicitly that interference with poles gives logarithms of the type  $\ln^p(N_1 N_2)$ . This argument does not work in the singly soft limit since, keeping fixed  $x_2$ , the soft scale will be multiplied by a certain function of  $x_2$  with a generic Mellin transform. In this case the Mellin DIS scale is simply  $\ln N_1$ .

Consider now the DY scale  $(1-x_1)^2$ . In dimensional regularization it emerges as  $(1-x_1)^{-1+2\epsilon}$ . Focusing on the doubly soft limit the Mellin-Mellin transform in the threshold limit gives

$$\begin{aligned} \int_0^1 dx_1 x_1^{N_1-1} \int_0^1 dx_2 x_2^{N_2-1} (1-x_1)^{-1+2\epsilon} &= \frac{1}{N_2} \beta(N_1, 2\epsilon) \approx \\ \approx \frac{1}{N_2} \frac{1}{2\epsilon} \frac{\Gamma(1+2\epsilon)}{N_1^{2\epsilon}} + \mathcal{O}\left(\frac{1}{N_1}\right). \end{aligned} \quad (3.6.4)$$

Now the large logarithm is of the form  $\ln^p N_1^2$ . However, since  $|N_2| \rightarrow \infty$ , these contributions are subleading with respect to the Mellin DIS scale  $\ln N_1 N_2$ . In the singly soft limit, since  $N_2$  is fixed, these terms are not subleading and are resummed together with the  $N_1 N_2$  logarithms.

### 3.6.2 Resummation formulae: doubly soft limit

In section 2.3 we have discussed the derivation of threshold resummation formulae in the case of differential distribution. The main complication with respect to total cross sections is the greater number of soft scales and therefore of singular logarithms that must be resummed. We have observed that by

generalizing the factorization assumption 2.2.26, resummation formulae can be derived straightforwardly. Now, for the case of rapidity distributions we have identified the scales from the phase space analysis, so it is sufficient to apply 2.3.2 and 2.3.3,

Consider first the doubly soft limit. From the first equation we have

$$C\left(N_1, N_2 m \frac{m_H^2}{\mu^2}, \alpha_s(m_H^2)\right) = C^{(c)}\left(\frac{m_H^2}{\mu^2}, \alpha_s(m_H^2)\right) \quad (3.6.5)$$

$$\exp\left\{\int_1^{N_1^2} \frac{dn}{n} \int_{n\mu^2}^{m_H^2} \frac{dk^2}{k^2} \hat{g}_1(\alpha_s(k^2/n), N_2) + \int_1^{N_1 N_2} \frac{dn}{n} \int_{n\mu^2}^{m_H^2} \frac{dk^2}{k^2} \hat{g}_2(\alpha_s(k^2/n))\right\}.$$

Following the previous discussion, the first integrals produces subleading contributions in the doubly soft limit so that consistently the resummation formula is simply

$$C\left(N_1, N_2 m \frac{m_H^2}{\mu^2}, \alpha_s(m_H^2)\right) = C^{(c)}\left(\frac{m_H^2}{\mu^2}, \alpha_s(m_H^2)\right) \exp\left\{\int_1^{N_1 N_2} \frac{dn}{n} \int_{n\mu^2}^{m_H^2} \frac{dk^2}{k^2} \hat{g}_2(\alpha_s(k^2/n))\right\}, \quad (3.6.6)$$

That is practically the total cross section formula with  $N_1 N_2 = N$ . This suggests that resummation in the doubly soft limit could have also been derived in Mellin-Fourier space. Indeed one can show [12] that Fourier transforming the coefficient function  $C(x, y)$  with respect to rapidity, expanding the Fourier exponential and reverting back the transformation, the coefficient function in the doubly soft limit factorizes as  $C(x, y) = C(x)\delta(y)$  plus subleading terms in  $x$ . Thus the resummation of the differential cross section can be reduced to that of the total.

This final formula we have obtained can be shown to be equivalent to the following formula already known for a long time [13]:

$$C\left(N_1, N_2, \frac{m_H^2}{\mu^2}, \alpha_s(m_H^2)\right) = C^{(c)}\left(\frac{m_H^2}{\mu^2}, \alpha_s(m_H^2)\right)$$

$$\exp\left\{\int_0^1 \int_0^1 dx_1 dx_2 \frac{x_1^{N_1-1} x_2^{N_2-1} - 1}{(1-x_1)(1-x_2)} g_2(\alpha_s(m_H^2(1-x_1)(1-x_2)))\right.$$

$$\left. \Theta(m_H^2(1-x_1) - \mu^2) \Theta(m_H^2(1-x_2) - \mu^2)\right\}. \quad (3.6.7)$$

### 3.6.3 Resummation formulae: singly soft limit

We finally get to the original result presented in [1], that is the first fully analytical resummation of the singly soft limit of Higgs boson production. The

result follows by applying the resummation formulae shown in 2.3.

The two hard scales are  $m_H^2$  and  $m_H^2(1 - x_2)$ . In Mellin-Mellin space they become  $m_H^2$  and  $m_H^2/N_2$ . The two soft scales are found by multiplying the hard scales by  $(1 - x_1)^2$  and  $(1 - x_1)$  respectively. In Mellin-Mellin space these factors become  $1/N_1^2$  and  $1/N_1$ . Using this identifications, the two resummation formulae are

$$C\left(N_1, \frac{m_H^2}{\mu^2}, \frac{m_H^2/N_2}{\mu^2}, \alpha_s(\mu^2)\right) = C^c\left(\frac{m_H^2}{\mu^2}, \alpha_s(\mu^2)\right) \quad (3.6.8)$$

$$\exp\left\{\int_1^{N_1^2} \frac{dn}{n} \int_{n\mu^2}^{m_H^2} \frac{dk^2}{k^2} g_1(\alpha_s(k^2/n), N_2) + \int_1^{N_1 N_2} \frac{dn}{n} \int_{n\mu^2}^{m_H^2/N_2} \frac{dk^2}{k^2} g_2(\alpha_s(k^2/n))\right\},$$

and

$$C\left(N_1, \frac{m_H^2}{\mu^2}, \frac{m_H^2/N_2}{\mu^2}, \alpha_s(\mu^2)\right) = C^c\left(\frac{m_H^2}{\mu^2}, \alpha_s(\mu^2)\right) \quad (3.6.9)$$

$$\exp\left\{\int_0^1 dx_1 \frac{x_1^{N_1-1} - 1}{1 - x_1} \int_{\mu^2}^{m_H^2(1-x_1)^2} \frac{d\lambda^2}{\lambda^2} \hat{g}_1(\alpha_s(\lambda^2), N_2) + \int_0^1 dx_1 \frac{x_1^{N_1-1} - 1}{1 - x_1} \int_{\mu^2}^{\frac{m_H^2}{N_2}(1-x_1)} \frac{d\lambda^2}{\lambda^2} \hat{g}_2(\alpha_s(\lambda^2), N_2)\right\}.$$

Clearly, the resummation formula for  $x_2 \rightarrow 1$  can be obtained by exchanging  $x_1$  and  $x_2$ .

### 3.7 The question of verification

Having derived the resummation formulae, the next natural steps are two. Firstly, check the predicted logarithms with the singular logarithms in the fixed order expression, secondly compare with other existing resummation results.

As mentioned, the only other resummation result for threshold rapidity distribution available in literature was derived in an unpublished paper by F.J. Tackmann et alii [8]. The formula is derived in the context of Soft-Collinear Effective Theory (SCET), in an implicit form which can be solved only numerically. Perturbative solutions however can give explicitly the resummed logarithms order-by-order. This was done in [14], where expressions in the SCET formalism were translated into the standard, or *direct*, QCD framework. The results shows that the resummation we have just presented has some logarithmic contributions that are in missing in [8], particularly relating the soft scale  $m_H^2(1 - x_1)^2$ .

This motivates us to first check our formula with the first non-trivial fixed order result of Higgs boson production, the next-to-next leading order. This

cannot be done by simple comparison neither in Mellin-Mellin space or in real space, since the soft scale we predicted,  $\ln(1 - x_1)^2$ , differs from simple  $\ln(1 - x_1)$  by a factor of 2. For this reason in the fixed-order expression we will not only check the explicit form of the singular logarithms, but also how they arise from calculations, in order to check whether their origin is the same predicted by our phase-space argument.

Eventually, to finally establish the resummation formula, it is necessary to fully understand the reason of the different results in our direct QCD approach and in the SCET formalism.

## Chapter 4

# Gluon fusion at NNLO

4.1	Gluon fusion at LO . . . . .	56
4.2	Gluon fusion at NLO . . . . .	56
4.2.1	Virtual contribution at NLO . . . . .	57
4.2.2	Real contribution at NLO . . . . .	57
4.2.3	NLO in $(x, u, m_H^2)$ . . . . .	60
4.2.4	NLO in $(x_1, x_2, m_H^2)$ . . . . .	62
4.3	Gluon fusion at NNLO . . . . .	63
4.3.1	Relevant variables . . . . .	63
4.3.2	Phase space at NNLO . . . . .	64
4.3.3	The fully differential distribution at NNLO . . . . .	69
4.3.4	Retracing logarithms . . . . .	75

In this section we study both the phase spaces and the final results of Higgs boson production through the gluon fusion channels at LO, NLO and NNLO in light of the phase space analysis conducted in the previous chapter. The scope is to verify whether the large logarithms predicted in section 3.5 and resummed by eqs. 3.6.8 and 3.6.9 do actually appear in the fixed order calculation and whether the origin is the same of the one predicted.

In the first two sections we derive the LO and NLO result from the squared amplitudes, discussing both the rapidity distribution and the fully differential cross section. In the last section we focus on the final result of the NNLO fully differential distribution published in [2]. After a brief discussion on the relevant variables, we apply the phase space machinery of the previous chapter in the special case of two emissions. This makes possible to predict the form of the singular logarithms in terms of the Mandelstam invariants  $t$  and  $u$  and in terms of the maximum mass of the extra radiation  $Q_{max}^2$ . In particular, we see that the collinear scale arises as  $\ln Q_{max}^2$  and the soft scale as  $\ln t$  (or, symmetrically,  $\ln u$ ). The phase space argument is finally verified in two steps: firstly, checking the actual form of singular logarithms from [2]. In order to study the threshold limit of the rapidity distribution on the fully



differential distributions, all variables are written in terms of a set of independent variables with extrema independent on  $x_1$  and  $x_2$ . Secondly, after having passed the first test, the actual origin of the logarithm is retraced from intermediate results contained in [5] and it is compared with the corresponding predictions.

## 4.1 Gluon fusion at LO

We have already discussed in section 3.1 the fundamentals of Higgs boson production. The most relevant partonic subprocess at LHC is gluon fusion

$$g + g \rightarrow H(p_H) + X(p_X), \quad (4.1.1)$$

that can be computed in the infinite top mass approximation. In this context the top loop (figure 3.1) collapses into an effective vertex proportional to the total cross section at this order (eq. 3.1.3).

The LO rapidity distribution is trivial since the Higgs boson is necessarily produced at rest. To review the variables defined in the previous chapter we write explicitly the result. First, in terms of  $(x, y, m_H^2)$ , at rest not only  $x = 1$  but  $y = 0$ , therefore

$$\frac{d\sigma^{(0)}}{dy} = \sigma_0 \delta(1 - x) \delta(y). \quad (4.1.2)$$

At rest  $x_1$  and  $x_2$  (eqs. 3.3.6) are 1, so in terms of these variables the LO rapidity distribution is

$$\frac{d\sigma^{(0)}}{dy} = 2\sigma_0 \delta(1 - x_1) \delta(1 - x_2). \quad (4.1.3)$$

Finally, in terms of  $x$  and  $u$  the rapidity distributions reads

$$\frac{d\sigma^{(0)}}{dy} = \frac{1}{2} \sigma_0 \delta(1 - x) \delta(u(1 - u)). \quad (4.1.4)$$

Clearly, the result does not display any large logarithms since at this order there are no QCD emissions. Notice that the doubly differential cross section would have in addition a  $\delta(p_T^2)$  that is left also after integration on the partonic momentum fractions  $\xi_1$  and  $\xi_2$ . For this reason, the fully differential distribution at LO is often ignored and the actual LO is taken to be the fully differential distribution at the next order.

## 4.2 Gluon fusion at NLO

In this section we derive the NLO gluon fusion rapidity distribution starting from the squared amplitude. This will serve mainly as a first application

to the basics of perturbative QCD presented in chapter 1 and for an introduction to some features we will see in the NNLO calculation, such as the  $p_T^2$  singularity. The final results will also clarify the discussion of the previous chapter on the dependence of the result on  $N_1 N_2$  in the doubly soft limit, elucidating what it does imply in the real space. Results are checked with existing literature [15].

As discussed in the first chapter, beyond LO inclusive cross sections are calculated by combining real and virtual contributions. The first is made up integrating on the phase space the sum of all the squared amplitudes of the  $2 \rightarrow 2$  process, that in this case is only  $gg \rightarrow Hg$ , while, similarly, the second comes from the squared amplitude of the 1-loop contributions to  $gg \rightarrow H$ .

Physically, we are already able to predict some features of the result. First, the extra radiation is an on-shell gluon that in the center-of-mass frame of reference it must recoil with the Higgs, so its momentum is completely determined by conservation laws. For this reason the transverse momentum and the rapidity of the Higgs are not independent: energy conservation constraint them to keep the gluon on-shell. Analytically, the virtuality of the extra radiation  $Q^2$  is 0, so the number of variables reduces and equation 3.2.2 fix the remaining.

#### 4.2.1 Virtual contribution at NLO

We take the virtual contribution from [16].

$$\sigma_{virt}^{(1)} = \sigma_0 \delta(1-x) \left[ \frac{\alpha_s}{2\pi} \left( \frac{4\pi\mu^2}{m_H^2} \right)^\epsilon \frac{\Gamma(1+\epsilon)\Gamma(1-\epsilon)^2}{\Gamma(1-2\epsilon)} \left( -\frac{2}{\epsilon^2} + \pi^2 \right) \right] \quad (4.2.1)$$

Expanding gamma functions in  $\epsilon$

$$\sigma_{virt}^{(1)} = \sigma_0 \delta(1-x) \left[ \frac{\alpha_s}{2\pi} \left( \frac{4\pi\mu^2}{m_H^2} \right)^\epsilon (1 - \epsilon\gamma_E) \left( -\frac{2}{\epsilon^2} + \pi^2 \right) \right]. \quad (4.2.2)$$

To get the rapidity distribution just add the correct  $\delta$  function in the desired variable. For later use we write explicitly

$$\frac{\sigma_{virt}^{(1)}}{du} = \sigma_0 \delta(u(1-u)) \delta(1-x) \left[ \frac{\alpha_s}{2\pi} \left( \frac{4\pi\mu^2}{m_H^2} \right)^\epsilon (1 - \epsilon\gamma_E) \left( -\frac{2}{\epsilon^2} + \pi^2 \right) \right]. \quad (4.2.3)$$

#### 4.2.2 Real contribution at NLO

We compute the real contribution to the NLO cross sections starting from the squared amplitude of the process

$$g(p_1) + g(p_2) \rightarrow H(p_H) + g(k). \quad (4.2.4)$$

Amplitudes are calculated considering four tree diagrams: two of these carry the extra emission on the two legs of the incoming partons. These are the origin of soft and collinear singularities we will regularize in  $d$ -dimensions. Notice that the collinear singularity comes from an initial-state emission, therefore we also expect poles proportional to splitting functions cancelled by PDFs renormalization. The unpolarized squared amplitude is [16]

$$|\mathcal{M}|_{unp}^2 = \frac{3\alpha^3}{72\pi v^2(1-\epsilon)^2} \left[ \frac{m_H^8 + s^4 + t^4 + u^4}{stu} (1-2\epsilon) + \frac{\epsilon}{2} \frac{(m_H^4 + s^2 + t^2 + u^2)^2}{stu} \right]. \quad (4.2.5)$$

Notice that, even if coming from the computation of tree diagrams, the result displays a dependency on  $\epsilon$ . Computing quantities in  $d$ -dimensions, all functions depending on the number of dimensions, such as polarizations and spin, carry a dependency on  $d$  and hence on  $\epsilon$ . The squared amplitude is regular for  $\epsilon = 0$ , but this limit must be taken only at the end of calculations because  $\mathcal{O}(\epsilon)$  terms contribute to the final result combining with order one  $\epsilon$  poles. The total real contribution is

$$\frac{d\sigma_{real}^{(1)}}{dy} = \Phi \int d\phi_2 |\mathcal{M}|_{unp}^2, \quad (4.2.6)$$

where  $\Phi = 1/2s$ . The regularized two-body phase space integral of the process is

$$d\phi_2(s; p_H, k) = \frac{d^{d-1}p_H}{(2\pi)^3 2p_H^0} \frac{d^{d-1}k}{(2\pi)^3 2k^0} \delta^{(d)}(p_1 + p_2 - p_H - k) (2\pi)^d. \quad (4.2.7)$$

This can be computed in different ways. Firstly, the phase space is equivalent to the result for the Higgs emission phase space  $d\phi_2$ , so the result can be recycled

$$d\phi_2 = \frac{(4\pi)^{-\epsilon} |p_T|^{-2\epsilon}}{16\pi\Gamma(1-\epsilon)p_H^0 k^0} dp_T^2 dp_z \delta(\sqrt{s} - p_H^0 - k^0) |\mathcal{M}|^2 \quad (4.2.8)$$

Choosing as variables  $(s, m_H^2, y)$ , the Dirac  $\delta$  can be written in order to eliminate the integration on the transverse momentum,

$$d\phi_2 = \frac{(4\pi)^\epsilon |p_T|^{-2\epsilon}}{16\pi\Gamma(1-\epsilon)} \frac{s + m^2}{2s \cosh^2 y} dp_T^2 dy \delta(p_T^2 - p_{T,max}^2), \quad (4.2.9)$$

Notice that at this point we have integrated on the gluon momentum measure  $d^{d-1}k$ , so one could naively ask where are the soft and collinear poles that we have repeatedly mentioned in previous chapters. We will see how these missing poles arise later, but we can understand physically what it is going on. The momentum of the gluon is fixed by conservation laws, this made possible to eliminate the corresponding differential with the Dirac delta. For this reason the actual configuration of the gluon is determined by  $p_T^2$  and  $y$ ,

and therefore we expect the squared amplitude to be singular for  $p_T^2 \rightarrow 0$  (collinear limit) and for  $p_T^2, y \rightarrow 0$  (soft limit), as we will shortly verify. Because of this, if we were calculating the fully differential cross section the result would already be established out of the collinear region, since it is not necessary to compute any divergent integral producing poles, and the virtual contribution, as mentioned in the previous section, does not exist since it has a completely trivial kinematics. The limit  $\epsilon \rightarrow 0$  can be safely taken, and the final result is

$$\frac{d^2\sigma^{(1)}}{dp_T^2 dy} = \frac{1}{2s} \frac{1}{16\pi} J \frac{3\alpha_s^3}{72\pi v^2} \frac{m_H^8 + s^4 + t^4 + u^4}{stu} = \frac{\sigma_0}{s} \alpha_s \frac{m_H^8 + s^4 + t^4 + u^4}{stu} \delta(Q^2) \quad (4.2.10)$$

where  $\sigma_0$  is given by equation 3.1.3 and for brevity the Jacobian  $(s+m_H^2)/2s \cosh^2 y$  coming from the variable transformation has been simply renamed  $J$ .

Getting back to the the rapidity distribution, combining what we have found so far

$$\begin{aligned} \frac{d\sigma_{real}^{(1)}}{dy} &= \frac{(4\pi)^\epsilon |p_{T,max}|^{-2\epsilon}}{\Gamma(1-\epsilon)} \frac{s+m^2}{2s \cosh^2 y} \frac{\sigma_0 \alpha_s}{2(1-\epsilon)^2} \frac{1}{s^2 t u} \\ &\quad [ (m_H^8 + s^4 + t^4 + u^4)(1-2\epsilon) + \frac{\epsilon}{2}(m_H^4 + s^2 + t^2 + u^2)^2 ]. \end{aligned} \quad (4.2.11)$$

Now it is time to choose a consistent set of independent variables. We choose two sets,  $(x, u, m_H^2)$  and  $(x_1, x_2, m_H^2)$ . The first one is needed to check the calculation with [15], the second one is the natural one to study resummation. From equations 3.2.6 and 3.2.2 we find the Mandelstam invariants  $t$  and  $u$ , the Jacobian  $J$  and  $p_{T,max}^2$  in terms of  $(s, y, m_H^2)$

$$\begin{aligned} t &= m^2 - \frac{s+m^2-Q^2}{2 \cosh y} e^{-y}, \\ u &= m^2 - \frac{s+m^2-Q^2}{2 \cosh y} e^y. \end{aligned} \quad (4.2.12)$$

These relations are valid at any order, but at LO they simplify because  $Q^2 = 0$ . From these relations it is now straightforward to get  $t$  and  $u$  in terms of  $(x_1, x_2, m_H^2)$

$$\begin{aligned} t &= -m^2 \frac{1-x_1^2}{x_1(x_1+x_2)} & J &= \frac{2(1+x_1x_2)x_1x_2}{(x_1+x_2)^2} \\ u &= -m^2 \frac{1-x_2^2}{x_2(x_1+x_2)} & p_{T,max}^2 &= m_H^2 \frac{(1-x_1)^2(1-x_2)^2}{(x_1+x_2)^2}, \end{aligned} \quad (4.2.13)$$

notice that  $t$  and  $u$  are correctly negative.

Equations 3.3.8 give the corresponding relations<sup>1</sup>

$$\begin{aligned} t &= -m^2 \frac{1-x}{x} u & J &= \frac{2[1+u(x-1)][x+u(1-x)]}{1+x} \\ u &= -m^2 \frac{1-x}{x} (1-u) & p_{T,max}^2 &= \frac{m^2(1-u)u(1-x)^2}{x}, \end{aligned} \quad (4.2.14)$$

#### 4.2.3 NLO in $(x, u, m_H^2)$

First let us carry on the computation in the variables  $(x, u, m_H^2)$ . In this set it is also necessary to consider the Jacobian given by changing the differential variable  $y$  into  $u$  written in equation 3.3.10. This greatly simplifies the multiplicative factors given by the other Jacobian in equation 4.2.14. Combining together

$$\begin{aligned} \frac{d\sigma_{real}^{(1)}}{dy} &= \frac{3\sigma_0\alpha_s}{2} \left( \frac{4\pi\mu^2}{m_H^2} \right)^\epsilon [1 - \epsilon\gamma_E](1 + 2\epsilon)[\ln x]^\epsilon [u(1-u)]^{-1-\epsilon} [1-x]^{-1-2\epsilon} \\ &\quad \left\{ \left[ 1 + x^4 + (1-x)^4(y^4 + (1-u)^4) \right] (1 - 2\epsilon) + \frac{\epsilon}{2} \left[ 1 + x^2 + (1-x)^2(u^2 + (1-u^2)) \right]^2 \right\}. \end{aligned} \quad (4.2.15)$$

Firstly, we have introduced the renormalization scale  $\mu^2$  regularizing the dimension of  $\alpha_s$ . Secondly, the expansion of the  $\Gamma$  function led to the Euler constant  $\gamma_E$ . These two factors can be ignored since, following the  $\overline{MS}$  cancellation scheme, they are always cancelled by the virtual contribution. Finally, notice that the Mandelstam invariants  $s, t$  and  $u$  in the denominator of the squared amplitude, being proportional to  $(1-z), (1-u)$  and  $u$ , have been included in the same factors that appeared in  $|p_{T,max}^2|^{-\epsilon}$ . Clearly, these are divergent in the singly and doubly soft limit and are exactly the  $p_T^2$  divergence we mentioned in the previous section, since at LO

$$p_T^2 = \frac{tu}{s}. \quad (4.2.16)$$

Applying the distributional identity 1.8.5, these terms give plus distributions that regularize the  $u$  integrals, necessary to get the total cross section, and the integrals on the parton momentum fractions  $\xi_1$  and  $\xi_2$ , since  $x = \tau/\xi_1\xi_2$  and  $\tau = \xi_1\xi_2$  in the inferior limit of the integration range. The same distributional identity gives an  $\epsilon$  pole from  $u(1-u)$  and another pole from  $(1-x)$ . Obviously, these are respectively the collinear and the soft pole. These are the missing poles we have mentioned in the previous section. Expanding the

---

<sup>1</sup>The Mandelstam variable and the angular variable  $u$  can be easily told apart from the context

relevant exponentials we find

$$\begin{aligned} \frac{dC_{real}^{(1)}}{dy} \propto [1 + \epsilon \log x] & \left[ -\frac{\delta(u(1-u))}{\epsilon} + \left( \frac{1}{u(1-u)} \right)_+ - \epsilon \left( \frac{\log(u(1-u))}{u(1-u)} \right)_+ \right] \\ & \left[ -\frac{\delta(1-x)}{2\epsilon} + \left( \frac{1}{1-x} \right)_+ - 2\epsilon \left( \frac{\log(1-x)}{1-x} \right)_+ \right] (1 + 2\epsilon) \\ & \left\{ \left[ 1 + x^4 + (1-x)^4(u^4 + (1-u)^4) \right] (1 - 2\epsilon) + \frac{\epsilon}{2} \left[ 1 + x^2 + (1-x)^2(u^2 + (1-u^2)) \right]^2 \right\}. \end{aligned} \quad (4.2.17)$$

The result contains both second order and first order poles. The double pole is proportional to  $\delta(u(1-u))\delta(1-x)$  and cancels with the pole in the virtual contribution 4.2.3, that has the same kinematics. The virtual contribution however carries also a finite term proportional to  $\pi^2$  which contributes to the final result. The first order poles are only proportional to  $\delta(u(1-u))$ . First order poles from  $\delta(1-z)$  cannot rise, since it implies  $u = 0 \vee u = 1$ , and so every term proportional to  $\delta(1-x)$  must also be proportional to  $\delta(u(1-u))$ . This is equivalent to say that the first order poles can only be collinear, since, if they were soft, they would also carry the collinear pole, since softness implies collinearity. The first order poles are cancelled by the Altarelli-Parisi term (see equation 1.3.28 in [16]), that is proportional to the gluon-gluon splitting function

$$P_{gg}(x) = 3 \left[ \frac{1 + x^4 + (1-x)^4}{(1-x)_+ x} \right] + \beta_0 \delta(1-x). \quad (4.2.18)$$

Clearly, the second term cancels single  $\epsilon$  poles coming from terms proportional to  $\delta(1-x)\delta(u(1-u))$ . Notice that the numerator of the splitting function exactly matches the expressions appearing in the squared amplitudes for  $u = 0 \vee u = 1$ .

Applying partial fraction decomposition the final result is [15]

$$\begin{aligned} \frac{d\sigma^{(1)}}{du} = 3\sigma_0 & \left\{ \frac{1}{2} \delta(u(1-u)) \delta(1-x) \left( \frac{\pi^2}{3} + \frac{11}{6} \right) + \right. \\ & + \delta(u(1-u)) \left[ 2 \left( \frac{\log(1-x)}{1-x} \right)_+ - (x^2 - x + 1)^2 \frac{\log(x)}{1-x} - 2x(x^2 - x + 2) \log(1-x) \right] \\ & \left. + 2 \left( \frac{1}{1-z} \right)_+ \left( \frac{1}{u(1-u)} \right)_+ - x(x^2 - x + 2) \left( \frac{1}{u(1-u)} \right)_+ - (1-x)^3 [2 - u(1-u)] \right\}. \end{aligned} \quad (4.2.19)$$

#### 4.2.4 NLO in $(x_1, x_2, m_H^2)$

We now shortly derive and interpret the same result in terms of the threshold variables  $(x_1, x_2, m_H^2)$ .

The starting point is

$$\begin{aligned} \frac{d\sigma_{real}^{(1)}}{dy} = & \frac{3\sigma_0\alpha_s}{2} J(x_1, x_2) \left( \frac{4\pi\mu^2}{m_H^2} \right)^\epsilon [1 - \epsilon\gamma_E](1 + 2\epsilon) \left[ \frac{(x_1 + x_2)^2}{(1 + x_1)(1 + x_2)} \right]^\epsilon [1 - x_1]^{-1-\epsilon} [1 - x_2]^{-1-\epsilon} \\ & \left\{ (x_1 + x_2)^4 (1 + x_1^4 x_2^4) + x_2^4 (1 - x_1)^4 + x_1^4 (1 - x_2)^4 (1 - 2\epsilon) + \right. \\ & \left. + \frac{\epsilon}{2} \left[ (x_1 + x_2)^2 (1 + x_1^2 x_2^2) + (1 - x_1)^2 x_2^2 + (1 - x_2)^2 x_1^2 \right]^2 \right\}. \end{aligned} \quad (4.2.20)$$

Now the the distributional identity 1.8.5 give rise to plus distributions in  $x_1$  and  $x_2$  regularizing the collinear and soft divergences in the denominator  $stu$  of the square amplitudes. While in terms of the variables  $x$  and  $u$  each type of divergence was clearly explicit, in terms of  $x_1$  and  $x_2$  the collinear divergence is obtained in the limit  $x_1 \rightarrow 1$  keeping  $x_2$  fixed and vice versa, while the soft divergence when  $x_1, x_2 \rightarrow 1$ , which of course implies the collinear divergence.

The result has the following structure

$$\begin{aligned} \frac{d\sigma_{real}^{(1)}}{dy} = & \frac{3\sigma_0}{2} J(x_1, x_2) \left\{ f_{00}(x_1, x_2) \delta(1 - x_1) \delta(1 - x_2) + \right. \\ & \delta(1 - x_2) \left[ f_{01}(x_1) \left( \frac{1}{1 - x_1} \right)_+ + f_{02}(x_1) \left( \frac{\ln(1 - x_1)}{1 - x_1} \right)_+ \right] + (x_1 \leftrightarrow x_2) + \\ & \left. + f_{11}(x_1, x_2) \left( \frac{1}{1 - x_1} \right)_+ \left( \frac{1}{1 - x_2} \right)_+ \right\}. \end{aligned} \quad (4.2.21)$$

$f_{ij}$  are regular functions of  $x_1$  and  $x_2$  in the threshold limit involving polynomials and logarithms. This structure comes naturally from expanding the product  $(1 - x_1)(1 - x_2)$  with the distributional identity 1.8.5. Under Mellin-Mellin transform this result displays terms which are not subleading in the doubly soft limit: this implies that at this order resummation formulae for the doubly soft limit 3.6.6 and for the singly soft limit 3.6.8 resum the same type of logarithms. In this context we can also test the argument made in the previous section, that is that the doubly soft limit logarithms must depend only on  $N_1 N_2$ . To simplify the calculation the doubly soft limit can be

directly taken from equation 4.2.20. This gives a result proportional to

$$32(1+\epsilon)(1-x_1)^{-1-\epsilon}(1-x_2)^{-1-\epsilon} \quad (4.2.22)$$

Expanding and transforming the logarithms with equation 2.2.14 we notice that they exactly combine so to form a binomial square (compare with [17])

$$\frac{C_{doublysoft}^{(1)}}{dy}(N_1, N_2) \propto \ln^2 N_1 N_2 + 2\gamma_E \ln N_1 N_2. \quad (4.2.23)$$

We have seen that at this order we can gain no insight in the subleading logarithms resummed by the singly soft limit formula. For this reason, it is necessary to get to NNLO.

### 4.3 Gluon fusion at NNLO

In this section we finally study the NNLO threshold scales of the rapidity distribution. Since the explicit result does not exist in literature, we study the doubly differential cross section in [2] comparing it to the phase space analysis of section 3.5 applied to the case of two emissions. In order to study the rapidity distribution in terms of the doubly differential cross section we must first study with more details the threshold behaviour of the variables introduced in section 3.2. Secondly, following section 3.5, we study the possible decomposition of the phase space for two extra-emissions, singling out the DY and DIS scale predicted and, most importantly, writing them in terms recognizable in the result from [2]. Finally, we get to the fully differential distribution. Some manipulations will highlight the singular scales in threshold limit revealing the predicted logarithms. Their origin is retraced from [5] and compared with the phase space argument for resummation.

#### 4.3.1 Relevant variables

Up to now, we have always preferred sets of variables including  $x_1$  and  $x_2$  in order to study threshold properties of the results. However, in order to check our knowledge on Higgs boson production acquired through phase space analysis, we will have to compare our result to those of [2] which uses mainly Mandelstam invariants. As a useful reference we provide here some relations between variables and their behaviour in the threshold limit. The variable we are interested in are  $x_1, x_2, p_T^2, Q^2, s, t, u$  and  $m_H^2$ . Definitions and some relations were already determined in the previous chapter, particularly section 3.2. First consider the set  $(s, t, u, m_H^2)$ , the other variables in terms of these



are

$$p_T^2 = \frac{(t - m_H^2)(u - m_H^2)}{s} - m_H^2, \quad (4.3.1)$$

$$y = \frac{1}{2} \ln \frac{u - m_H^2}{t - m_H^2}, \quad (4.3.2)$$

$$Q^2 = s + t + u - m_H^2. \quad (4.3.3)$$

Consider now the threshold limit for the rapidity distribution. Since at NNLO we only know the doubly differential distribution, it is important to consider that some variables, such as  $Q^2$  and  $p_T^2$ , are not adequate since their kinematic boundaries depend on the threshold variables  $x_1$  and  $x_2$ . For this reason we define dimensionless variables ranging on fixed intervals. We have already determined the limits of  $Q^2$  in equation 3.2.9. Defining in an obvious way  $Q_{max}^2$ , let  $q$  be the slider variable

$$Q^2 = qQ_{max}^2, \quad (4.3.4)$$

such that for  $q = 0$   $Q^2$  is minimum and for  $q = 1$   $Q^2$  is maximum. Consider now the set  $(x_1, x_2, q, m_H^2)$ . This is special among the possible sets since in the threshold limit their boundaries are all effectively fixed and makes possible studying how the other variables behave in the threshold limit. In particular, consider the following relations

$$t = -m^2 \frac{(1 - x_1)}{x_1(x_1 + x_2)} [1 + x_1 + q(1 - x_2)], \quad (4.3.5)$$

$$u = -m^2 \frac{(1 - x_2)}{x_2(x_1 + x_2)} [1 + x_2 + q(1 - x_1)], \quad (4.3.6)$$

$$Q_{max}^2 = m_H^2 \frac{(1 - x_1)(1 - x_2)}{x_1 x_2}, \quad (4.3.7)$$

$$p_T^2 = m^2 \frac{(1 - q)(1 - x_1)(1 - x_2)}{(x_1 + x_2)^2} [(1 + x_1)(1 + x_2) - q(1 - x_1)(1 - x_2)]. \quad (4.3.8)$$

Notice that  $t$  and  $u$  are singular for the two possible singly soft limit, while  $Q_{max}^2$  and  $p_T^2$  are always singular.

### 4.3.2 Phase space at NNLO

At NNLO processes with two emissions start contributing. These have a more complex phase space that makes finally possible to see in practice some features of the space phase decomposition argument presented in section 3.3.1. Since in the threshold limit for any given value of the rapidity at least one gluon must be collinear to the Higgs boson for momentum conservation, the

two singular kinematical configurations contributing to the threshold limit that are integrated on are when the second emitted gluon is either collinear or soft.

Since the rapidity is fixed, the case where also the recoiling parton is soft manifests as a divergence in  $y \rightarrow 0$ . Similarly, in the doubly differential cross section, where  $p_T^2$  is fixed, the configuration where the recoiling gluon is collinear manifests as a divergence in  $p_T^2 \rightarrow 0$ .

Following section 3.5, we compute the phase space in two ways, highlighting the two different configurations we mentioned. Firstly, we include the extra gluon with the recoiling one in a DIS-like phase space (fig. 4.1), then we separate the extra emission in a DY-like phase space (fig. 4.2). We see the emergence of the two singular scales that we had already discovered in the previous chapter, and, most importantly, we rewrite them in terms of variables that will make them manifest in the result we will compare. Of course, the two phase spaces are still simplified relatively to the decomposition made in the previous chapter, but they are still enough to gain insight.

Consider the process

$$g(p_1) + g(p_2) \rightarrow g(k_1) + g(k_2) + H(p_H), \quad (4.3.9)$$

the phase space is

$$d\phi_3 = \frac{d^{d-1}k_1}{(2\pi)^{d-1}2k_1^0} \frac{d^{d-1}k_2}{(2\pi)^{d-1}2k_2^0} \frac{d^{d-1}p_H}{(2\pi)^{d-1}2p_H^0} (2\pi)^d \delta(p_1 + p_2 - k_1 - k_2 - p_H) \quad (4.3.10)$$

Now we employ the first factorization that will highlight the collinear scale: the two gluons are included in a two-body DIS-like phase space. (Fig. 4.1).

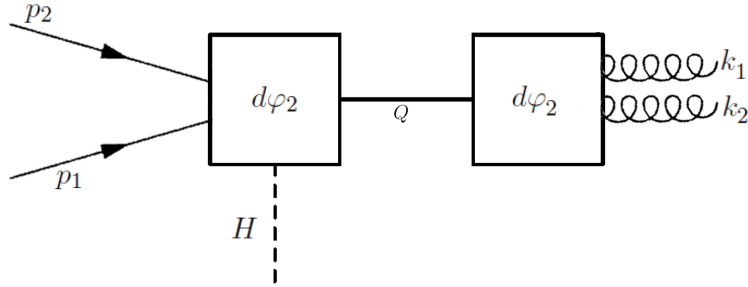


Figure 4.1: Phase space for Higgs boson production with two emissions. The three-body phase space is factorized into two two-body phase spaces. The first is the Higgs boson production phase space, the second is a DIS-like phase space with two emissions.

Using equation 2.2.2 this becomes

$$d\phi_3(p_1, p_2; k_1, k_2, p_H) = \int \frac{dQ^2}{2\pi} d\phi_2(p_1 + p_2; p_H, Q) d\phi_2(Q; k_1, k_2). \quad (4.3.11)$$

Where  $Q^2 = (k_1 + k_2)^2$  according to the notation introduced in section 3.2. The technique to calculate the first phase space is well-known

$$d\phi_2(p_1 + p_2; p_H, Q) = \frac{(4\pi)^\epsilon |p_T^2|^{-\epsilon}}{16\pi\Gamma(1-\epsilon)} \frac{dp_T^2 dy}{\sqrt{Q^2}} \delta(\sqrt{Q^2} - p_H^0 - \sqrt{s}). \quad (4.3.12)$$

The natural set of independent variables in this context, as explained in section 3.2, is  $(m_H^2, s, y, p_T^2)$  or  $(m_H^2, s, y, Q^2)$ . In both cases  $p_T^2$  and  $Q^2$  are not independent and the Dirac  $\delta$  can be used to eliminate the integral  $dp_T^2$  or  $dQ^2$ . If we were calculating the doubly differential cross section, the natural choice is the second, leaving thus

$$\frac{d\phi_2}{dp_T^2 dy} = \frac{(4\pi)^\epsilon |p_T^2|^{-\epsilon}}{16\pi^2\Gamma(1-\epsilon)} \int d\phi_2(Q; k_1, k_2), \quad (4.3.13)$$

where we have made explicit the integral on partonic momenta  $k_1$  and  $k_2$ . Calculating the rapidity distribution, following the approach in section 3.5, we may already eliminate the measure in  $dp_T^2$  using the Dirac  $\delta$ , leaving the integral in  $Q^2$  multiplied and the Jacobian of the  $\delta$  transformation  $|\frac{dp_T^2}{dQ^2}|$ .

Now consider the two-body phase space  $d\phi_2(Q; k_1, k_2)$ . Exploiting Lorentz invariance we compute it in the partonic center-of-mass frame of reference applying equation 2.2.3.

$$d\phi_2(Q; k_2, p_H) = \frac{1}{(4\pi)^{2-2\epsilon}} (Q^2)^{-\epsilon} d\Omega_\epsilon. \quad (4.3.14)$$

Notice that, since this phase space is DIS-like, the soft scale emerging is  $(Q^2)^{-\epsilon}$ , that is equivalent to the  $(k')^2$  scale found in section 3.5 and the scale  $s$  in section 2.2.1. Combining together we get

$$\frac{d\sigma_{real}^{(2)}}{dy}(s, y, m_H^2) = \frac{1}{2s} \frac{1}{512\pi^3\Gamma(1-\epsilon)} \int dQ^2 \left| \frac{dp_T^2}{dQ^2} \right| \left( \frac{4\pi}{\tilde{p}_T^2} \right)^\epsilon \left( \frac{4\pi}{Q^2} \right)^\epsilon \int d\Omega_\epsilon |\mathcal{M}(\Omega_\epsilon, s, y, m_H^2, Q^2)|^2, \quad (4.3.15)$$

Where  $\tilde{p}_T^2$  specifies that we are considering  $p_T^2$  in terms of the other 4 independent variables. If interested in getting the fully differential cross section,

$$\frac{d\sigma_{real}^{(2)}}{dy dp_T^2}(s, y, m_H^2, p_T^2) = \frac{1}{2s} \frac{1}{512\pi^3\Gamma(1-\epsilon)} \left( \frac{4\pi}{\tilde{p}_T^2} \right)^\epsilon \left( \frac{4\pi}{Q^2} \right)^\epsilon \int d\Omega_\epsilon |\mathcal{M}(\Omega_\epsilon, s, y, m_H^2, Q^2)|^2. \quad (4.3.16)$$

As both discussed and verified in the previous section,  $(p_T^2)^\epsilon$  combined with

collinear divergences in the squared amplitude regularizes them introducing a collinear pole proportional to  $\delta(p_T^2)$  and plus distributions. This makes the integral on  $p_T^2$  finite in the inferior extremum (or, as we will see shortly, the integral on  $Q^2$  finite in the superior extremum). If only interested in the fully differential hadronic cross section these factors can be ignored, as the integrals on partonic momentum fractions require regularization only with respect to longitudinal variables. such as  $x_1, x_2, x, u, y$ . Regularization or not, the fully differential distribution is of course divergent for  $p_T^2 \rightarrow 0$ , a problem that can be solved with  $p_T$  resummation. Now, following the strategy applied in section 3.5, we write the  $Q^2$  integral in terms of the slider variables  $q$  defined in the previous section. The scale  $(Q^2)^{-\epsilon}$  becomes

$$(Q^2)^{-\epsilon} = q^{-\epsilon} (Q_{max}^2)^{-\epsilon}. \quad (4.3.17)$$

The exponential  $q$  regularizes the  $Q^2$  integral for  $q \rightarrow 0$ , the remaining quantity is the DIS scale discussed in the previous chapter, as the explicit form of  $Q_{max}^2$  shows

$$Q_{max}^2 = m_H^2 \frac{(1-x_1)(1-x_2)}{x_1 x_2}. \quad (4.3.18)$$

Considering  $p_T^2$  in terms of the threshold variables and  $q$  in eq. 4.3.5, we notice that  $q \rightarrow 1$  implies  $p_T^2 \rightarrow 0$ , that is to say that the  $(p_T^2)^\epsilon$  makes possible the regularization the  $q$  integral in its other extremum. .

Now we get to the second factorization of the phase space, that will highlight the soft scale. The second gluon is produced with the massive state  $l = k_1 + k_2$  in a DY-like phase space (Fig. 4.2). Employing the usual fac-

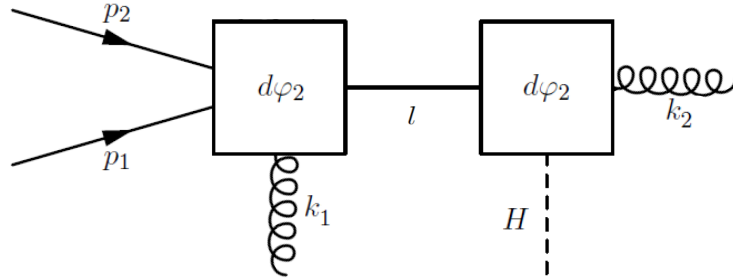


Figure 4.2: Phase space for Higgs boson production with two emissions. The three-body phase spaced is factorized into two two-body phase spaces. The first is a DY-like phase space with a single emission, the second is the Higgs boson production phase space.

torization identity 2.2.2, the phase space is

$$d\phi_3(p_1 + p_2; k_1, k_2, p_H) = \int \frac{dl^2}{2\pi} d\phi_2(p_1 + p_2; k_1, l) d\phi_2(l; p_H, k_2), \quad (4.3.19)$$

the second term is the usual Higgs boson production phase space,

$$d\phi_2(l; k_2, p_H) = \frac{(4\pi)^\epsilon}{8(2\pi)^2\Gamma(1+\epsilon)} |p_T^2|^{-\epsilon} \frac{dp_T^2 dy}{\sqrt{k_2^0}} \delta(k_2^0 + p_H^0 - \sqrt{l^2}). \quad (4.3.20)$$

The first phase subspace can be computed with equation 2.2.3

$$d\phi_2(p_1 + p_2; k_2, p_H) = \frac{1}{2(4\pi)^{2-2\epsilon}} s^{-\epsilon} \left(1 - \frac{l^2}{s}\right)^{1-2\epsilon} d\Omega_i \quad (4.3.21)$$

Combining all together

$$d\sigma_{real}^{(2)} = \Phi\mathcal{C}(\pi, \epsilon) \int dl^2 \left(\frac{4\pi}{p_T^2}\right)^\epsilon s^\epsilon \left(1 - \frac{l^2}{s}\right)^{1-2\epsilon} \frac{dp_T^2 dy}{\sqrt{k_2^0}} \delta(k_2^0 + p_H^0 - \sqrt{l^2}) \int d\Omega_i |\mathcal{M}|^2. \quad (4.3.22)$$

Now we use the Dirac delta to eliminate the integration on  $p_T^2$  (or, if interested in computing the doubly differential cross section, to eliminate the  $l^2$  integration), thus leaving

$$\frac{dC^2}{dy} = \Phi\mathcal{C}(\pi, \epsilon) \int \frac{dl^2}{\sqrt{l^2}} \left| \frac{dp_T^2}{dl^2} \right| \left( \frac{4\pi}{\tilde{p}_T^2} \right)^\epsilon \frac{1}{s - l^2} \left( \frac{(s - l^2)^2}{s} \right)^{1-\epsilon} \int d\Omega_i |M(\Omega, s, y, m_H^2, l^2)|^2, \quad (4.3.23)$$

where we have rewritten the soft scale emerged from the DY-like phase. Notice that this is really a soft scale since in the threshold limit, when  $k_1$  is soft,  $l^2 = s$ . Now we exchange  $l^2$  with the dimensionless slider variable  $w$ . We have already determined the maximum and minimum of  $l^2$  in section 3.5, however we will now repeat the computation in terms of the variables relevant for [2], that is  $s, t$  and  $u$ . We had obtained for  $l_{min}^2$  in the case  $y > 0$

$$l_{min}^2 = m^2 e^{2y}. \quad (4.3.24)$$

Writing the exponential of rapidity in terms of  $(s, t, u, m_H^2)$  we have

$$l_{min}^2 = m^2 \frac{u - m^2}{t - m^2}, \quad (4.3.25)$$

So  $w$  is defined such that

$$l^2 = m^2 \frac{u - m^2}{t - m^2} + w \left( s - m^2 \frac{u - m^2}{t - m^2} \right) = s \left[ \frac{m^2}{s} \frac{u - m^2}{t - m^2} + w \left( 1 - \frac{m^2}{s} \frac{u - m^2}{t - m^2} \right) \right] \quad (4.3.26)$$

Scale	Origin	logarithms $(x_1, x_2)$	logarithms $(t, u, Q_{max}^2)$
Collinear	DIS	$\ln(1-x_1)(1-x_2)$	$\ln Q_{max}^2$
Soft	DY	$\ln(1-x_1)^2$	$\ln t^2$

Table 4.1: Soft and collinear scales arising from the two different phase space factorizations depicted in figure 4.1 and 4.2.

And the  $\epsilon$  exponential becomes

$$\frac{(s-l^2)^2}{s} = \frac{s^2[1 - \frac{m^2}{s} \frac{u-m^2}{t-m^2} + w(1 - \frac{m^2}{s} \frac{u-m^2}{t-m^2})]^2}{s} = s(1-w)^2 \left(1 - \frac{m^2}{s} \frac{u-m^2}{t-m^2}\right)^2. \quad (4.3.27)$$

Notice that  $(1-w)$  regularizes the extremum  $w=1$ . We know that the left-over must be singular for  $x_1 \rightarrow 1$ , but it is not manifest in the way it is written. However we know  $t$  to be singular in the threshold limit. This suggests to factorize  $t$  from the expression so that

$$\frac{(s-l^2)^2}{s} = s(1-w)^2 \frac{t^2}{(t-m^2)^2} \left(1 - m^2 \frac{s+u-m^2}{st}\right)^2, \quad (4.3.28)$$

and, indeed, the last factor is finite for  $x_1 \rightarrow 1$ , so that the final singular scale is  $t^{2\epsilon}$ .

We have thus learnt that in the configuration of the threshold limit where one gluon is soft, a divergent scale in  $t$ , and symmetrically in  $u$ , must arise. Notice that in such configuration  $Q^2 = k_2^2 = 0$ , hence, in the doubly differential cross section, only terms proportional to  $\delta(Q^2)$  feature logarithms in  $t$ . This prediction is not trivial and will be explicitly checked in NNLO result.

It is worth to repeat an important point. The two factorization we have employed (figs. 4.1 and 4.2) are just two different ways of writing the same phase space. However, they highlight two different configurations in the threshold limit that contribute to two different enhanced logarithms,  $\ln Q_{max}^2$ , from the collinear configuration, and  $\ln t^2$ , from the soft configuration. Table 4.1 sums up these findings. Eventually, from both phase spaces both singular logarithm must arise. In the next sections we see explicitly how from the first factorization the  $t$  logarithms arise.

### 4.3.3 The fully differential distribution at NNLO

NNLO result of the doubly differential cross section for Higgs boson production has been computed for the first time in [10] and a year later was repeated in [2], succeeding in obtaining the results in a totally explicit and compact way. As already noted, the computation in this references is referred to as NLO, since the LO doubly differential distribution is completely trivial,

however for uniformity we will keep calling it NNLO. The result by [2], which from now on we will simply call GS, is detailed, for the production channel  $gg \rightarrow Hgg$ , in J.C. Glosser's Ph.D. thesis [5]. In this section we first present the result of the computation and inspect it to check our phase space analysis. Finally, the kinematical origin of the logarithms is retraced using [5].

First, define the coefficients of the perturbative expansion

$$\frac{d^2\sigma_{gg}}{dp_T^2 dy} = \frac{\sigma_0}{s} \left[ \frac{\alpha_s(\mu_R)}{2\pi} C^{(1)} + \left( \frac{\alpha_s(\mu_R)}{2\pi} \right)^2 C^{(2)} \right], \quad (4.3.29)$$

This gives the hadronic cross section by the usual convolution on parton momenta fractions. The NLO is

$$C^{(1)} = g_{gg}\delta(Q^2) = \frac{s^4 + t^4 + u^4 + m_H^8}{stu}\delta(Q^2), \quad (4.3.30)$$

which we have already discussed in depth.

The NNLO of the fully differential distribution is found by combining the real contribution  $C_{real}^{(2)}$  from  $gg \rightarrow Hgg$  and  $gg \rightarrow Hq\bar{q}$ , with the one loop contribution from  $gg \rightarrow Hg$ ,  $C_{virt}^{(1)}$ . As discussed, the  $gg \rightarrow H$  contribution is not included. In order to cancel collinear poles, the Altarelli-Parisi contribution  $C_{AP}^{(2)}$  must also be added. Each of these functions is computed in  $d$  dimensions, so they depend on the regularization parameter  $\epsilon$ . Only their sum is finite for  $\epsilon \rightarrow 0$ .

Concerning the doubly differential cross section, in order to get the finite hadronic cross section, integration on parton momenta requires regularization on  $Q^2$ , therefore, through the usual identity 1.8.5, the final result will display distributions in  $Q^2$ . In practice, however, integration on partonic momenta can be carried easily in terms of the dimensionless variables (see appendix B of GS)

$$z_t = \frac{-t}{Q^2 - t}, \quad z_u = \frac{-u}{Q^2 - u}, \quad (4.3.31)$$

so that the results also displays plus distributions in terms of these two. Notice that for  $x_1 \rightarrow 1$   $z_u \rightarrow 1$  while for  $x_2 \rightarrow 1$   $z_t \rightarrow 1$

Terms singular in  $p_T^2$  needs to be regularized only if interested in the rapidity distribution. Moreover, poles arising from  $\delta(p_T^2)/\epsilon$  can be cancelled only by adding the  $gg \rightarrow H$  contribution. For this reason, from the final result only the rapidity distribution cannot be really obtained, but it can be used to study its threshold behaviour.

To isolate the most prominent numerical contributions to the hadronic cross section, the result in GS is presented separating non singular and singular terms. We are interested in the second. The result is the following

$$\begin{aligned}
C_{sing}^{(2)} = & \delta(Q^2) \left\{ (11 + \delta + N_c U) g_{gg} \right. \\
& + (N_c - n_f) \frac{N_c}{3} \left[ \frac{m_H^4}{s} + \frac{m_H^4}{t} + \frac{m_H^4}{u} + m_H^2 \right] \Big\} \\
& + \left\{ \left( \frac{1}{-t} \right) \left[ -P_{gg}(z_t) \log \frac{\mu_F^2 z_t}{-t} + p_{gg}(z_t) \left( \frac{\log(1-z_t)}{1-z_t} \right)_+ \right] g_{gg,t}(z_t) \right. \\
& + \left( \frac{1}{-t} \right) \left[ -2n_f P_{qg}(z_t) \log \frac{\mu_F^2}{Q_{max}^2} + 2n_f z_t (1-z_t) \right] g_{qg,t}(z_t) \\
& + \left( \frac{z_t}{-t} \right) \left[ \left( \frac{\log(1-z_t)}{1-z_t} \right)_+ - \log \frac{Q_T^2 z_t}{-t} \left( \frac{1}{1-z_t} \right)_+ \right] \\
& \quad \cdot \frac{N_c^2}{2} \left[ \frac{m_H^8 + s^4 + t^4 + u^4 + Q^8 + z_t z_u (m_H^8 + s^4 + Q^8 + (u/z_u)^4 + (t/z_t)^4)}{sut} \right] \\
& - \left( \frac{z_t}{-t} \right) \left( \frac{1}{1-z_1} \right)_+ \frac{\beta_0}{2} N_c \left( \frac{m_H^8 + s^4 + z_t z_u ((u/z_u)^4 + (t/z_t)^4)}{sut} \right) \\
& + (t \leftrightarrow u) \Big\} \\
& + N_c^2 \left[ \frac{(m_H^8 + s^4 + Q^8 + (u/z_u)^4 + (t/z_t)^4)(Q^2 + Q_T^2)}{s^2 Q^2 Q_T^2} + \right. \\
& \left. + \frac{2m_H^4((m_H^2 - u)^4 + (m_H^2 - t)^4 + t^4 + u^4)}{sut(m_H^2 - t)(m_H^2 - u)} \right] \frac{1}{p_T^2} \log \frac{p_T^2}{Q_T^2}
\end{aligned} \tag{4.3.32}$$

where  $P_{gg}$  and  $P_{qg}$  are the splitting functions

$$P_{gg}(z) = N_C \left[ \frac{1 + z^4 + (1-z)^4}{(1-z)_+ z} \right] + \beta_0 \delta(1-z), \quad P_{qg}(z) = \frac{1}{2} [z^2 + (1-z)^2], \tag{4.3.33}$$

$p_{gg}$  is the regular coefficient of  $P_{gg}$ . If  $g_{ij}$  are the partonic NLO functions,  $g_{ij,t}(z_t) := g_{ij}(z_t \xi_1, \xi_2)$ ,  $g_{ij,u}(z_u) := g_{ij}(\xi_1, z_u \xi_2)$ , where  $\xi_1$  and  $\xi_2$  are partonic momentum fractions. Clearly, in the singly soft limits they reduce to the ordi-



nary functions. Explicitly

$$\begin{aligned}
g_{gg,t}(z_t) &= \frac{m_H^8 + (z_t s)^4 + t^4 + \left(\frac{z_t s p_T^2}{t}\right)^4}{z_t^2 s^2 p_T^2} & g_{gg,u}(z_u) &= \frac{m_H^8 + (z_u s)^4 + u^4 + \left(\frac{z_u s p_T^2}{u}\right)^4}{z_u^2 s^2 p_T^2} \\
g_{qg,t}(z_t) &= C_F \frac{(t^2 + z_t^2 s^2)t}{-z_t s p_T^2} & g_{qg,u}(z_u) &= C_F \frac{\left(\frac{z_u s p_T^2}{u}\right)^2 + z_u^2 s^2}{-u}
\end{aligned} \tag{4.3.34}$$

Finally,

$$\delta = \frac{3\beta_0}{2} \left( \ln \frac{\mu_R^2}{-t} + \ln \frac{\mu_R^2}{-u} \right) + \left( \frac{67}{18} N_c - \frac{5}{9} n_f \right), \tag{4.3.35}$$

$$U = \frac{1}{2} \ln^2 \frac{-u}{-t} + \frac{\pi^2}{3} \tag{4.3.36}$$

$$\begin{aligned}
& - \ln \frac{s}{m_H^2} \ln \frac{-t}{m_H^2} - \ln \frac{s}{m_H^2} \ln \frac{-u}{m_H^2} - \ln \frac{-t}{m_H^2} \ln \frac{-u}{m_H^2} \\
& \ln^2 \frac{m_H^2}{s} + \ln^2 \frac{m_H^2}{m_H^2 - t} + \ln^2 \frac{m_H^2}{m_H^2 - u} \\
& + \text{Li}_2 \left( \frac{s - m_H^2}{s} \right) + \text{Li}_2 \left( \frac{m_H^2}{m_H^2 - t} \right) + \text{Li}_2 \left( \frac{m_H^2}{m_H^2 - u} \right), \\
Q_T^2 &= Q^2 + p_T^2
\end{aligned} \tag{4.3.37}$$

and  $N_c = 3$ ,  $n_f = 5$  (remember the infinite top mass approximation). First notice that all the singularities in  $Q^2$  have been regularized<sup>2</sup>. Because we are interested in the behaviour of the result in threshold limit of the rapidity distribution, we must set up the integration on transverse momentum, even if we cannot compute it explicitly. We have already discussed that the best variables to write the integral are  $(x_1, x_2, q, m_H^2)$  therefore the integration is written in the  $q$  variable through the variable changes  $p_T^2 \rightarrow Q^2 \rightarrow q$

$$\int_0^{p_{T,max}^2} dp_T^2 = \int_0^{Q_{max}^2} dQ^2 \left| \frac{dp_T^2}{dQ^2} \right| = \int_0^1 dq \frac{dQ^2}{dq} J = \int_0^1 dq J(x_1, x_2, q) Q_{max}^2, \tag{4.3.38}$$

where  $J$  is the regular function

$$J = \frac{2x_1 x_2}{(x_1 + x_2)^2} [1 + x_1 x_2 - q(1 - x_1)(1 - x_2)]. \tag{4.3.39}$$

The plus distributions in  $z_t$  and  $z_u$  can be rewritten in terms of  $q$  by applying

---

<sup>2</sup>The  $\frac{1}{Q^2} \ln \frac{p_T^2}{Q_T^2}$  terms in the last line are finite

the following identities, proved in the appendix,

$$\begin{aligned}
\delta(1 - z_t) &= \frac{-t}{Q_{max}^2} \delta(q), \\
\frac{z_t}{-t} \left( \frac{1}{1 - z_t} \right)_+ &= \frac{1}{Q_{max}^2} \left\{ \left( \frac{1}{q} \right)_+ + \delta(q) \ln \left( \frac{Q_{max}^2}{-t} \right) \right\}, \\
\frac{z_t}{-t} \left( \frac{\ln(1 - z_t)}{1 - z_t} \right)_+ &= \frac{1}{Q_{max}^2} \left\{ \left( \frac{\ln q}{q} \right)_+ + \ln \frac{Q_{max}^2 z_t}{-t} \left( \frac{1}{q} \right)_+ + \frac{\delta(q)}{2} \ln^2 \frac{Q_{max}^2}{-t} \right\}.
\end{aligned} \tag{4.3.40}$$

Now, defining obviously the coefficients  $\mathcal{V}, \mathcal{A}_{t,u}, \mathcal{B}_{t,u}, \mathcal{C}_{t,u}, \mathcal{D}_{t,u}, E$ , we finally rewrite the result as

$$\begin{aligned}
C_{sing,rap}^{(2)} &= \int_0^1 dq J(x_1, x_2, q) Q_{max}^2 \left\{ \frac{\delta(q)}{Q_{max}^2} \mathcal{V} + \right. \\
&\quad \frac{1}{-t} \mathcal{A}_t \left[ -p_{gg} \left( \left( \frac{\ln(1 - z_t)}{1 - z_t} \right)_+ + \ln \frac{\mu^2 z_t}{-t} \left( \frac{1}{1 - z_t} \right)_+ \right) - \beta_0 \ln \frac{\mu^2 z_t}{-t} \frac{\delta(q)}{Q_{max}^2} \right] + \\
&\quad \frac{1}{-t} \left[ \mathcal{B}_{1,t} \ln \frac{1}{q Q_{max}^2} + \mathcal{B}_{2,t} \right] + \\
&\quad \frac{z_t}{-t} \mathcal{C}_t \left[ \left( \frac{\ln(1 - z_t)}{1 - z_t} \right)_+ - \ln \frac{Q_T^2 z_t}{-t} \left( \frac{1}{1 - z_t} \right)_+ \right] - \\
&\quad \frac{z_t}{-t} \mathcal{D}_t \left( \frac{1}{1 - z_t} \right)_+ + (t \leftrightarrow u) \\
&\quad \left. + \mathcal{E} \right\}
\end{aligned} \tag{4.3.41}$$

Expanding distributions in  $z_t$  and  $z_u$  and rearranging

$$\begin{aligned}
C_{sing,rap}^{(2)} = \int_0^1 dq J(x_1, x_2, q) \Bigg\{ & \\
& Q_{max}^2 \left[ \mathcal{E} + \frac{\mathcal{B}_{2,t}}{-t} - \frac{\mathcal{B}_{1,t}}{-t} \ln \frac{1}{q Q_{max}^2} \right] \\
& + \delta(q) \left[ \mathcal{A}_t \beta_0 \ln t + \frac{\mathcal{A}_t p_{gg}}{2} \ln^2 Q_{max}^2 - \frac{\mathcal{A}_t p_{gg}}{2} \ln^2 t - \mathcal{C}_t \ln Q_{max}^2 \ln p_{T,max}^2 + \frac{1}{2} \mathcal{C}_t \ln^2 Q_{max}^2 \right. \\
& \left. - \frac{1}{2} \mathcal{C}_t \ln^2 t + \mathcal{C}_t \ln p_{T,max}^2 - \mathcal{D}_t \ln Q_{max}^2 + \mathcal{D}_t \ln t + \mathcal{V} \right] \\
& + \left( \frac{1}{q} \right)_+ \left[ \frac{\mathcal{A}_t p_{gg}}{z_t} \ln Q_{max}^2 + \mathcal{C}_t \ln Q_{max}^2 - \mathcal{C}_t \ln Q_T^2 - \mathcal{D}_t \right] \\
& + \left( \frac{\ln q}{q} \right)_+ \left[ \frac{\mathcal{A}_t p_{gg}}{z_t} + \mathcal{C}_t \right] + (t \leftrightarrow u) \Bigg\}
\end{aligned} \tag{4.3.42}$$

Where in the parenthesis proportional to  $\delta(q)$  we have set  $z_t = z_u = 1$  and  $Q_T^2 = p_{T,max}^2$  and the coefficients  $\mathcal{A}, \mathcal{C}, \mathcal{D}$  are all proportional to  $(1 - x_1)^{-1}(1 - x_2)^{-1}$ . Keeping in mind eqs. 4.3.5, the threshold logarithms that appear in the final result are

$$L_1 = \ln t, \quad L_2 = \ln u, \quad L_3 = \ln Q_{max}^2. \tag{4.3.43}$$

Or, in terms of the threshold variables

$$L_1 = \frac{\ln(1 - x_1)}{1 - x_1}, \quad L_2 = \frac{\ln(1 - x_2)}{1 - x_2}, \quad L_3 = \frac{\ln(1 - x_1)(1 - x_2)}{(1 - x_1)(1 - x_2)}. \tag{4.3.44}$$

These are exactly the kind of logarithms we have predicted in the previous section (table 4.1).

Moreover, logarithms in  $t$  and  $u$  appear only in terms proportional to  $\delta(q)$ , in the second line of the result, as we expected, since we know that they should come from the kinematic configuration where one gluon is soft, and hence  $Q^2 = 0$ .

These logarithms do not feature any plus distribution for the reasons we have discussed. In a complete calculation of the fully differential distribution they must appear as plus distributions, since the rapidity distribution must be finite.

#### 4.3.4 Retracing logarithms

We have thus verified that the result has the predicted logarithms. It is now interesting to retrace their origin following the calculations in [5], to confirm that they do appear from the expected kinematical configurations. In this work, only details on the  $gg \rightarrow Hgg$  channel are given, no intermediate results are available for  $gg \rightarrow Hq\bar{q}$ , but for our scope this is sufficient.

The computation is carried following the usual steps, that is adding the real and virtual coefficient functions with the Altarelli-Parisi term that cancels the collinear poles

$$C^{(2)} = \lim_{\epsilon \rightarrow 0} \left[ C_{real}^{(2)} + C_{virt}^{(2)} + C_{AP}^{(2)} \right]. \quad (4.3.45)$$

To get the real contributions, squared amplitudes are integrated using the phase space decomposition 4.3.16. The explicit angular integration is

$$\frac{1}{2\pi} \int_0^\pi d\phi \int_0^\pi d\theta (\sin \theta)^{1-2\epsilon} (\sin \phi)^{-2\epsilon} |\mathcal{M}(\theta, \phi)|^2, \quad (4.3.46)$$

where  $\theta$  and  $\phi$  are the polar angles of the back-to-back gluons jet in their center-of-mass frame of reference. Details on their calculations can be found in [5], [10] and subsequent older articles. Terms proportional to  $\epsilon^{-1}$  and  $(Q^2)^{-1}$  give the singular part of the real contribution

$$\begin{aligned} C_{real}^{(2)} = \sigma_\epsilon \Bigg\{ & -\frac{1}{N_c \epsilon} \frac{p_{gg}(z_t)}{-t} g_{gg,t}(z_t) \\ & -\frac{1}{\epsilon} \left[ \left( \frac{Q^2}{Q_T^2} \right)^{-\epsilon} \left( 1 + \frac{\pi^2 \epsilon^2}{6} \right) - 1 \right] \frac{g_{gg,t}(z_t)}{Q^2} \\ & -\frac{1}{2} \left( \frac{11}{6} + \frac{67\epsilon}{18} \right) \frac{g_{gg,t}(z_t)}{Q^2} + (t \leftrightarrow u) + \text{Regular terms} \Bigg\}, \end{aligned} \quad (4.3.47)$$

where  $\sigma_\epsilon$  collects all the remaining factors from the phase space. These include  $(Q^2)^{-\epsilon}$  and  $(p_T^2)^{-\epsilon}$ . The first factor combined with the  $Q^2$  singularities gives the  $Q_{max}^2$  logarithms, exactly as predicted by the phase space argument. The second exponential is necessary to regularize collinear divergences. As discussed, these are ignored by GS, thus resulting in poorly behaved expressions for  $p_T^2 \rightarrow 0$ . We could in principle repeat the calculation considering the full regularization, but in order to cancel the new  $\epsilon$  poles arising, we should include the two-loop calculation of  $gg \rightarrow H$ , which in turn gives also finite contributions. We have thus understood the origin of the  $\ln Q_{max}^2$  appearing in the GS final result 4.3.42: it is exactly the one predicted by the phase space decomposition depicted in fig. 4.1.

After combining exponentials and singularities, the expression can be summed

to the AP contribution

$$C_{AP}^{(2)} = \frac{1}{N_c \epsilon} \frac{P_{gg}(z_t)}{-t} g_{gg,t}(z_t) + \frac{1}{N_c \epsilon} \frac{P_{gg}(z_u)}{-u} g_{gg,u}(z_u), \quad (4.3.48)$$

that is calculated considering the cross section in the limit of a single collinear gluon emission from the first or second initial-state gluon, carrying a momentum fraction, fixed by conservation of energy, of  $(1 - z_t)$  or  $(1 - z_u)$ . Since  $P_{gg}(z_t)$  contains plus distributions in  $z_t$ , to make the cancellation explicit, in place of the usual 1.8.5 identity, the following expansion was adopted

$$\left( \frac{1}{Q^2} \right)^{1+k\epsilon} = -\frac{1}{k\epsilon} (-t)^{-k\epsilon} \delta(Q^2) + \left( \frac{z_t}{-t} \right)^{1+k\epsilon} \left\{ \left( \frac{1}{1-z_t} \right)_+ - k\epsilon \left( \frac{\ln(1-z_t)}{1-z_t} \right)_+ \right\}, \quad (4.3.49)$$

which can be easily verified at any fixed order by expanding both sides in  $\epsilon$ . This finally introduces the  $t^{-\epsilon}$  scale which we expected from the phase space analysis. Thinking back to its meaning it is not a surprise that we could find it in this place. The  $t$  (or  $u$ ) scale arises writing the phase space in such a way to highlight an initial soft emission (fig. 4.2) which reduces the energy of the process from  $s$  to  $l^2$  while the other is collinear. Thus, the kinematical configuration that contributes to the singularity is exactly the one considered in 4.3.48, where there is a single collinear emission.

Now, the sum of the two terms leave only poles proportional to  $\delta(q)$ , that are cancelled by the virtual contribution from the 1-loop of single emissions diagrams, that indeed has exactly a kinematics proportional to  $\delta(q)$ . Adding all together we get all the singular terms of the  $gg \rightarrow Hgg$  process contributing to 4.3.32.

In conclusion, from the resummation argument we have predicted the two kinds of logarithmic contributions (table 4.1), the *collinear*  $\ln Q_{max}^2$  and the *soft*  $\ln t$ , coming respectively from the region of the phase space where both gluons are collinear to the Higgs boson and from the region of the phase space where one gluon is collinear and the other is soft. These two regions can be highlighted by writing the phase space in two different ways (figs. 4.1 and 4.2).

In the NNLO fully differential distribution we have effectively observed these two logarithms (eqs. 4.3.42), in particular we have seen  $\ln t$  being proportional only to  $\delta(q)$ , as expected from the phase space region where it arises. Following [5], we have explicitly seen that  $\ln Q_{max}^2$  in the final results do come from the first phase space factorization (fig. 4.1). From the same reference we have seen that  $\ln t$  comes from the cancellation of singular poles with the Altarelli-Parisi contribution, that are calculated from the phase space region where we expect these logarithms to come from.

It should be noted, however, that, even if the kinematical origin of the soft scale is clearly the one predicted, we could not observe in the complete cal-

culation the factor of 2 that the phase argument predicts from the DY-like phase spaces (tables 2.1, 4.1 and eq. 4.3.28). We mentioned in section 3.7 that this is important in order to understand the difference with the resummation by Tackmann in [8]. We do not expect this to be due to an error in the phase space argument, but only in the way the calculation is actually performed that does not make the factor of 2 evident.

We have thus confirmed the appearance and the origin of the enhanced logarithms resummed by the resummation formulae 3.6.8 and 3.6.9, making progress in the verification of this approach to the resummation of the rapidity distribution.

# Conclusions

In this thesis we considered the rapidity distribution of Higgs boson production through gluon fusion. The threshold limit is the limit where the center-of-mass energy is barely enough to produce an Higgs boson with fixed mass and rapidity. We parametrized the threshold limit with the scaling variables  $x_1$  and  $x_2$  and, particularly, we defined the singly soft limit, where  $x_1 \rightarrow 1$  and  $x_2$  is fixed (or vice versa), and the doubly soft limit, where both  $x_1, x_2 \rightarrow 1$ , that is when the rapidity is 0.

Following the approach in [1], we derived the resummation formulae for rapidity distribution identifying the threshold enhanced logarithms  $\ln m_H^2(1 - x_1)^2$  and  $\ln m_H^2(1 - x_1)(1 - x_2)$  arising respectively from the DY-like phase subspace of soft emissions and the DIS-like phase subspace of collinear emissions in the threshold limit.

In order to verify these findings we moved onto the analysis of the first leading orders of Higgs boson production. To identify the two singular scales we wrote them in terms of natural kinematical quantities appearing in actual calculations. We found the soft scale  $m_H^2(1 - x_1)^2$  to be proportional to the Mandelstam invariant  $t$ , and the collinear scale  $m_H^2(1 - x_1)(1 - x_2)$  to be related to the maximum energy of the emitted radiation  $Q_{max}^2$ . In particular at NNLO we observed that the soft scale must always be multiplied by a  $\delta(Q^2)$ , since in the kinematical configuration where we expect it to arise,  $Q^2$  must be 0.

Since the first two leading orders are trivial, we considered the NNLO rapidity distribution starting from the only complete result in literature, the fully differential distribution in [2]. We first found that in order to study the threshold limit of the rapidity distribution from the fully differential distribution, the transverse momentum integration must be exchanged with the integration on the dimensionless variable  $q$  defined in the fixed range  $[0, 1]$ . Rewriting the result in terms of this variable we could finally single out the soft and collinear logarithms in the form we predicted,  $\ln Q_{max}^2$  and  $\ln t$ .

Finally, to further support our findings, we retraced the origin of these two logarithms in the computation of the fully differential distribution detailed in [5]. The origin of  $Q_{max}^2$  logarithms can be clearly identified from the phase calculation, and it is fully corresponding to the phase space decomposition

we employed to predict its origin.  $t$  logarithms appear from the Altarelli-Parisi contribution to the cross section. We argued that the kinematics of such terms is really the same of the kinematical configuration where we predicted  $\ln t$  factors to come from in the phase space argument.

To fully establish the resummation formula, it must be compared with the results in SCET obtained by F.J. Tackmann et alii [8], where some differences have been observed, likely by virtue of factorization scheme-dependent factors. If the resummation approach we adopted passes also this test, it is natural to extend it to the threshold resummation of the fully differential distribution, where both the rapidity and the transverse momentum of the Higgs boson are fixed.



# Appendix A

## Mathematical tools

### A.1 Plus distribution

Given a logarithmic divergent function  $f(x)$  in  $x = a$ , we define the *plus distribution*  $(f(x))_+$ , such that on any test function  $g(x)$

$$\int_0^a dx g(x) (f(x))_+ = \int_0^a [g(x) - g(a)] f(x). \quad (\text{A.1.1})$$

If  $f(x)$  is divergent in  $x = 0$ , then

$$\int_0^{x_{max}} dx g(x) (f(x))_+ = \int_0^{x_{max}} dx [g(x) - g(0)] f(x). \quad (\text{A.1.2})$$

In this thesis the correct definition is always implicit in the properties of  $f$ , for example in equation 4.3.40 plus distributions on the LHS are defined in the first way for  $a = 1$ , while on the RHS in the second way.

Integrals with plus distributions are finite, since the difference in the square brackets cancels the logarithmic divergence in  $f$ . For the same reasons higher divergences are not regularized.

Plus distributions can be also written straightforwardly in terms of other distributions. In the first case, for example, if  $a = 1$

$$(f(x))_+ = \lim_{\Delta \rightarrow 0} \left[ \Theta(1 - \Delta - x) f(x) - \delta(1 - x) \int_0^{1-\Delta} d\xi f(\xi) \right], \quad (\text{A.1.3})$$

where the parameter  $\Delta$  separates the regular and the divergent regions of the integral on  $x$ . Sometimes, cross sections are written in terms of  $\Delta$ , rather than plus distributions [10, 18].

Plus distribution arise from  $d$ -dimensional regularized calculations from the

following identity

$$x^{-1+\epsilon} = \frac{\delta(x)}{\epsilon} + \left(\frac{1}{x}\right)_+ + \epsilon \left(\frac{\ln x}{x}\right)_+ + \mathcal{O}(\epsilon^2), \quad (\text{A.1.4})$$

for divergences in  $x = 0$ , or, alternatively, exchange  $x$  with  $1 - x$  for divergences in  $x = 1$ . The identity can be derived acting on a test function  $g(x)$  and with a few expansions

$$\begin{aligned} \int_0^1 dx x^{-1+\epsilon} g(x) dx &= \int_0^1 dx x^{-1+\epsilon} [g(x) - g(0)] + \frac{g(0)}{\epsilon} = \\ &= \int_0^1 dx \left[ \frac{1}{x} + \epsilon \frac{\ln x}{x} + \mathcal{O}(\epsilon^2) \right] [g(x) - g(0)] + \frac{g(0)}{\epsilon} = \\ &= \int_0^1 dx \left[ \left(\frac{1}{x}\right)_+ + \epsilon \left(\frac{\ln x}{x}\right)_+ + \frac{\delta(x)}{\epsilon} \right] g(x). \end{aligned} \quad (\text{A.1.5})$$

This identity can also be used to compute change of variables in plus distributions. Consider in particular the relations we are interested in, eqs. 4.3.40. The relation between the two variables is

$$q = \frac{-t}{Q_{max}^2} \frac{1 - z_t}{z_t}. \quad (\text{A.1.6})$$

Consider now

$$q^{-1+\epsilon} = \left( \frac{-t}{Q_{max}^2 z_t} \right)^{-1+\epsilon} (1 - z_t)^{-1+\epsilon}, \quad (\text{A.1.7})$$

the LHS and the second factor of the RHS can be expanded in  $\epsilon$  using the distributional identity we have just shown, while the first can be expanded into ordinary logarithms. Since the relation holds for all values of  $\epsilon$ , equating in the LHS and in the RHS terms in the same  $\epsilon$  order we relate all  $\left(\frac{\ln^k q}{q}\right)_+$  distributions with  $\left(\frac{\ln^k(1-z_t)}{1-z_t}\right)_+$  distributions and vice versa, if we started from the inverse variable transformation.

## A.2 Mellin transform

Given a function  $f(x)$  with  $x \in [0, 1]$ , its *Mellin transform*  $\mathcal{M}[f](N)$  is

$$\mathcal{M}[f](N) := \int_0^1 dx x^{N-1} f(x), \quad (\text{A.2.1})$$

where  $N \in \mathbb{C}$ . Notice that, since in the limit  $|N| \rightarrow \infty$   $x^{N-1} \rightarrow \delta(1 - x)$ , the equivalence

$$\lim_{|N| \rightarrow \infty} \mathcal{M}[f](N) = \lim_{x \rightarrow 1} f(x) \quad (\text{A.2.2})$$

holds.

Analogously to the Fourier transform, we can define a convolution between two functions that factorizes under a Mellin transform. Given the functions  $f$  and  $g$  we define the Mellin convolution

$$(f \otimes g)(x) := \int_x^1 \frac{dy}{y} f(y) g\left(\frac{x}{y}\right). \quad (\text{A.2.3})$$

Rewriting it as

$$(f \otimes g)(x) = \int_0^1 dy \int_0^1 dz f(y) g(z) \delta(x - yz), \quad (\text{A.2.4})$$

it is obvious to see how it factorizes under a Mellin transform

$$\begin{aligned} \mathcal{M}[f \otimes g](N) &= \int_0^1 dx x^{N-1} \int_0^1 dy \int_0^1 dz f(y) g(z) \delta(x - yz) \\ &= \int_0^1 dy y^{N-1} \int_0^1 dz z^{N-1} f(y) g(z) = \mathcal{M}[f](N) \mathcal{M}[g](N). \end{aligned} \quad (\text{A.2.5})$$

# Bibliography

- [1] Lorenzo De Ros. Resummation of rapidity distributions in the singly and doubly soft limits, 2022.
- [2] Christopher J. Glosser and Carl R. Schmidt. Next-to-leading corrections to the Higgs boson transverse momentum spectrum in gluon fusion. *JHEP*, 12:016, 2002.
- [3] Stefano Forte and Giovanni Ridolfi. Renormalization group approach to soft gluon resummation. *Nucl. Phys. B*, 650:229–270, 2003.
- [4] John Collins. *Foundations of Perturbative QCD*. Cambridge Monographs on Particle Physics, Nuclear Physics and Cosmology. Cambridge University Press, 2011.
- [5] Christopher James Glosser. *Higgs boson production in hadron hadron colliders*. PhD thesis, Michigan State U., 2001.
- [6] Stefano Forte, Giovanni Ridolfi, and Simone Rota. Threshold resummation of transverse momentum distributions beyond next-to-leading log. *JHEP*, 08:110, 2021.
- [7] T. R. Rabemananjara. *Resummation and Machine Learning Techniques Towards Precision Phenomenology at the LHC*. PhD thesis, Milan U., 2021.
- [8] Gillian Lustermans, Johannes K. L. Michel, and Frank J. Tackmann. Generalized Threshold Factorization with Full Collinear Dynamics. 8 2019.
- [9] D. Westmark. *Threshold Resummation and the Determination of Parton Distribution Functions*. PhD thesis, Florida State U., 2015.
- [10] V. Ravindran, J. Smith, and W. L. Van Neerven. Next-to-leading order QCD corrections to differential distributions of Higgs boson production in hadron hadron collisions. *Nucl. Phys. B*, 634:247–290, 2002.

- [11] Paolo Bolzoni, Stefano Forte, and Giovanni Ridolfi. Renormalization group approach to Sudakov resummation in prompt photon production. *Nucl. Phys. B*, 731:85–108, 2005.
- [12] Eric Laenen and George F. Sterman. Resummation for Drell-Yan differential distributions. In *7th Meeting of the APS Division of Particles Fields*, pages 987–989, 11 1992.
- [13] S. Catani and L. Trentadue. Resummation of the QCD Perturbative Series for Hard Processes. *Nucl. Phys. B*, 327:323–352, 1989.
- [14] Davide Maria Tagliabue. Threshold resummation of rapidity distributions in scet vs. direct qcd, 2020.
- [15] Charalampos Anastasiou, Lance J. Dixon, and Kirill Melnikov. NLO Higgs boson rapidity distributions at hadron colliders. *Nucl. Phys. B Proc. Suppl.*, 116:193–197, 2003.
- [16] Claudio Muselli. *Resummations of Transverse Momentum Distributions*. PhD thesis, Milan U., 2017.
- [17] Pulak Banerjee, Goutam Das, Prasanna K. Dhani, and V. Ravindran. Threshold resummation of the rapidity distribution for Drell-Yan production at NNLO+NNLL. *Phys. Rev. D*, 98(5):054018, 2018.
- [18] T. Matsuura and W. L. van Neerven. Second Order Logarithmic Corrections to the Drell-Yan Cross-section. *Z. Phys. C*, 38:623, 1988.